

# **For Reference**

**NOT TO BE TAKEN FROM THIS ROOM**

# For Reference

NOT TO BE TAKEN FROM THIS ROOM

Ex LIBRIS  
UNIVERSITATIS  
ALBERTAEASIS



A faint, grayscale background image of a classical building, possibly a library or courthouse, featuring multiple columns and a prominent pediment at the top.

Digitized by the Internet Archive  
in 2020 with funding from  
University of Alberta Libraries

<https://archive.org/details/Chance1970>







THE UNIVERSITY OF ALBERTA

FLIGHT MECHANICS OF

*AGROTIS ORTHOGONIA MORRISON* (LEPIDOPTERA: PHALAENIDAE)

by



MARTIN ALAN CHARLES CHANCE

A THESIS

SUBMITTED TO THE FACULTY OF GRADUATE STUDIES

IN PARTIAL FULFILMENT OF THE REQUIREMENTS FOR THE DEGREE

OF MASTER OF SCIENCE

DEPARTMENT OF ENTOMOLOGY

EDMONTON, ALBERTA

SPRING 1970



thesis  
1970  
21

UNIVERSITY OF ALBERTA  
FACULTY OF GRADUATE STUDIES

The undersigned certify that they have read, and recommend  
to the Faculty of Graduate Studies for acceptance, a thesis  
entitled: Flight Mechanics of *Agrotis orthogonia* Morrison  
(Lepidoptera: Phalaenidae) submitted by Martin Alan Charles Chance  
in partial fulfilment of the requirements for the degree of  
Master of Science.



## Abstract

The flight mechanism of *Agrotis orthogonia* Morrison is extremely complicated. However, it functions in a relatively simple way. This function can be approximated by four stiff rods which hinge on each other to form a diamond shaped structure and lie in a vertical plane. The wing attaches proximally to the dorsal apical hinge of the diamond. A fifth rod attaches between the ventral apical hinge of the diamond and the wing distal to its proximal hinge. Pulling the anterior and posterior ends of the diamond together produces downstroke movements. Pulling the dorsal and ventral hinges together produces upstroke movements.

Wing pronation and supination is automatic and occurs about the dorsal second axillary-, dorsal subcosta - first axillary hinge. The subalar musculature, along with the remainder of the downstroke muscles, pronates as well as depresses the wing. The upstroke muscles and the aerodynamic forces produced on the wing supinate it during the upstroke.

The contraction of the lateral oblique dorsal longitudinal muscle acts on the laterophragma and third axillary system to protract or unfold the wing at flight initiation and during the upstroke. The aerodynamic forces produced on the wing protract it during the downstroke.



## Acknowledgements

I would like to thank Drs. R. H. Gooding, B. Hocking, and J. Sharplin for their supervision of this work, and M. M. Chance and Drs. D. A. Craig, B. Hocking, and J. Sharplin for their valuable suggestions and criticism of this manuscript.

I am indebted especially to Dr. J. Sharplin for her inexhaustible encouragement and enthusiasm throughout.

I would also like to thank L. A. Jacobson (Canada Department of Agriculture, Lethbridge, Alberta) for providing me with reared and field caught specimens, and J.D. Shorthouse for making field collections for me in the fall of 1967.

I am grateful to the National Research Council of Canada and the Defence Research Board of Canada for financing this project.



## Autobiographical Sketch

I attended Sir George Williams University in Montreal. I graduated with a B.A. in 1964 and with a B.Sc. with a major in mathematics and physics in 1966.

During my final years at Sir George Williams, after taking some courses in biology I decided to continue my university education by studying some aspect of biophysics. I spent the summer of 1965 working on a biophysics project in the Department of Physics at Sir George Williams as a summer assistant to Dr. A. E. Smith. On a visit to Edmonton I had the opportunity to meet Dr. B. Hocking, and became interested in insect flight.

Smith, A.E. and M.A.C. Chance. 1966. Coacervate behaviour in an alternating electric field. Nature, London 209:74-75.



## Table of Contents

	Page
1. Introduction .....	1
2. Literature Review .....	2
3. Methods and Materials .....	5
4. Morphology and Functions of the Flight Structures .....	9
4.1. General description .....	9
4.2. The notum .....	11
4.2.1. Deflection of the notum .....	11
4.2.2. The anterior margin of the notum .....	13
4.2.3. The anterolateral margin of the notum ....	14
4.2.4. The posterolateral margin of the notum ...	17
4.2.5. Deflection of the margins of the notum ...	22
4.3. The pleuron and sternum .....	25
4.3.1. Structure of the pleuron and sternum ....	25
4.3.2. The pleurites .....	30
4.3.3. Deflection of the pleurites .....	33
4.3.4. Deflection of the pleuron and sternum ....	39
4.4. The wing base .....	57
4.4.1. The first axillary sclerite .....	57
4.4.2. The second axillary sclerite .....	58
4.4.3. The subcosta, costa, radial plate, radius, second cubitus, and the wing .....	61
4.4.4. The third axillary sclerite, first median plate, and second median plate ....	66



	Page
4.4.5. Movement of the first axillary sclerite, second axillary sclerite, subcosta, radial plate and the wing .....	68
4.4.6. Movement of the third axillary and median plate and wing retraction and protraction .....	83
5. Discussion .....	90
6. Conclusion .....	100
7. Tables and Figures .....	101
8. Literature Cited .....	137



List of Tables

	Page
Table 1. Abbreviations of terms used in the figures for the flight structures of <i>A. orthogonia</i> ....	101-102
Table 2. Abbreviations of terms used for the flight muscles of <i>A. orthogonia</i> , and the equivalent abbreviated terms used for the flight muscles of <i>T. polyphemus</i> by Nüesch (1953) .....	103-104
Table 3. The limits of movement of the right side of the mesothoracic notum of <i>A. orthogonia</i> and the associated sclerites of its wing base ....	105



## List of Figures

	Page
Fig. 1. Semi-diagrammatic dorsal view of the right fore wing base .....	106
Fig. 2. Semi-diagrammatic side view of the left mesothoracic pleural and notal region, and ventral region of the fore wing .....	106
Fig. 3. Semi-diagrammatic dorsal view of the right hind wing base .....	107
Fig. 4. Semi-diagrammatic ventral view of the left hind wing base .....	107
Fig. 5. Lateral inside view of the right side of a sagittal section of the pterothorax .....	108
Fig. 6. Lateral inside view of the right side of a sagittal section of the pterothorax with the longitudinal muscles and the phragma removed .....	108
Fig. 7. Lateral inside view of the right side of a sagittal section of the pterothorax with the longitudinal and proximal dorsoventral muscles, and the phragma removed .....	109
Fig. 8. Lateral inside view of the right side of a sagittal section of the pterothorax with the longitudinal and dorsoventral muscles, and the phragma removed .....	109



Fig. 9. Lateral inside view of a sagittal section of the pterothorax with all the longitudinal, indirect acting dorsoventral, and most of the large direct acting muscles, and the phragma removed .....	110
Fig. 10. Left side view of the pterothorax with the wing, wing base, and tegula removed .....	110
Fig. 11. Side view of the left pterothorax with the levels and orientations of sections 11a, 11b, and 11c indicated .....	111
Fig. 11a. Cross-section of the mesothoracic dorsal longitudinal muscles .....	111
Fig. 11b. Cross-section of the mesothoracic dorso- ventral muscles .....	111
Fig. 11c. Cross-section of the metathoracic dorso- ventral muscles .....	111
Fig. 12a. Top view of the left half of the mesonotum with the line of buckling indicated (cross hatched) ..	112
Fig. 12b. Top view of the right half of the mesonotum with the insertions of the flight muscles indicated .....	112
Fig. 13a. Top view of the left side of the pterothorax ....	113
Fig. 13b. Top view of the right side of the mesothorax with the maximum upstroke positions indicated by solid lines, and the maximum downstroke positions indicated by broken lines .....	113



Fig. 14. Side view of the left side of the mesothorax with the maximum upstroke positions indicated by solid lines, and the maximum downstroke positions indicated by broken lines .....	114
Fig. 15a. Top view of the right fore wing .....	115
Fig. 15b. Top view of the right hind wing .....	115
Fig. 16. Top view of the right fore wing base with the levels and orientations of sections 16a and 16b indicated .....	116
Fig. 16a. Dorsoposterior view of a section through the right fore wing base just posterior to the first and second axillaries, and the radial plate .....	116
Fig. 16b. Posterior view of a section through the right fore wing dorsal subcosta, radial plate, ventral radius, and second median plate .....	116
Fig. 17. Top view of the right fore wing base with the levels and orientations of sections 17a and 17b indicated .....	117
Fig. 17a. Posterior view of a section through the right fore wing ventral subcosta, dorsal subcosta, ventral radius, and radial plate .....	117
Fig. 17b. Posterior view of a section through the right fore wing ventral subcosta, dorsal subcosta, ventral radius, and costal-subcostal	



	Page
margin .....	117
Fig. 18. Side view of the second axillary complex of the right fore wing .....	118
Fig. 19. Side view of the left mesothoracic basalar complex .....	118
Fig. 20. Dorsal view of the left mesothoracic first axillary and adjacent sclerites with the levels and orientations of sections 20a to 20e indicated .....	119
Fig. 20a. Section through the anterior median notal wing process-first axillary ligament .....	119
Fig. 20b. Section through the posterior median notal wing process-first axillary ligament .....	119
Fig. 20c. Section through the anterior first-second axillary ligament .....	119
Fig. 20d. Section through the posterior first-second axillary ligament .....	119
Fig. 20e. Section through the anterior arm of the first axillary .....	119
Fig. 21. Side view of the left mesothoracic scutum and basalar complex with the level and orientation of section 21a indicated .....	119
Fig. 21a. Section through the left mesothoracic scutum and basalar complex .....	119
Fig. 22. Dorsolateral view of the left mesothoracic	



	Page
first-second basalar hinge with the level and orientation of section 22a indicated .....	119
Fig. 22a. Section through the left mesothoracic first- second basalar hinge .....	119
Fig. 23. Posterodorsal view of the dorsal side of the third axillary complex of the right fore wing .....	120
Fig. 24. Dorsal view of the third axillary complex with the levels and orientations of sections 24a to 24c indicated .....	120
Fig. 24a. Section through the dorsal second axillary- first median plate ligament .....	120
Fig. 24b. Section through the first median plate- anterior third axillary articulation .....	120
Fig. 24c. Section through the anterior-posterior third axillary articulation .....	120
Fig. 25. Section parallel to the longitudinal axis of the insect through the left mesothor- acic wing base .....	121
Fig. 26. Dorsal view of the right mesonotum with the level and orientation of section 26a indicated .....	122
Fig. 26a. Inside ventrolateral view of the right side of the mesonotum .....	122
Fig. 27. Side view of the right mesothoracic	



	Page
laterophragma .....	123
Fig. 28. Side view of the right mesothoracic phragma with the laterophragma removed .....	123
Fig. 29. Dorsolateral view of the right mesothoracic laterophragma .....	123
Fig. 30. Mesothoracic right first axillary, dorsal subcosta, and anterior notal wing process viewed from a position above and towards the midline of the insect .....	124
Fig. 31. Top view of the right mesothoracic anterior notal wing process .....	124
Fig. 32. Cross-section through the mesothoracic first axillary-anterior notal wing process junction at the level of the resilin block .....	124
Fig. 33. Side view of the left mesothoracic notum and phragma with the levels and orientations of sections 33a to 33d indicated .....	125
Fig. 33a. Cross-section of the mesothoracic scutal-scutellar suture at a level about half way between the central axis and the lateral margin of the insect .....	125
Fig. 33b. Section through the left mesothoracic epimeral-laterophragmal articulation .....	125
Fig. 33c. Section through the dorsal end of the	



left mesothoracic phragma-scutal-scutellar articulation .....	125
Fig. 33d. Section through the ventral end of the left mesothoracic phragma-scutal-scutellar articulation .....	125
Fig. 34. Lateral inside view of the right mesonotum with the levels and orientations of sections 34a and 34b indicated .....	126
Fig. 34a. Section through the right mesonotum at the level of the base of the anterior arm of the laterophragma .....	126
Fig. 34b. Section through the right mesonotum at the level of the anterior tip of the anterior arm of the laterophragma .....	126
Fig. 35a. Diagrammatic top view of the mechanism of the mesonotum .....	127
Fig. 35b. Diagrammatic side view of the mechanism of the right side of the mesonotum .....	127
Fig. 36. Inside lateral view of the right mesothoracic pleuron and sternum .....	128
Fig. 37. Side view of the right mesothoracic pleuron with the levels and orientations of sections 37a to 37f indicated .....	129



	Page
Fig. 37a. Section through the right mesothoracic pleural region at the level of the furcopleural muscle .....	129
Fig. 37b. Section through the right mesothoracic pleural region at the level of the origin of the pleural-third axillary muscle .....	129
Fig. 37c. Section through the right mesothoracic pleural region at the level of the dorsal end of the origin of the pleural-third axillary muscle .....	129
Fig. 37d. Section through the right mesothoracic pleural region at the level of the proximal process of the second basalare .....	129
Fig. 37e. Section through the right mesothoracic pleural region at the level of the distal process of the second basalare .....	129
Fig. 37f. Section through the right mesothoracic pleural region at the level of the pleural wing process .....	129
Fig. 38. Inside lateral view of the right mesothoracic pleuron and sternum with the levels and orientations of sections 38a to 38e indicated .....	130
Fig. 38a. Section through the mesothoracic	



	Page
furcasternal region at a level immedi-	
ately ventral to the presternum .....	130
Fig. 38b. Section through the mesothoracic furca-	
sternal region at a level immediately	
ventral to the furcal blade .....	130
Fig. 38c. Section through the ventral region of	
the right mesothoracic furca .....	130
Fig. 38d. Section through the dorsal region of	
the right mesothoracic furca .....	130
Fig. 38e. Section through the right mesothoracic	
furcal-epimeral junction .....	130
Fig. 39. Side view of the left mesothoracic	
basalar complex and anepisternum with	
the hinge points of figs. 39a to 39c	
indicated .....	131
Fig. 39a. Diagrammatic representation of the side	
view of the left mesothoracic basalar	
complex and anepisternum .....	131
Fig. 39b. Diagrammatic representation of the front	
view of the left mesothoracic basalar	
complex and anepisternum .....	131
Fig. 39c. Diagrammatic representation of the top	
view of the left mesothoracic basalar	
complex and anepisternum .....	131
Fig. 40a. Diagrammatic representation of the left	



	Page
side of the mesothorax during the downstroke .....	132
Fig. 40b. Diagrammatic representation of the left side of the mesothorax during the upstroke .....	132
Fig. 41a. Diagrammatic representation of the left side of the mesothorax at the beginning of the downstroke .....	133
Fig. 41b. Diagrammatic representation of the left side of the mesothorax at the beginning of the upstroke .....	133
Fig. 42. Side view of the left tegula in position over the left fore wing base .....	134
Fig. 43. Diagrammatic representation of the front view of the left mesothoracic first and second axillary limiting positions in flight .....	135
Fig. 44. Side view of the mean left fore wing path for three individuals .....	136
Fig. 45. Mean variation of the frontal angle made by the wing to the ventral axis of a single insect with time .....	136



## 1. Introduction

The Lepidoptera are particularly good experimental animals for use in flight studies because their thoracic flight movements are large, and the wing beat frequencies of species in this order vary from very slow to the fastest representatives of the neurogenic flight system. The thorax of lepidopterans is more loosely articulated than that of other highly successful flying insects. This may reduce the dependence on the resonant characteristics of the wings and sclerites in the determination of the wing beat frequency. Such animals should be interesting subjects for the study of motor neuron impulse patterns.

Here I describe in detail the flight structures and their functions in *Agrotis orthogonia* Morrison. I place emphasis on anatomical and mechanical, rather than electrophysiological, studies. However, I must rely on electrophysiological studies in the literature to determine the patterns of muscle activity in flight. This study will permit the evaluation of the forces developed by the flight muscles in subsequent investigations. I could not obtain accurate estimates of the relative positions of the flight structures to each other in flight posture by the methods used. These estimates and the forces developed in the flight muscles will be the subject for further studies.



## 2. Literature Review

Hocking (1953), Weis-Fogh and Jensen (1956a), Boettiger (1957), and Pringle (1957, 1965, and 1968) all review the literature on insect flight. Wilson (1968) reviews specifically the topics of nervous control of insect flight. Greenewalt (1960) reviews the dimensional relationships for flying animals established by a number of authors. FitzPatrick (1952) provides a literature list on 'natural flight.'

For the purposes of this work two specific fields are of interest, the morphology of the lepidopteran thoracic wing mechanism, and the functional morphology of the flight system of any insect. Snodgrass (1935) and Imms (1964) provide the bases for the nomenclature used here for the flight structures. Berlese (1909) (*Herse convoluli* (L.)), Michener (1952) (*Eacles imperialis* Drury), Nüesch (1953) (*Telea polyphemus* Cramer), and Ehrlich and Davidson (1961) (*Danaus plexippus* L.) all describe muscles, muscular attachment, and to some extent the wing base and thoracic sclerites of lepidopterans. Nüesch's description is particularly complete for the thorax. Sharplin (1963a, 1963b) describes in detail the comparative morphology of the lepidopteran wing base and the thorax, and includes some ideas about the function of both muscular and cuticular parts. Even this very detailed paper contains inadequate information to explain completely the function of the wing mechanism of any one species. Sharplin (1963b, 1963c) includes references to the naming



systems used by earlier authors. Sharplin (1964) describes the wing folding mechanism of moths.

Kammer (1967) indicates the function of the muscles of a number of lepidopterans based on electrophysiological studies, and includes reference to the functions of lepidopteran muscles indicated by earlier authors. Kammer's work illustrates the inadequacy of electrophysiological studies alone. These functions presumably parallel Wilson's (1962) studies of muscle function in grasshoppers from which the muscle function of *A. orthogonia* at least does not follow exactly. Chadwick (1959) compares the furcopleural muscles of Lepidoptera, and notes the relatively small ratio of muscle to nonmuscular elements in the entire furcopleural element. Hence, he claims static bracing as the function of the furcopleural union. He misses the fact that because of the arrangement of the fibers of the furcopleural muscle, it is very powerful. Alexander (1968) provides a review of the basic properties of muscular contraction.

Snodgrass (1935), Smart (1959), and Tiegs (1955) all describe the functional morphology of the flight system of the Diptera based on anatomical studies. Ritter (1911) considered the mechanics of the dipterous system together with the anatomy. Boettiger and Furshpan (1952) first described the 'click mechanism' of the dipterous thorax from anatomical studies. Pringle (1957) expresses the ideas of Boettiger and Furshpan (1952) in a more easily understood fashion. Nachtigall and Wilson (1967)



confirm many of Ritter's (1911) conclusions electrophysiologically and show in addition that the furcopleural muscle is a main controller of wing beat frequency in dipterans.

Tiegs (1955) and Parsons (1960a) describe the anatomy of the flight system of a number of homopterans and base their description of function on anatomical studies. Barber and Pringle (1966) study the homopteran system electrophysiologically.

Tiegs (1955) describes the flight structure morphology and muscle function on the basis of anatomy of *Blattella germanica* L. Carbonell (1948) describes the flight structure anatomy of *Periplaneta americana* (L.) and Ewer and Mayler (1967) that of *Deropeltis erythrocephala* (Fabricius). Kammer (1967) describes the electrophysiological flight responses of the lateral oblique dorsal longitudinal muscle of *P. americana*.

Russenberger and Russenberger (1959) study in very great detail the function of the flight mechanism of *Aeschna cyanea* (Müller), a dragonfly. Their treatment of insect material by embedding and milling is a novel if not particularly useful approach.

Jensen and Weis-Fogh (1962) describe the physical properties of normal cuticle and the rubber-like cuticle resilin. Sharplin (1963a) describes a flexible cuticle in the wing bases of Lepidoptera, bending cuticle.



### 3. Methods and Materials

I studied only the male of *A. orthogonia* except as noted in section 4. I observed some of the movements of the wing base of live flying specimens, reared and field caught, with a dissecting microscope with micrometer and protractor eyepieces. A stroboscope illuminated the preparations. Brushing with a soft brush facilitated removal of scales. I brushed the anterodorsal section of the abdomen, the dorsal section of the metathorax, and the pleuron near the meron-epimeral suture to remove the scales (figs. 1 and 2), and spread a thin layer of wax (1:1 beeswax:rosin, 62C m.pt.) on these areas. I then applied these areas to a prewaxed mount, and reheated the applied wax with a fine heating wire. The insect was thus held firmly to the mount, or tethered. For photography I used a simple mount which attached to the dorsal region only.

Live tethered specimens, which flew into a head wind of about  $1\text{m}\cdot\text{sec}^{-1}$  provided by a small fan, were photographed from the front with a high-speed cine camera, and from the side by multiple flash and a single exposure camera. Dr. Sharplin and the University of Alberta photo services department carried out the high-speed cinematography with a 'Fastax' camera on a single specimen. The 'Fastax' camera accelerated the film from the beginning to the end of the film sequence. Thus the time intervals between the individual frames varied. To minimize this variation, I analysed only the last section of the film where



the film speed was greatest and its acceleration least. I measured wing angles to the ventral axis on individual frames. I took the wing angle along the stiff proximal 2/3 of the radial vein, throughout the wing beat cycle. The lowest wing angle in two adjacent downstrokes, approximated by extrapolation to the nearest millisecond, marked the beginning and end points of any cycle. I then plotted wing angle variation with frame number for 40 individual cycles. I divided each of the frame number axes arbitrarily into 10 equal units and obtained the average wing angle from each of the 10 units over the 40 cycles. The mean wing beat frequency for 20 tethered individuals, measured with a stroboscope, was 40 Hertz (Hz): a stroke cycle period of 25msec. I then set the 10 units equal to 25msec and plotted a curve of the mean wing angle for the 10 units with time (fig. 45).

The 'Fastax' camera was not available for further use, so I obtained the side view of the wing position in flight by another method. Photographs taken with an exposure time of 1/60sec and a stroboscope flash-rate of 360Hz produced an image of five to six successive wing positions. Since the exposure times were less than the wing beat cycle period, the wing positions were always adjacent to one another in the stroke cycle. I obtained a complete wing beat cycle for three individuals from several photographs of each individual. Fig. 44 shows the side view of the mean path for the three specimens



traced out by the distal end of a stiff extension of the stiff proximal 2/3 of the radial vein arbitrarily set at 15mm distal to the first axillary-subcostal ligament. By neither photographic method could I quantitatively estimate the angles of wing pronation or supination. Therefore I only indicate pronation or supination during the stroke (figs. 44 and 45).

I placed 10 of the fresh specimens in weak solutions of methylene blue (Weis-Fogh 1960) to test for the presence of resilin ligaments (resilin becomes sapphire blue in about 24 hours), and the remainder of the fresh specimens in 70% ethanol for all other studies. I examined the muscles by cross-section and sequential dissections of sagittally split preserved specimens. I examined the skeletal parts from the muscle preparations and from preserved specimens heated at 90C in 2% w/v aqueous potassium hydroxide for 45 minutes. I treated some of the specimens in each of the following ways:

1. The upper and the lower halves of the wing base were split apart and stained in Mallory's triple stain (Pantin 1948), dehydrated and cleared in xylene (Sharplin 1963b). The notum with the upper half and the pleuron with the lower half were mounted separately in Canada balsam.

2. Some of the specimens were soaked in a 1:1 polyvinyl lactophenol:glycerin (v/v) mixture for several days. So treated, the thorax and wing base could be flexed, to mimic the flight movements, without danger of cracking the cuticle.



3. The first and second axillary sclerites from one side of 10 specimens were dissected apart and mounted in Canada balsam for measurement. Each sclerite was removed from an insect of wing length 15mm (from the first axillary-subcostal ligament to the distal tip of the wing).

All other methods are indicated in section 4.



#### 4. Morphology and Function of the Flight Structures

##### 4.1 General description

I base the nomenclature used here for the integument on that of Snodgrass (1935), with the modifications of Sharplin (1963b) and Nüesch (1953) (table 1). Both Sharplin and Nüesch provide reference to the nomenclature of earlier papers. The style of figs. 1 - 4 is after that of Sharplin (1963b, 1963c), to facilitate comparison of *A. orthogonia* with her descriptions. As function is of prime interest here, I name the muscles by their origin-insertion in the sense of Snodgrass (1935), except for the longitudinal muscles. Table 2 lists the muscles with their abbreviations for *A. orthogonia* and those of Nüesch (1953) for *T. polyphemus*. Kammer (1967) provides reference to some of the other muscle nomenclature. Figs. 5 - 9 show sequential dissections of sagittally split specimens. I base each figure on at least five specimens.

I studied in especial detail the functional morphology of the mesothorax for a number of reasons. First, the metanotum and its musculature is greatly reduced. Fig. 13a shows the relative size of the mesonotum and metanotum. Fig. 5 shows the relative size of the first dorsal longitudinal ( $d_{11}$ ) muscle in these segments; the first dorsal longitudinal muscle mass is absent from the metathorax. Second, the fore wing overlaps the hind wing (fig. 13a) and certainly transfers power to the hind wing in the downstroke. On the upstroke the hind wing frenulum



(F.), which is coupled into a flap on the fore wing subcosta (Sc.), the retinaculum (Re.) (figs. 13a and 15a,b) also transfers power from the fore wing to the hind wing. Stiff hairs between the first and second cubital veins ( $Cu_1, Cu_2$ ) of the fore wing contact the hind wing only where the wings are folded. Third, the hind wing base has not paralleled the evolutionary development of its mesothoracic counterpart. It lacks the lever extending system of the medial notal wing process (m.n.w.Pr.) and the laterally enlarged first axillary sclerite (1Ax.) (Sharplin 1963b,c).

The metathoracic pleural and sternal regions are relatively less reduced than the notal parts (figs. 6-10). The metathoracic direct and indirect acting musculature is quite large (figs. 11c, 7-10), and must have a considerable power output. This must be the topic of further work.

Figs. 59 and 60 show the variation of wing position with time during the stroke cycle. Because the number of individuals used to obtain these curves was small (sect. 3) the curves represent only a first approximation of the wing position with time. Although the gross wing positions could be estimated from the photographs, the degree of pronation or supination could not. To observe in more detail pronation and supination, I studied tethered flying specimens with a stroboscope. In flight the angle of pronation is smaller than that of supination. The wing camber increases in the upstroke



but is at all times convex dorsally.

#### 4.2 The notum

##### 4.2.1. *Deflection of the notum*

Figs. 13b and 14 show the maximum flight deflection positions of the notum (N.). The values are relative to the transverse axis between the epimeral-furcal (epm.-fu.) junction on both sides, the central longitudinal axis parallel to the coxal-pleural (cx.-p.) suture, and the dorsoventral axis at right angles to the transverse and longitudinal axes. Contraction of the large first dorsal longitudinal muscles pulls the anterior end of the notum posteriorly. This deflects the notum so that its lateral margins rise and move distally. The greatest bending occurs along a line of buckling just anterior to the scutal-scutellar (sct.-scl.) suture (cross-hatched area fig. 12a). Contraction of the dorsoventral muscles deflects the notum such that its anterior end moves anteriorly, and its lateral margins move proximally and down. The line of buckling straightens. Some gross features of the notum contribute to this action.

The notum is indented on both sides near the anterior notal wing process (a.n.w.Pr.) (fig. 12a). This provides clearance for the wing base at the top of the upstroke. The corrugation so formed (figs. 12a, sects. A , B , and C ) also stiffens this region. The line of bending is just posterior to the indented area.

The maximum force a muscle fiber can produce is propor-



tional to its cross-sectional area, but reduces as it shortens (Alexander 1968). Therefore, the force produced by any muscle must be a function of the fraction of the total length of the muscle by which it has shortened. A long muscle produces the same force per unit of cross-sectional area as a short muscle over a larger displacement.

The individual muscle fasciculae of both the dorsolongitudinal and dorsoventral muscles vary in length (figs. 5, 6, and 7). The long muscles attach to regions of the cuticle which move the furthest, the short, to regions which move the least. Although the lateral oblique dorsal longitudinal (lat.obl.d.1.) muscle is active during the upstroke (Kammer 1967), it probably contributes little to the straightening of the notum. It is important in wing protraction and the maintenance of the wing in the protracted position (sect. 4.4.6).

The large indirect flight muscles (table 2, figs. 5, 6, and 7) attach to the dome-shaped notum over broad areas of the prescutum and scutum (fig. 12b). The cuticle of these areas is uniform in thickness, and flexible because the exocuticle is thin. Because the large indirect muscles do not taper significantly to their origins and insertions on the notum, tensions in the large indirect muscles place a uniform force distribution on these origins and insertions, whether due to passive elastic and inertial forces during stretching, or active forces of contraction. The upstroke and downstroke muscle forces are directed



at about  $70^\circ$  to each other, both towards the interior of the notal dome (figs. 5 and 6). Hence, the stress on the cuticle between the antagonistic muscle connections is small. However, the regions of maximum bending, the line of buckling and the anterolateral corner of the notum have little muscle attachment. The cuticle of the lateral margins of the notum is thickened (sects. 4.2.3. and 4.2.4.) and transfers the forces from the flight muscles to the wing and the remainder of the thorax. It also greatly influences the deflections of the notum.

#### 4.2.2. *The anterior margin of the notum*

The prescutum (Psc.) and scutum are continuous centrally but split laterally (fig. 26a). It should be noted that fig. 26a illustrates most of the notal margin because the anterior section has been folded distally. The first dorsal longitudinal<sub>a</sub> and the ventral part of the first dorsal longitudinal<sub>b</sub> muscle insert on the prescutum (fig. 26a), the remainder of the first dorsal longitudinal muscle inserts on the scutum (fig. 12b). The lateral arm of the prescutum has only muscle directed into the prothorax inserting on it except for the prescutal-basalar (psc.-ba.) muscle at the ventral tip (fig. 9). Also at the ventral tip, the lateral arm is attached to the subtegula (Stg.) by a resilin (Weis-Fogh 1960) ligament (figs. 2 and 26a). This ligament appears to be short when viewed from the side as in figs. 2 and 26a but is 0.28mm long.



The prescutum is stiffened to transverse bending because of its cross-sectional shape and a flange (figs. 5 and 26a) which splits the first dorsal longitudinal muscle insertion on the prescutum. Tensions developed in the muscle fibers tend to orient this flange parallel to the fibers. The flange stiffens the prescutum to its lateral edges where the flange and the bracing of the lateral arms is continuous (fig. 26a). The lateral arm itself is very stiff to bending in any direction because it is braced by its cross-section and its cuticle is thick. Membrane lightly bridges the incision between the prescutum, its lateral arm, and the scutum. This area acts as a hinge between the laterally stiff anterior margin and the bracing of the lateral margin of the notum. A small region of bending cuticle (Sharplin 1963a) at the anterior end of the prescutum-scutal incision acts as a transition zone between the membrane of the incision and the cuticle of the notum.

#### 4.2.3. *The anterolateral margin of the notum*

The anterolateral margin of the notum is truss-like (fig. 26a). Distally the upper member of the truss is formed by the 'U' cross-sectioned margin of the scutum, and proximally, the muscle-bearing part of the scutum (fig. 21a). The posterior end of the 'U'-shaped member tapers into the anterodorsal edge of the anterior notal wing process (fig. 31). Anteriorly the 'U'-shaped member increases in size, turns ventrally, and



tapers into the lower member of the truss (fig. 26a). A large block of resilin lies between the outer edge of the 'U'-shaped margin and the subtegula (fig. 21a).

The anteroventral margin of the truss is formed by a solid rod of cuticle (figs. 21a and 26a). This rod splits posteriorly to form part of two triangular braces (fig. 26a). The outer brace forms a deep triangle between the anterior edge of the anterior notal wing process and the scutum (figs. 26a and 31). The inner brace forms a shallow triangle with the dorsal member (fig. 26a). This brace narrows to a rod-like thickening which extends posteriorly into the notal incision where it ends in a swelling (fig. 26a). The proximal brace and thickening extends along the proximal edge of the anterior notal wing process.

The anterior section of the scutum along the lower region of the prescutum-scutal incision is thickened and takes on the curve of the anterolateral corner of the notum (figs. 26a and 12a). This, together with the ventrally directed anterior part of the 'U'-shaped upper member, forms a rigid cross piece between the upper and lower members of the truss (fig. 26a). A second cross brace lies posterior to this region and completes the first triangle of the truss. This brace takes the form of a thin triangle, with its short base fused to the upper member, and its apex fused to the lower member (fig. 26a). The second triangle of the truss is formed by this brace, the upper member, and the inner and outer braces (fig. 26a). A thin sheet of cuticle is



continuous with the cross braces, and with the upper and lower members of the truss (figs. 21a and 26a).

Figs. 12b and 26a illustrate the insertions of the muscles in the region of the anterior truss system. The origin of the tergo-basalar (t.-ba.) muscle extends from the apex of the split in the ventral member of the truss, to about half the distance along the outer brace. The anterior tergo-coxal (a.t.-cx.) muscle inserts anteriorly almost to the apex of the split between the braces. The distal end of the anterior notal wing process carries no muscle insertions, but is rigidly braced (fig. 31).

The anterior region of the truss hinges on the prescutum at an angle of  $130^{\circ}$  to the prescutum in dorsal aspect (figs. 12a,b), and is inclined out at its ventral edge  $10^{\circ}$  to the dorsoventral axis of the insect (fig. 21a). The hinge line, the prescutum-scutal incision, lies at  $49^{\circ}$  to the transverse axis of the insect in front view. The anterior region is stiffened dorsoventrally by its truss-like shape, and stiff to transverse bending along its axis by the cross-section of the upper and lower members of the truss, and by the 'L'-shaped cross-section formed by the truss and scutum (fig. 21a). Both contribute to the dorsoventral stiffness.

The anterior notal wing process region of the truss is also stiff dorsoventrally and transversely. In dorsal aspect the dorsal surface of the anterior notal wing process is convex anteriorly and concave posteriorly (fig. 31). The concave region



extends to the posterior end of the inner brace (fig. 12a), but is deepest in the region of the anterior notal wing process. The transverse corrugation of the scutum and anterior notal wing process, together with the inner and outer triangular braces, contributes to the dorsoventral stiffness of the anterior notal wing process region. The longitudinal axis of the anterior notal wing process corrugations lies directed posteriorly at  $65^\circ$  to the midline and that of the scutum, about  $90^\circ$  to the midline at the distal edges. Thus, the corrugations are important in transverse stiffness. Although the posterior edge of the anterior notal wing process is not braced, muscle insertions cover the ventral surface of the anterior notal wing process. This reduces the tendency of the anterior notal wing process to fold posteriorly and thus increase the transverse stiffness.

Posterior to the anterior notal wing process the lateral bracing is less rigid. It is at the posterior end of this region that the scutum becomes convex again. The line of buckling occurs in this region (fig. 12a). Initiation of buckling is from an area of bending cuticle (bd.Ct.) (Sharplin 1963a) at the posterior end of the notal incision (n.In.) (figs. 2, 12a and 26a). A ligament, the notal-median notal wing process ligament, extends between the anterior margin posterior to the anterior notal wing process and the median notal wing process (fig. 1).

#### 4.2.4. *Posterolateral margin of the notum*

The posterolateral margin of the scutum is stiffened to



bending, especially dorsoventrally, by a series of flanges (figs. 26a, 34a, and 34b). The stiffened region extends anteriorly at the ventral end of the notal incision into the median notal wing process (figs. 2, 16a, and 26a), and posteriorly to a region immediately anterior to the scutal-scutellar suture (fig. 26a). It is hinged at the line of buckling on the notum, and along its posterior edge. A single layer of thin cuticle composes the region between the stiffened margin and the scutal-scutellar suture. The scutal-scutellar suture is flattened centrally, expands to a 'T'-cross-sectioned region laterally (fig. 33a), and then becomes smaller (fig. 33c) and participates with the ventral margin of the scutellum in the formation of a triangular articulation for the phragma (Ph.) (figs. 26a and 27).

There is a ball and socket articulation formed by the phragma and scutum-scutellar socket dorsally (figs. 26a and 33c). Ventrally the ball and socket the phragma is flanged such that its anterior edge fits into a groove in the triangular scutal-scutellar process. A ligament connects the flange and triangular process ventrally (figs. 26a, and 33d). The membrane connection between the phragma and scutellum continues into the articulation (figs. 33c, and 33d).

The phragma is a large cupped sheet of flexible cuticle (figs. 2, and 26a), on which the first dorsal longitudinal muscles all originate (fig. 5). All power is transferred to the remainder of the notum through the lateral articulations (fig. 26a).



These articulations are at the dorsal ends of a hollow strengthening ridge (fig. 37a) which runs close to the periphery of the phragma. The strengthening ridge tapers to the surface of the phragma at the ventral end of the phragma. Posterior to the articulations, the phragma extends dorsally under the posterior end of the scutellum, and is attached to it by membrane (figs. 2 and 26a). The ventral end of the phragma extends deep into the thorax (fig. 2).

The postnotum, here the laterophragma (Lph.) and phragma, is a complicated structure made up of an acrotergite, and a prescutal element. The mesothoracic (acrotergite) half of both laterophragma and phragma is sclerotized, the metathoracic half is membranous except for the dorsal region where the metathoracic prescutum is separated from the phragma. Here the cuticle is sclerotized but thin. The mesaprescutum joins the phragma across the posterior side of the phragma and on each side along the lateral strengthening ridges (figs. 2 and 26a). The three-sided box-like shape of the metaprescutum stiffens it, but the meta-prescutum-metascutum junction is not stiff. The lateral extensions of the metaprescutum and the metascutum join along a strip of bending cuticle (fig. 3), but the remainder of the metaprescutum and metascutum junction is membranous. The remainder of the metathoracic-mesothoracic cuticular junction is also membranous.

The laterophragma (figs. 1, 2, 26a, 27 and 29) hinges on



the phragma, scutum, and scutellum. Only the anterior (acrosternite) side is sclerotized; the posterior side (metaprescutum) is membranous. The lateral sides of the sclerotized portion of the metaprescutum, which attach to the lateral sides of the phragma, carry the membranous connection between the central and lateral regions high, close to the ventral side of the mesoscutellum (figs. 28 and 29). A loop of bending cuticle (fig. 28) joins the dorsal ends of the two ridges which split dorsally from the peripheral ridge of the phragma (fig. 26a). This loop of bending cuticle extends anteriorly and distally (figs. 27 and 28). The membrane connection between the scutellum and phragma continues anteriorly interior to the bending cuticle (figs. 28, 33c, and 33d). The bending cuticle loop is braced dorsally and ventrally. The ventral brace continues at almost a right angle from a small region of bending cuticle, which separates it from the dorsal end of the posterior member of the split peripheral ridge of the phragma (fig. 29). The dorsal brace continues from the most dorsal of three ridges which split from the ventral margin of the scutellum at the phragma articulation (figs. 27 and 28). The braced dorsal arm of the laterophragma extends anteriorly (figs. 34a and 34b) and a 'V' cross-sectioned blade, ventrally (figs. 1, 2, 27, 29, and 33c). The lateral oblique dorsal longitudinal muscle (fig. 6) inserts on the ventral blade. The muscle insertion and the cross-section of the ventral blade stiffen it. A socket is formed at the anterior edge of the ventral blade-anterior arm angle into which the epimeron inserts.



(figs. 26a, 27, 29, and 33b). This junction completes the postalar bridge. The epimeron is held in the socket by a short strong ligament which joins the epimeron and dorsal arm of the laterophragma anterodistal to the socket (figs. 27, 33b, and 34a).

The metaprescutal apodeme (psc.Ad.) is a small cuticular disc which has a ligamentous connection to the posterior edge of the fused dorsal end of the epimeron and furca (fig. 27), not to the laterophragma as in many other Lepidopterans (Sharplin 1963c). Hence the muscle which inserts on this apodeme (p.-psc.ad.) probably functions as a tonic controller of mesothoracic posture, rather than as an antagonist for the mesothoracic lateral oblique dorsal longitudinal muscle as suggested by Sharplin (1963c). Nüesch (1953) refers to this muscle as mesothoracic, and possibly corresponding to the first tergo-pleural muscle in the metathorax, not as the spiracular dilator muscle as indicated by Sharplin (1963c).

Proximally there is a large sheet of bending cuticle between the dorsal arm of the laterophragma and the scutellum (figs. 1, 29, and 34a). At the anterior end of this sheet the posterior notal wing process (po.n.w.Pr.) hinges on the scutum (figs. 1 and 29). The posterior notal wing process is closely attached to the anterior tip of the laterophragma by a ligament (figs. 1, 2, and 27). A long thin ligament joins the ventral side of the anterior arm of the laterophragma to the subalare



(Sa.) (figs. 2, 27, and 29).

The central region of the scutellum protects the large heart underlying it. The third dorsal longitudinal muscle (fig. 5) originates on the anterodorsal edge of the phragma and inserts on the heart close to the scutum-scutellar suture.

#### 4.2.5. *Deflection of the margins of the notum*

Fig. 35a,b illustrates schematically the stiffened regions and hinges of the notal margin in the extreme up- and downstroke positions. All positions represented in figs. 13b, 14 and 35a,b and table 3 are the means of maximum values measured with a stroboscope on at least 10 flying individuals tethered in still air. Table 3 lists the amount of mutilation of specimens required to observe the various structures.

Contraction of the first dorsal longitudinal muscle in the downstroke pulls the prescutum and the anterior end of the scutum posteriorly. This bends the notum upwards centrally. The anterolateral margin of the scutum hinges dorsodistally about the prescutal-scutal incision. The angle to the transverse axis swept out by the anterior notal wing process (table 3, figs. 35a,b) is approximately the complement of the hinge angle to this axis. The posterolateral margin of the scutum hinges dorsodistally about an area of flexible cuticle between it and the scutal-scutellar suture. Midway along the posterolateral margin and at the posterior end of the anterolateral margin the two margins hinge upon each other. The hinge moves dorsodistally



as the notum bends along a line of buckling. The median notal wing process - first axillary junction extends past the line of buckling. Hence the dorsodistal movement of the posterolateral margin at its connection with the wing base is amplified (Sharplin 1963b).

The proximal end of the posterior notal wing process moves dorsodistally with the posterolateral margin. The ventral ends of the semi-circular scutal-scutellar suture, with the articulation and lateral arms of the phragma, widen slightly.

The phragma moves less than any other part of the notum relative to the remainder of the thorax, for five morphological reasons. First, I mounted the thorax by the epimeron and metanotum. The metanotum connects directly but not rigidly to the posterior side of the phragma (fig. 2), and to the epimeron through the laterophragma and lower membrane (sect. 4.3.2.). Second, the cross-sectional areas, and hence the forces produced by the first dorsal longitudinal muscle (Alexander 1968) which insert on the phragma, are equal dorsal and ventral to the articulation axis of the phragma (fig. 11a). Third, the ball and socket articulation allows some rotational, but little translational, movement. The flanged lower process stops the ventral end of the phragma from rotating anteriorly about the articulation. However, the angle of the articulation changes with the posterolateral margin of the notum. Fourth, the ventral end of the phragma is close to the gut, ventral nerve



cord, and metafurca. Any large movements of the phragma would abrade or interfere with these structures, and cause a large haemolymph displacement. Fifth, the heart attaches to the anteriodorsal edge of the scutellum, and the heart muscle (third dorsal longitudinal) to the dorsal edge of the phragma (fig. 5). Any large displacement of the dorsal edge of the phragma might break this muscle, since it is only about one third as long as the first dorsal longitudinals.

Contraction of the dorsoventral muscles during the upstroke straightens the notum, which is bent upwards centrally during the downstroke. Thus these muscles pull the lateral margins of the scutum ventroproximally about their respective hinge areas, the prescutum-scutal incision and the scutal-scutellar suture. The line of buckling straightens, and the median notal wing process- and anterior notal wing process-first axillary junctions also move ventroproximally. The prescutum and the anterior end of the scutum is pushed anteroventrally; the dorsal part of the scutal-scutellar suture, pulled anteriorly; and the ventral part, with the articulation and the lateral arms of the phragma, narrowed slightly. The scutellar margin tilts, moving dorsally at its posterior end.

The deformation of the notal cuticle during the up- and downstroke must store energy to be released during the adjacent portion of the stroke. I have not measured any parameters from which this energy could be estimated.



#### 4.3. The pleuron and sternum

##### 4.3.1. *Structure of the pleuron and sternum*

Figs. 2, 10, and 36 illustrate the main structural features of the pleuron and the sternum (S.). It should be noted that the pre-episternal (peps.) region and the region anterior to the pleural ridge have been folded anterolaterally in figs. 2 and 36 respectively. The musculature is shown in figs. 6-9, and 11a,b and the muscle origins and insertions in fig. 36. The origins of all the large dorsoventral muscles are located on sternal or coxal elements (fig. 36). Forces placed on these elements by tensions developed in muscles during flight must be transmitted through the pleural walls to the wing and notum. The pleural wing process is the ventral pivot for the wing (sect. 4.4.5.). It is the force couples, which the indirect and direct flight muscles can develop about the margins of the notum, the pleurites and the pleural wing process (p.w.Pr.), that move the wing in flight (sect. 4.3.4.). The pleuron and notum articulate anteriorly through the subtegula, and posteriorly through the epimeron and laterophragma (fig. 2).

The pleural ridge (p.Ri.) separates the episternum and epimeron. Dorsally it carries the pleural ridge-subtegular apodeme and the pleural wing process (figs. 2, 19, and 36). Ventrally it articulates with the coxa (fig. 36). The coxal suture (cx.Su.), an involution which divides the coxa and meron (Mer.), extends ventrally from this articulation to the



posteroventral corner of the coxa, immediately posterior to the coxal-trochanteral (cx.-tr.) articulation (figs. 19 and 36).

Both the pleural ridge and coxal suture are strengthening elements.

At its ventral end the pleural ridge is a simple flange which projects inwards at right angles to the pleuron (figs. 36 and 37a). Posterior to this flange an oblong cell in the epimeron wall surrounds the insertion of the furcal-pleural (fu.-p.) muscle (figs. 8 and 36). The ventral wall of the cell is a flange which tapers dorsoposteriorly from the pleural ridge into a shallow invagination (figs. 36 and 37a). This invagination deepens dorsally, and the ventral pleural ridge flange joins its inner wall (fig. 37b). Its outer wall forms the origin for the pleural-third axillary<sub>b</sub> (p.-3ax<sub>b</sub>) muscle (figs. 2, 19, and 37b). The inner flange of the pleural wing process attaches to its posterior edge and lies approximately parallel to the pleural wall (figs. 36 and 37b). Dorsal to the pleural-third axillary muscle insertion the invagination becomes shallow (fig. 37c), and disappears (fig. 37d). Anterior to this region the hollow pleural ridge-subtegular apodeme (figs. 21a, 36, and 37f) has been invaginated from the pleural ridge leaving a pit in the pleural ridge (figs. 19 and 36) (Sharplin 1963b). This pit has a hinge function in the basalar system (sect. 4.3.2., 4.3.3.). The ventral (fig. 37c) and dorsal edge (figs. 37d and 37e) of the pit are composed of thick stiff cuticle. The upper brace is continuous with the anterior edge of the pleural wing



process (fig. 36). The inner flange of the pleural wing process, which is not sclerotized, braces the posterior region of the pleural wing process, and forms the posterior margin of the pit (figs. 36, 37c, 37d, and 37e). The pleural wing process and pleural ridge-subtegular apodeme form a rigid unit. The anterior end of the pleural ridge-subtegular apodeme attaches to the ventral end of the subtegula by a tough flexible ligament (figs. 2 and 36). The subtegula is a stiff rod, 'U'-shaped in cross-section. The 'U'-shaped cavity forms the insertion for the pleuro-subtegular (p.-stg.) muscle, which originates on the pleural ridge-subtegular apodeme (figs. 8, 19, and 21a).

The coxa is suspended by membrane on the katepisternum (Keps.) from the coxal articulation with the pleural ridge dorsally to the coxal articulation with the sternocoxale (Stcx.) ventrally (fig. 36). A stiff flange-like apodeme interior and ventral to this membrane, the basicosta (Bc.) is the origin for the anterior coxal flight muscles on its dorsal surface (fig. 36). Two coxal muscles originate from its ventral surface and insert on the coxal suture. The sternocoxale bridges the ventral interior gap of the coxa. Anteriorly sternocoxale and coxa articulate; posteriorly they fuse (fig. 36). Centrally the dorsal edge of the sternocoxale articulates with the furcasternum (Fus.) (fig. 36). The coxa and trochanter articulate ventral to the sternocoxale (fig. 36). The trochanteral apodeme (tr.Ad.) or "median tendon of the trochanter" (Nuesch



1953) extends dorsally into the coxal cavity (fig. 36). This is the origin for all the trochanteral flight muscles (figs. 6-8 and 36).

Posterior to the coxal articulation with the pleural ridge, the meron and epimeron fuse (figs. 27 and 36). The posterior edge of the meron connects to the furcasternum, furca, and metathorax by membrane (figs. 36, 37a, 38a, 38b, 38c, and 38d). The meron is the origin for all the large flight muscles posterior to the trochanteral muscles (fig. 36). The epimeron has a slender thickened ridge extending dorsoposteriorly which fuses with the furca at a dorsal triangular plate (fig. 36). The central region anterior and posterior to the thickened ridge is membranous (figs. 2 and 36).

The presternum is a triangular plate reinforced centrally by the median ridge, laterally by the episternal ridge (eps.Ri.), and across its dorsal base by a ridge and the spinasternum (Ss.) (fig. 36). The episternal ridge extends dorsally between the preepisternum and the katepisternum (fig. 36). The presternum is the origin for the tergo-sternal muscles and the anterior part of the sternal-basalar muscles (fig. 36). At its ventral apex the presternum and its median ridge fuse to the furcasternum (figs. 36 and 38a).

The furcasternum is highly invaginated into the thorax. It lies dorsal to the articulations with the sternocostral sclerites in the form of a partial cylinder with lateral flanges



(figs. 36 and 38b). The furcal blade (fu.B1.) attaches to its anterodorsal edge (figs. 36 and 38c). Dorsal to the blade the two lateral furcae branch from their common base, the furca-sternum (figs. 36 and 43). The ventral regions of both furcae are tubular (figs. 36 and 38c). Anterodorsally the tubular region accepts the apodemes from the prothoracic first ventral longitudinal (I v<sub>1</sub>) muscle (figs. 5, 8, 36, and 37a); posteriorly it accepts the mesothoracic first ventral longitudinal (II v<sub>1</sub>) muscle (figs. 5 and 36). Above the tubular region the furca is 'U'-shaped in cross-section (figs. 36, 38d, and 38e). The metathoracic furcal-basalar (III fu.-ba.) muscle originates in the ventral part of the 'U'-shaped cavity (figs. 7, 36 and 38d).

The dorsal end of the furca fuses to the epimeron at a dorsal triangular plate (fig. 27). The dorsal apex of this triangle forms a head which fits into the socket articulation of the laterophragma (figs. 27, 29, and 33b) (sect. 4.2.4.). A ligament between the anterior edge of the triangle and the ventral edge of the laterophragma holds the head in the socket. The axis of this articulation lies in the anterodistal plane at 70° to the longitudinal axis of the insect. Immediately below this articulation the metathoracic prescutal apodeme attaches to the posterior surface of the furca by a short ligament (figs. 2, 9, 27, and 36). The large pleuro-subalar (p.-sa.) muscle originates on the anterolateral surface of the



triangular plate (figs. 9 and 36).

From the coxal articulation to the dorsal end of the oblong cell of the epimeron, the pleural ridge fuses to the katepisternum, anepisternum (Aeps.), epimeron, and the thickened margins of these areas (figs. 2 and 36). The katepisternum and preepisternum fuse along the episternal ridge (fig. 36). Membrane separates the anterior region of the katepisternum and anepisternum but they fuse posteriorly (figs. 2 and 36). A large thickened ridge extends along the ventral and anterior margin of the anepisternum. This ridge turns ventrally close to the pleural ridge and becomes smaller as it tapers into the ventral edge of the katepisternum (figs. 5 and 36). The anterior edge of the anepisternum and an apodeme known as the basalar tendon cap (ba.Te.) (Nüesch 1953) fuse along the dorsoanterior ridge (fig. 37c), which is continuous with the ventral ridge of the anepisternum. A thin strip of hard but flexible cuticle joins the first basale and anepisternum along the dorsoanterior edge of the anepisternum (fig. 21a). A strip of bending cuticle separates the anepisternum from the anterodorsal edge of the pleural ridge (figs. 2 and 36). The epimeron is membranous posterodorsal to its contribution to the pleural ridge (figs. 2 and 36).

#### 4.3.2. *The pleurites*

The large subalar pleurite lies along the membranous upper edge of the epimeron (figs. 2 and 36). All of the subalar musculature inserts on an apodeme known as the subalar tendon



cap (sa.Te.) (Nüesch 1953) (figs. 8 and 36). The fibers of the large coxosubalar (cx.-sa.) muscles extend dorsoventrally approximately parallel to the pleural ridge. The pleurosubalar muscle fibers extend anteroposteriorly (fig. 8). A dorsal ridge with an anteriorly directed projection extends anterodorsally from the tendon cap (figs. 2 and 36). It supports the major subalar ligaments to the ventral second axillary sclerite and the pleural wing process. The pleural-third axillary<sub>b</sub> muscle passes under the inner surface of this ridge and projection. A thin round ligament connects the posterior tip of the subalare to the anterior arm of the laterophragma (figs. 27 and 29). The central region of the subalare is indented (fig. 2). This provides clearance for the posterior notal wing process and the posterior third axillary sclerite when the wings are folded or near their maximum downstroke position (figs. 10 and 29), and increases the area of insertion for the subalar dorsoventral muscles.

The basalar pleurites lie at the dorsal edge of the episternum (figs. 2, 19, and 36). The anepisternum and the first basalare are not separated anteriorly, but lie at right angles to each other in the frontal plane (fig. 21a). Membrane separates the first basalare and the second basalare from the anepisternum posteriorly (figs. 2, 19, and 36). A sheet of bending cuticle extends along the dorsal edge of the anepisternum to this membrane. The bending cuticle then tapers posteroventrally



along the anepisternal-pleural ridge junction (figs. 2, 19, and 36).

The first basalare and its tendon cap (figs. 21a and 36) receive the insertions of the basalar muscles (figs. 7, 11, and 36). The fibers of the dorsoventral basalar muscles extend approximately parallel to the pleural ridge; those of the prescutal-basalar anterodorsally from the basalare to the prescutum and tergobasalar muscles posterodorsally from the basalare to the lateral brace of the anterior notal margin (fig. 7). The first basalare is stiff longitudinally by virtue of its cross-section (fig. 21a), but the proximal wall of the basalar tendon cap is endocuticular and flexible.

A complex bending-cuticle hinge joins the first basalare and second basalare (figs. 19, 22a, 36, 37d, and 37e). A ligament, the ventral subcostal-basalare ligament, extends dorsodistally to the ventral subcosta from the dorsal edge of the second basalare immediately posterior to the hinge (figs. 2 and 19). This ligament transfers most of the power from the basalares to the wing base (sect. 4.3.3. and 4.4.5.). The posterior end of the second basalare is split into two processes; the distal one is hollow, and its cuticle thin and flexible, and the proximal one is solid and its cuticle thick and rigid, from the first basalar-second basalar hinge to its posterior articulation (figs. 19, 37d, and 37e). A second ligament, the ventral radial-second basalar ligament, extends dorsally to the



ventral radius from the posterodorsal end of the flexible distal process (figs. 2 and 19). This ligament and process place a moment about the axis of the second basalare (sect. 4.3.3.), but contribute little to power transfer. It is important to the function of the proprioceptive system (sect. 4.4.5.). A resilin ligament connects the posterior tip of the rigid proximal process to a cup-shaped receptacle in the invaginated pit of the pleural ridge at the base of the pleural ridge-subtegular apodeme (figs. 19, 36, and 37d).

#### 4.3.3. Deflection of the pleurites

I neither measured nor observed in detail the movement of the pleurites of *A. orthogonia*. I observed two other species of noctuids, four specimens of *Euxoa ochrogaster* (Guenée) and two specimens of *Chorizagrotis auxiliaris* (Grote). I used these specimens because they were available and very similar to *A. orthogonia* in size, structure, and movement of flight structures. I observed tethered flying specimens with a stroboscope. Table 3 lists the means of the limiting positions of the pleurites.

Kammer (1967) reports that the large dorsoventral subalar muscles in a number of lepidopterans are electrophysiologically active during the downstroke at about the same time as the first dorsal longitudinal muscles. I observed the subalare moving ventrally approximately parallel to the pleural wall, but obliquely to the pleural ridge (table 3) during the downstroke.



The subalar muscles act directly on the wing base through the subalare and the large ligaments to the ventral second axillary sclerite (fig. 2) (sect. 4.4.5.). The cross-sectional area of the subalar muscles of one side is slightly larger than 1/4 that of the first dorsal longitudinal muscles of one side (figs. 11a, b). Because of their direct mechanical advantage on the wing base (sect. 4.4.5.) and their relative size, they contribute significantly to the downstroke power. As well, the large pleurosubalar and the dorsoventral subalar muscles apply an anteroventral force to the epimeron-furca, and a ventral force to the laterophragma through the subalar-laterophragmal ligament (figs. 2 and 31) (sect. 4.3.4.). The tensions developed in the ventral second axillary sclerite ligaments, and the subalar muscles, do not have the same line of action (figs. 2 and 36) and so create a moment about subalare. The pleural-subalar muscle produces a moment of opposite sense and determines the position of the triangular dorsal epimeron-furca junction (sect. 4.3.4.). The upstroke muscles through the wing base, the ventral second axillary sclerite (sect. 4.4.5.), and the laterophragma (sect. 4.3.4.), apply a restoring force to the subalare during the upstroke.

Figs. 39a, 39b, and 39c illustrate the approximate limiting positions of the parts of the basalar complex as lettered in fig. 39. AB represents the region where the first basalare and anepisternum fuse; AC represents the first



basalare; CGD, the second basalare; F, some point on the ventral subcostal-basalar ligament; GF, part of the ventral subcostal-basalar ligament; and AE, the anterior edge of the anepisternum. AB, C and D are the hinges. The cross-sectional area of the basalar muscles of one side is about one-fourth that of the first dorsal longitudinal muscles of one side (fig. 11a,b). As in the case of the subalar muscles, the basalar muscles contribute significantly to the downstroke power because of their size, and the leverage by which their power is applied to the wing base (sect. 4.4.5.). Contraction of the dorsoventral basalar muscles during the downstroke places a force on ABC which is directed ventrally, and slightly posteroproximally. The muscle fibers of the sternobasalar and coxobasalar muscles, which insert on the distal side of the first basalare, are shorter than those on the proximal side. The fibers of the dorso-ventral basalar muscles which insert on the anterior end of the first basalare are shorter than those of the posterior end (figs. 8 and 36). Since a long muscle can produce the same force as a short muscle per unit cross-sectional area, over a larger contraction displacement (sect. 4.2.1., Alexander 1968), contraction of the basalar muscle produces a moment which moves the proximal side of the first basalare more ventrally than the distal side, and the posterior end more ventrally than the anterior. Any other moment placed on the first basalare stretches the muscle fibers unequally, and the muscles produce an opposing moment. However,



the cuticular parts of the basalar complex determine the path of C during the contraction of these muscles.

During the downstroke, ABC rotates ventroproximally about its axis, AB (figs. 39, 39a, 39b, and 39c). The endocuticle and exocuticle of AB is thin and bellows-like in cross-section (fig. 21a), which permits AB to be pulled ventrally about the anepisternum wall as ABC rotates. Both actions require little force to bend the cuticle. The cuticle of the proximal wall of the basalar tendon cap is very flexible, and is probably readily bent proximally by the basalare muscles as ABC rotates.

ABC hinges on CGD at C. C rotates ventroproximally, and slightly posteriorly during the downstroke (figs. 39a, 39b, and 39c). Although all of the hinge cuticle at C is bending cuticle, most of the bending is along a region of thin cuticle (figs. 22a, 37d, and 37e), which lies at approximately a right angle to the path followed by C in flight. AC and CD may rotate on C independently about their longitudinal axis by about 15°. A flap of cuticle, which extends posteriorly into the hinge from the most proximal flange of the first basalare (fig. 22a), limits the hinge movement when C is in a ventroproximal position. At this position C may move further only if the points A or D move, or if ACD rotates as a unit about AD. The latter requires that AC rotate about its longitudinal axis. Moments produced by the basalar muscles, and the moment required to twist ABC, limit the amount ABC rotates. The anterior edge of the anepisternum,



and the anterior end of the basalar tendon cap join along a ridge, AE (Figs. 37c and 39), to which the anterior end of ABC fuses. This ridge bends about the dorsoventral axis of the anepisternum to allow lateral movement of ABC, and ABC bends about the upper edge of the ridge to move dorsoventrally. However, the upper ridge and the upper edge of the anepisternum and basalar tendon cap limit the amount ABC rotates about its axis AC. ABC is resistant to twisting and bending by its cross-section (Fig. 21a).

I assume CGD (second basalare) lies in a plane parallel to the dorsal axis in Figs. 39a, 39b, and 39c. Although this is not strictly true in the flying insect, CGD remains approximately in this plane for a number of reasons. The torsion developed in ABC, and transmitted through C, and the torsion developed in the resilin ligament at C, limit the rotation of CGD about CD. Tension in the ventral radius - second basalar ligament, which acts on the distal process of the second basalare, produces a moment about CD which tends to rotate G proximally, and the ventral end of the distal process distally. A ventrally directed force produced by the tegula, which lies on the distal process of the second basalare (sect. 4.4.5.), produces a moment of opposite sense. Thus, it reduces the moment produced by this ligament. The ventral subcostal-basalar ligament, GF, sags during the upstroke, but at the beginning of the downstroke it snaps taut by the rotation of the wing base (sect. 4.4.5.), and remains



taut throughout the downstroke. However, the angle which GF makes to CD in the ventral plane is small (fig. 39c), hence GF produces only a small component of force which may produce a moment on CGD about CD. This moment is of the opposite sense to that produced by the ventral radial-second basalar ligament at the top of the downstroke. CGD is rigid by the thickness of its cuticle.

The central region of C bends ventrally slightly under the tension developed by the dorsoventral basalar muscles, which reduces the distance between A and C. Throughout the stroke, the distance between C and D remains approximately constant, because CGD is rigid except for the region of bending cuticle at C. D moves anterodistally as the pleural ridge-subtegular apodeme and pleural wing process rotate in the down-stroke (sect. 4.3.1.). A moves ventrally about its bellows-like connection to the anepisternum. The reaction at A, due to forces developed on the basalar complex, twists the dorsoanterior end of the anepisternum proximally slightly, particularly after the hinge limit of C has been reached. As the length between A and D decreases, the angle ACD increases. However, most of the motion of C is due to the rotation of ACD about AD. CGD carries G anteroproximally as C rotates ventrally (figs. 39a, 39b, and 39c). Because the angle between the ventral subcostal-basalar ligament, GF, and CGD is small in the anterodistal plane (fig. 39c), because CGD is much more rigid than AC, and because



the pleural ridge is more rigid than the anepisternum, the reaction force of CGD produces a large part of the posteriorly and distally directed components of the tension in GF at G.

Tension in the prescutal-basalar muscles and tergobasalar muscles, the elasticity of the anepisternal cuticle, and to a small extent tension in the ventral subcostal-basalar and ventral radial-second basalar ligaments, return the basalar complex to its position at the top of the downstroke, during the upstroke. Both ventral subcostal-basalar and ventral radial-second basalar ligaments were cut on two specimens of *C. auxilaris*. In flight, the basalare sclerites returned to their normal upstroke positions. When the prescutal-basalar and tergal-basalar muscles were cut as well, the basalares returned only about 10% of the distance to their former top of the stroke positions in flight. But, when flight stopped, the basalares were returned to their normal resting position, close to the top of the stroke position, by the elasticity of the cuticle.

#### 4.3.4. Deflection of the pleuron and sternum

Figs. 13b and 14 and table 3 illustrate the notal and relative pleural wing process maximum up- and downstroke positions. I estimated the pleural wing process positions from three sets of observations with a stroboscope, on tethered individuals flying in still air. In the first two sets of observations the insects were mounted by the abdomen and epimeron; in the third set, by the epimeron only. I observed all specimens



from the side opposite to the epimeron mount. First, I removed the wing and all but the first and second axillary sclerites (figs. 1 and 2) of the wing base from one side of four specimens. This left the pleural wing process unobscured during the complete cycle except for the lateral view of the maximum downstroke position. This I estimated.

Second, I removed the wing and wing base from one side of five specimens. This left the pleural wing process unobscured during the complete cycle. In the first and second cases the mutilation reduced wing stroke amplitude and frequency of the other side by about 15%. It also increased the difficulty of initiating the maintaining flight activity. Tiegs (1955) and Sotavalta (1954) show that reduction of wing base loading by partial removal of wings in noctuids increases their wing beat frequencies. Roeder (1951) reports a decrease in wing beat frequency for *Agrotis* when all of the wings were removed close to the thorax. These results and those for other lepidopterans (Kammer 1967) are dependent on the change in wing loading and the extent of removal of the wing receptors (Kammer 1967). Increases in wingstroke amplitude are also associated with wing loading reduction in lepidopterans (Kammer 1967). Asymmetrical wing loading and loss of all sensory receptors for one wing may explain my findings. When I cut only the subalar muscle from one side on four specimens of *A. orthogonia*, the wing beat frequency was reduced by an average of 10%. When I cut only the



ventral subcostal-basalar ligament on five specimens of *A. orthogonia*, the wing beat frequency was reduced by an average of 20%. Asymmetrical muscle loading may also be an important factor which determines wing beat frequency in these experiments.

Third, I observed two other species of noctuid, two specimens of *E. ochrogaster* and two specimens of *C. auxiliaris*. Only the tegulae (fig. 13a) were removed from these specimens, hence the wing in its lowest positions in the stroke cycles obscured the pleural wing process. I estimated the maximum downstroke positions from front and oblique views. The values obtained by the first two methods were smaller than those of the third. I use the mean value obtained by the third method in figs. 13b, 14, 35a, 35b, and table 3 because the performance of the specimens was less changed by experimental conditions than in either of the first two methods. I base the function of the various muscles and structures on their morphology, but observed directly the movements of the pleural ridge, subtegula and the upper regions of the pleuron on flying individuals illuminated by stroboscope.

Figs. 40a and 40b represent a much simplified model of the pleuron, sternum and notum. Points ABCD lie in the plane of the page, E above the page. AB, BC, CD, DA and DE are stiff two-force members which represent the anterolateral margin of the scutum, epimeron, pleural ridge-subtegular apodeme, and pleural ridge respectively. In the model, the wing base lies between BE and F.



This and the wing form a stiff unit. E is the articulation of the wing base to the pleural wing process; F, the point where the subalar and basalar ligaments attach to the wing base. A,B,C,D, and E are frictionless joints.

The tension which acts between A and C (fig. 40a) represents the tension developed during the contraction of the indirect downstroke first dorsal longitudinal muscle. The tension, which acts between D and F, represents the tensions developed by the direct downstroke muscles, the dorsoventral and the subalar and basalar muscles. Under these tensions A and C move together; B and D, apart. DE moves ventrally with D. The wing rotates downwards as the wing base hinges about B and E. Therefore, the force couples produced at B and E by the first dorsal longitudinal muscles, and at B and F by the basalar and subalar muscles, must be larger than the sum of the force couples required to stretch the now passive indirect dorsoventral muscles between B and D, and to overcome the inertial and aerodynamic moments of the wing. Because I assume the wing produces lift, and because the cross-sectional area of the first dorsal longitudinal muscles is about twice as large as the sum of the cross-sectional areas of the basalar and subalar muscles, I assume DE to be in tension under the action of the first dorsal longitudinal muscles as well as DF. In both the up- and downstroke cases an external system constrains the anteroposterior movement of the wing and E and D remain in the plane of the page, in equilibrium



laterally, because for any lateral component of force produced by DE at D, which is directed out of the plane of the page, the symmetrical system for the other wing produces an equal and opposite component of force.

The tension, which acts between B and D (fig. 40b), represents the tension developed during the contraction of the indirect dorsoventral muscles. Under this tension, B and D move together, A and C apart. DE moves dorsally with D. The wing rotates upwards as the wing base hinges about B and E. Therefore, the sum of the force couples produced at B and E by the indirect dorsoventral muscles, and the aerodynamic moments of the wing, must be larger than the sum of the force couples required to stretch the now passive first dorsal longitudinal, subalar, and basalar muscles, and overcome the inertial moment of the wing.

In the insect none of the joints A,B,C,D, or E are frictionless, nor are any of the members true two-force members. The tensions developed in the first dorsal longitudinal muscles place a distributed load on AB, but a concentrated load on C; those developed in the dorsoventral muscles place distributed loads on AB and DC; those developed in the dorsoventral basalar and subalar muscles, a distributed load on DC; and those developed in the prescutum-basalar and tergo-basalar muscles, a distributed load on AB. The movements of the notum are described in section 4.2.5. The hinge at A corresponds to the subtegular



hinge; at B, to the line of buckling; and at C, to the latero-phragma and phragma articulations. The epimeron mount holds DC stationary, hence A and B move dorsoposteriorly during the down-stroke. Since the plane of the page represents a sagittal section of the insect, the motions of B (fig. 35a) and D (figs. 41a and 41b) are not in the plane of the page but above it. Symmetrical lateral components of force from both sides of the insect, which act across the prescutum and phragma, hold A and C in equilibrium laterally.

Added to the forces which the active muscle tensions must overcome to move the wing and stretch the passive muscles are the forces required to bend the cuticle at A,B,C, and D in the latter part of each stroke. At the beginning of each stroke, the elastic recoil of the cuticle deflected in the latter part of the preceding stroke contributes a force in the same sense as that which the active muscles are producing. The forces produced by the deflection of the cuticle at B and D act at A and C on a line between AC. Gravitational forces, and the inertial forces of the parts of the system other than the wing, are small and will be neglected here.

During the downstroke, the proximal and distal members of the force couple at the wing base produced by the inertial and aerodynamic moment of the wing, and tensions developed in the passive dorsoventral muscles and active dorsoventral basalar and subalar muscles, place approximately ventrally directed



forces on ABC, and dorsally directed forces on ADC. A and C move together by tension in the first dorsal longitudinal muscles. Hence, hinges at A and C are held in compression dorsoventrally.

During the upstroke, the force couples of the wing base produced by the aerodynamic moment and tension placed on ABC and ADC by the dorsoventral muscles again act approximately ventrally on ABC and dorsally on ADC. The dorsoventral compression of A and C depends upon the resisting tension between A and C. At the beginning of the upstroke, the elastic recoil of the cuticle is large. Since elastic tension developed in passive muscle depends upon the relative extension of the muscle (Alexander 1968), the elastic tensions developed in the first dorsal longitudinal and dorsoventral basalar and subalar and pleural-subalar muscles are small because the muscle length is at its smallest value. The dorsoventral components of force which compress A and C are small. Later in the upstroke, when the cuticle must be deformed, the elastic tensions developed by the muscles are larger because the muscle length is close to its maximum value. Hence, dorsoventral components of force which compress A and C are larger than earlier in the stroke.

During the contraction of the indirect downstroke muscles, the anterolateral margin of the scutum moves dorsoposteriorly, and rotates dorsodistally about the distal ends of the prescutum (sect. 4.2.5.) (figs. 35a and 35b). The anterolateral margin carries the dorsal end of the subtegula with it. Since the



subtegula lies close to the prescutal hinge, it moves distally very little, but moves dorsoposteriorly with the prescutum. The lower end of the subtegula drives the pleural ridge-subtegular apodeme posteriorly, but rotates anteriorly itself because tension in the basalar and subalar muscles and in DE place a dorso-anteriorly directed force at A, and a dorsoposteriorly directed force at C on ADC. This twists the resilin subtegular-notal ligament, and stretches the resilin prescutal-subtegular ligament. As the prescutum moves dorsoposteriorly, the tension developed in the prescutal-subtegular ligament increases and pulls the subtegula - pleural ridge - subtegular apodeme junction slightly proximal.

During the contraction of the indirect dorsoventral muscles, and in the resulting deflection of the notum, the anterolateral margin of the scutum moves ventroanteriorly, carrying with it the dorsal end of the subtegula. The subtegula - pleural ridge apodeme - subtegula angle increases because the anterolateral margin of the scutum moves further anteriorly than the pleural ridge - subtegular apodeme and the lower end of the subtegula. The elastic resilin subtegular-notal and prescutal-subtegular ligaments release the energy stored by their deflection in the downstroke, into the system during the first part of the up-stroke. During the last part of the upstroke, the ventral region of the subtegula twists further posteriorly, which twists the subtegular-notal ligament and stretches the prescutal-



subtegular ligament. These ligaments release the energy thus stored in the first part of the downstroke. The proximal force, placed on the ventral end of the subtegula by the prescutal-subtegular ligament tension, initiates rotation of the pleural wing process and pleural ridge - subtegular apodeme unit on the pleural ridge at the end of the upstroke, and increases this rotation towards the end of the downstroke.

I observed no activity of the pleurosubtegular muscle in most of the flying specimens. However, several specimens exhibited either tonic or phasic activity. With tonic activity, the contraction of the pleurosubtegular muscles rotated the ventral end of the subtegula anteriorly at the initiation of flight. This reduced the subtegula - pleural ridge apodeme - subtegular angle, and its variation in flight. At the cessation of flight, the subtegula slowly rotated to its resting position. With phasic activity, the contraction of the pleurosubtegular muscles reduced the subtegula - pleural ridge apodeme - subtegular angle during the downstroke only. The increased subtegula - pleural ridge apodeme - subtegular angle decreases the deflection of the pleural wall and the pleural wing process, but increases the tension and torsion, and hence the energy stored, in the prescutal-subtegular and subtegular-notal ligament during the downstroke. The upstroke is unchanged. With tonic activity, during the upstroke, deflection of the pleural wall and pleural wing process increases, but little storage



of energy by either ligament takes place. The prescutal-subtegular ligament releases the increased amount of energy it stores during the downstroke into the upstroke cycle, but the subtegular-notal ligament does not.

The hind wing base covered much of the laterophragma in any of the intact specimens that I studied. For this reason I rely on the morphology of the laterophragma system to explain its function. Sharplin (pers. comm.) first noted that if the ventral blade of the laterophragma was pressed proximally in a freshly killed specimen with its wings retracted, the wings protracted. Thus the laterophragma has other functions than simply providing a posterior hinge about which the notum and pleuron may rotate. The function of the laterophragma is described below; its effects on the wing, in section 4.4.6.

The laterophragma rotates about the axis of its laterophragma epimeron-furcal junction on the ball and socket, and ligament connection anteriorly, and the laterophragmal-phragmal and scutal-scutellar hinge posteriorly. The force couple, which can be developed about this articulation, requires that for any other rotation, the triangular plate formed by the dorsal end of the epimeron-furca must twist, or the area between the scutal-scutellar and the laterophragma articulation must bend sharply. Neither is likely. The lateral oblique dorsal longitudinal muscle contracts during the upstroke (Kammer 1967). The proximal force thus developed on the ventral blade of the laterophragma



rotates the anterior arm, which lies at  $50^{\circ}$  to the laterophragma hinge line, dorsodistally about this hinge. The anterior tip of the arm carries the posterior notal wing process with it, and stretches the subalar-laterophragma ligament. The posterior notal wing process hinges about its articulation with the scutum. The posterior region of the laterophragma twists about the scutellum, and the bending cuticle hinges on the phragma. As noted earlier, during the upstroke the dorsoventral compressive forces developed about the laterophragma hinge are small. The posterior components of force on both scutal-scutellar and epimeron-furcal sides of the laterophragma hinge, due to the elastic recoil of the cuticle, and the passive stretching of the first dorsal longitudinal, subalar, and basalar muscles, are small, approximately equal in magnitude, and act in the same direction. The moment arm about which the forces may act on the laterophragma epimeron-furcal hinge is also small. Therefore, the moments developed on the laterophragma by the reactions about the laterophragma epimeron-furcal hinge are small and have little effect.

During the downstroke the laterophragma rotates so that its tip moves ventroproximally, which stretches the passive lateral oblique dorsal longitudinal muscles, and rotates the posterior notal wing process ventrally about its hinge on the scutum. Moments developed about the laterophragma epimeron-furcal hinge from four sources contribute to this rotation. First, the



subalare moves ventrally. The tension developed in the subalar-laterophragma ligament pulls the anterior tip of the laterophragma ventroproximally. Second, the cuticle of the laterophragma, between the laterophragma-epimeral hinge and the scutellum, which was twisted in the upstroke, recoils. This twists the anterior arm of the laterophragma ventroproximally. Third, the contraction of the first dorsal longitudinal muscles tends to move the scutal-scutellar suture anteriorly, but must first overcome the forces required to bend the notal and pleural cuticle, and the force, which acts dorsoposteriorly at the laterophragma, produced by the subalar and basalar muscles. Thus, although a net anteriorly directed force acts on the scutal-scutellar suture, a posteriorly directed one acts on the dorsal end of the epimeron-furca. Since the scutal-scutellar connection to the laterophragma lies more dorsally than the epimeron-furcal connection, the forces produce a moment which contributes to the ventroproximal rotation of the anterior tip of the laterophragma. Fourth, the downstroke forces compress the laterophragma articulation. However, the couple, produced between the ligament and ball and socket articulation at the laterophragmal epimeron-furcal junction, stops the laterophragma from rotating dorsally appreciably under the action of the downstroke forces.

Between the subtegula and laterophragma, the pleural and sternal regions consist of two stiff units, which hinge upon each other. The pleural ridge-subtegular apodeme and pleural wing



process make up the anterior unit. The pleural ridge-subtegular apodeme is a straight, sclerotized thick-walled tube (figs. 21a and 37f). It resists bending under compression or torsional forces by its shape. The cuticle of the pleural wing process is thick, curved in cross-section, and heavily sclerotized (figs. 37d, 37e, and 37f). It resists bending under compressive and laterally or anteroposteriorly directed forces. A thick endocuticular flange continues from the posterior edge of the pleural wing process ventrally on the posterior side of the pleural ridge (figs. 36, 37b, and 37c). Although the cuticle of this flange is not sclerotized it is stiff enough to prevent the pleural ridge-subtegular apodeme and pleural wing process from bending posteriorly over the dorsal part of the pleural ridge. The pleural ridge-subtegular apodeme and pleural wing process together form a rigid unit which does not deform in flight, but twists on the pleural ridge just dorsal to the reinforced cell in the epimeron, which surrounds the furcopleural muscle insertion (fig. 36). The pleural and sternal regions, which attach to the pleural ridge below the area of the pleural ridge which twists, form the posterior unit.

Anterior to the laterophragma articulation the posterior unit splits into two sections. The distal, the epimeron, extends anteriorly on the distal side of the thorax to the posterior edge of the pleural ridge. The medial, formed by the furca, furcasternum, presternum, and katepisternum, extends



ventromedially to the anterior edge of the pleural ridge (fig. 36). The sclerotized arm of the epimeron is slender from its triangular junction with the furca at the laterophragma to its ventral region (fig. 2). However, this area resists bending because of its curved cross-sectional shape (fig. 37a). The ventral region fuses broadly to the posterior edge of the pleural ridge, and to the dorsal edge of the meron (figs. 2 and 36). The meron articulates ventrally with the furcasternum through the sternocoxale (fig. 36).

The furca is stiff dorsally in the region where its cross-section is 'U'-shaped (figs. 38d and 38e). Ventrally the lower tubular portions of the furca fuse with the invaginated 'U'-shaped furcasternum (figs. 38a and 38b), and the anterior region of the furcasternum fuses with the prescutum (figs. 36 and 38a). All three structures form a rigid unit. The median ridge makes the prescutum and furcasternum junction rigid dorsoventrally. Since the lateral forces placed on this region in flight are symmetrical, they do not deflect it laterally. The box-like structure of the prescutum, median ridge and episternal ridge is also rigid. The katepisternum extends posteriorly from the stiff dorsal end of the episternal ridge to fuse broadly with the pleural ridge (figs. 2 and 36). The ventral ridge of the anepisternum tapers into the ventral region of the katepisternum, where it ends before it reaches the episternal ridge.



Figs. 41a and 41b illustrate the movements of the thorax and wing during the downstroke. This model differs from that of figs. 40a and 40b in that B moves dorsodistally; AZ, the subtegula, replaces the simple joint A of figs. 40a and 40b; ZDE, the pleural ridge-subtegular apodeme and pleural wing process, moves as a unit; CD is split; D, the pleural ridge just dorsal to the reinforced cell in the epimeron which surrounds the furcal-pleural muscle insertion, moves distally; F, the point of attachment of the subalar and basalar muscles to the wing base, lies below the wing on the ventral second axillary and ventral subcosta (sect. 4.4.2. and 4.4.3.); and the tension in the first dorsal longitudinal muscle acts between C and AB. At the beginning of the downstroke (fig. 41a), ZDE lies in a plane approximately parallel to the anterodorsal plane. As Z moves dorsoposteriorly, D moves distally, the subalar and basalar muscles apply a tension at F, and the wing rotates ventrally; ZDE twists about D such that E moves antero-distally and ventrally. Tension in the prescutal-subtegular ligament pulls Z proximally at the beginning of the downstroke to initiate the rotation of ZDE, and at the end of the downstroke to complete the rotation of ZDE.

When D moves distally, the epimeron bends very little, but rotates distally at its anterior end about its junction with the triangular epimeral furcal plate. The ventral region of the epimeron and the pleural ridge move as a stiff unit.



The dorsal end of the meron and coxa rotates distally on the epimeron and pleural ridge, bending along the epimeron-meral suture so that the ventral end of the meron and coxa remains articulated to the furcasternum through the sternocoxale. The furcasternal articulation stops the anterodorsal movement of the ventral part of the meron and coxa at the furcasternum. The anterior edge of the coxa moves distally on its membranous connection to the katepisternum, and episternal ridge. The furca, furcasternum, presternum and episternal ridge move slightly posterior but not laterally. The katepisternum and anepisternum rotate distally about the episternal ridge, bending on a dorsoventral line, and bending cuticle between the anepisternum and pleural ridge just anterior to the pleural ridge. The ventral ridge of the anepisternum and its projection into the katepisternum and the basalar complex rotate the anepisternum with the katepisternum.

The katepisternum bends laterally freely to allow the ventral region of the pleural ridge to move laterally. However, the moment which can be developed about the broad dorsoventral katepisternal-pleural ridge attachment, without twisting or bending the katepisternum dorsoventrally, is large. Hence, the furca, furcasternum, presternum, episternal ridge, katepisternum and pleural ridge move dorsoventrally as a unit, and rotate as a unit in the plane of the katepisternum-pleural ridge. Large anteriorly directed forces can also be placed on the pleural



ridge through the episternal ridge by tension which can be transmitted through the katepisternum. A large moment can also be developed about the broad dorsoventral attachment of the epimeron to the pleural ridge without deflecting the cuticle. The slender arm of the epimeron, and the dorsoventrally stiff articulation of the epimeron to the meron and coxa, brace the lower region of the epimeron to the laterophragma and furcasternum. The furcasternal articulation limits the dorsoanterior movement of the meron and coxa. Tension in the direct and indirect dorsoventral muscles, during the up and downstroke, hold the meron-coxa articulation with the furcasternum at this limit. The meron and coxa are rigid dorsoventrally by their shape and the coxal-sternal suture brace. When the pleural ridge moves distally the episternal ridge, presternum, furcasternum and furca move slightly posterior, which bends the furca just ventral to the triangular epimeron-furcal junction.

The forces placed on the meron and coxa by the tension developed at the subalar and basalar muscle origins (fig. 36), act dorsally on the merocoaxal - epimeral and merocoaxal - furcosternal articulation. These forces decrease the ventral movement of the pleural ridge. As the first dorsal longitudinal muscles draw Z and C together, the pleural ridge must move further distally. Tension in the furcopleural muscle (fig. 37a) reduces the distal movement of the pleural ridge, and probably the posterior movement of the furca, furcasternum, presternum and episternal ridge would increase the tension in the katepisternum and further reduce the distal movement of the pleural ridge. The



pinnate arrangement of the fibers of the furcopleural muscle permit it to exert large forces over a small displacement (Alexander 1968). Contraction of the pleurosubalar muscle pulls the ventral end of the triangular epimeron-furcal junction anteriorly, and through either the wing base or the pleural wing process-subalar ligament, may pull the pleural wing process posteriorly. The furca and epimeron bend at their junction with the triangular plate. This action lowers the posterior end of the notum and increases the distal displacement of the pleural ridge. The metathoracic first ventral longitudinal muscle is large and by its tension pulls the ventral end of the metathorax anteriorly. It also pulls the episternal ridge, presternum, furcasternum and furca posteriorly, which by an increase in the tension placed on the furcopleural muscle, reduces the distal movement of the pleural ridge. The metathoracic pleural-prescutal apodeme muscle (fig. 9) also pulls the metathorax anteriorly and the epimeron-furcal junction posteriorly, but because of the small size of this muscle its effect must be small.

During the upstroke, tension in the indirect upstroke coxal and trochanteral muscles places dorsally directed forces on the coxa and meron. The coxa and meron transfer these forces directly to the epimeron and pleural ridge dorsally and to the furcasternum ventrally. The furcasternum and furca transfer these forces, and the dorsally directed forces produced by the tension in the tergo-sternal muscles, to C (fig. 41b), and the furcasternum, presternum, episternal ridge and katepisternum transfer them to the pleural ridge. The epimeron mount held C stationary. The dorsally directed force on ZDC and the ventrally



directed force on ABC pushes A and Z anteriorly, which pulls D proximally. ZDE rotates about D such that E moves dorsoproximally and posteriorly. The wing rotates upwards.

#### 4.4. The wing base

##### 4.4.1. *The first axillary sclerite*

Two ligaments suspend the first axillary sclerite on the median notal wing process (figs. 1 and 16a). The anterior ligament (fig. 20a) suspends the first axillary loosely below the median notal wing process. The posterior ligament (fig. 20b) is thin anteriorly but thick posteriorly where it is continuous with the distal edge of the median notal wing process. The ligament holds the posterior end of the first axillary sclerite close to the dorsal surface of the median notal wing process. The thin pleural-first axillary (p.-1 ax.) muscle (figs. 8 and 20b) inserts along the proximal edge of first axillary sclerite. Its origin is on the anepisternum (fig. 36).

The central region of the first axillary sclerite is tubular (figs. 16b and 33a). At each end, the tube flattens to form flanges. From the two proximal flanges ligaments suspend the first axillary sclerite on the median notal wing process (figs. 16a, 20c, and 20d). The flanges and tubular region form a rigid unit.

Although the anterior arm (fig. 1) is composed of bending cuticle from its base to the hard plate at its anterior end,



the arm bends little in flight because of the thickness of its cuticle and its cross-section (fig. 20e). This arm extends dorsally centrally to form a vaulted structure (fig. 31) under which the pleural wing process probably lies during part of the stroke. Strong ligaments extend from the hard plate of the anterior arm to an anterior notal wing process and scutum (figs. 1, 16b, and 31). The hard plate sweeps out an angle approximately the same as the angle swept out by the wing in flight; the first axillary sclerite, a smaller angle. Hence the anterior arm of the first axillary sclerite is twisted in flight. Ventroproximal to the base of the anterior arm an anteriorly directed cuticular arm underlies a resilin pad (fig. 32). The dorsal edge of the resilin pad attaches to a cup-shaped region of the anterior notal wing process (figs. 1, 31, and 32).

#### 4.4.2. *The second axillary sclerite*

Two sclerites make up the second axillary sclerite. The sclerite which lies in the dorsal wing membrane, the dorsal second axillary sclerite, is plate-like dorsally, has a ventral projection distally, and follows the dorsal wing membrane ventrally posteriorly. Along its proximal edge, the dorsal plate articulates with the first axillary sclerite. The anterior articulation (fig. 20c) limits the maximum and minimum angles through which the second axillary sclerite may rotate relative to the first axillary sclerite. The posterior articulation (fig. 20d) limits only the maximum angle. Translational movement of the second



axillary sclerite on the first axillary sclerite is possible on the ligament of the posterior articulation only. Fig. 1 shows the maximum separation of the first and second axillary with the ligament of the posterior articulation fully extended. When the first and second axillary sclerites are minimally separated the dorsal edge of the posterodistal flange of the first axillary sclerite fits into the notch formed between the proximal articulations of the second axillary sclerite.

At the posterior edge of the second axillary sclerite where the dorsal wing membrane dips ventrally, the posterior edge of the second axillary sclerite forms a cup-shaped articulation with the first median plate (figs. 1, 16a, 18, and 23). The distal ventral projection is triangular. The curved dorsal base plate forms its base. The apex points ventrally at the ventral second axillary sclerite (fig. 18).

The ventral second axillary sclerite lies in the ventral wing membrane. It is an inverted 'T'-shape. The dorsal arm of the ventral second axillary sclerite forms the shaft of the 'T'; the ventral plate to which the ligaments attach, the cross-piece (fig. 18). The anterior end of the ventral plate becomes almost cylindrical at its attachment to the heavy ventral second axillary sclerite-pleural wing process ligament (figs. 16b and 18). The membrane from the dorsal edge of the ligament invaginates and attaches to the ventral second axillary sclerite part of the way up the dorsal arm (fig. 18). This membrane attaches to



the dorsal process of the ventral radius distally (figs. 16b and 25). From the posterior base of the invagination, the membrane continues along the dorsodistal edge of the ventral plate to the ventral second axillary-median plate ligament (figs. 2, 18, and 23). The ridge of cuticle to which this membrane attaches, and the posterior edge of the posterior end of the ventral plate which twists dorsally into the dorsal arm, form a socket into which the ventral apex of the dorsal second axillary sclerite fits. However, this peg-in-socket structure (Sharplin 1963a) does not form the functional articulation, as the ventral apex is quite flexible and does not fully reach into the socket. The dorsal second axillary sclerite and ventral second axillary sclerite hinge on a bending cuticle connection only. This connection extends from the anterior edge of the triangular ventral projection of the dorsal second axillary to the anterior surface of the dorsal arm of the ventral second axillary sclerite (fig. 18). Dorsally the bending cuticle continues distally to form a flange on the dorsal edge of the dorsal arm of the ventral second axillary sclerite, the radial bridge, which continues to the radial plate (figs. 1, 16a, and 18). A sensory organ (Sharplin 1963a), the scale plate, lies in the membrane between the radial bridge and the dorsal second axillary sclerite (figs. 1 and 16a).

A number of ligaments lie with the ventral second axillary in the ventral wing base membrane. From the anterior and posterior edges of the ventral apex of the ventral second axillary



sclerites two ligaments (anterior and posterior ventral second axillary sclerite-subalar ligaments) curve proximally then ventrally to the subalare (figs. 2 and 18). The anterior ligament is thicker, and curves proximally less than the posterior ligament. It is shorter than the posterior ligament because the second axillary sclerite lies at an angle of about 30° to the subalare in the anterodistal plane. At the posterior tip of the ventral second axillary sclerite a thin ligament extends to the posterior third axillary sclerite (ventral second axillary-posterior third axillary ligament) (figs. 2, 18, and 23), and a thick ligament extends to the dorsal wing base first medial plate (ventral second axillary - first median plate ligament) (figs. 2, 18, 23, and 25).

#### 4.4.3. *The subcosta, costa, radial plate, radius, second cubitus, and wing*

The proximal tip of the dorsal subcosta attaches to the sclerotized plate at the anterior end of the anterior arm of the first axillary sclerite by a thick ligament (figs. 1, 16a, and 31). All lie in the dorsal wing membrane. The proximal arm of the dorsal subcosta is thick and rigidly braced on its ventral side by a continuation of the invagination in the dorsal wing membrane between the costa, subcosta and radius (figs. 16b and 17a). Anterodistally the dorsal subcosta expands into a hollow bulb (figs. 1, 17a, and 17b). This bulb is rigid and connects rigidly to the ventral subcosta and ventral radius, which lie in the ventral wing membrane, proximally through the wall of the internal subcostal bulb, and by 2 struts, the dorsal-ventral subcostal, and subcostal-ventral radial struts (figs. 17a and 17b).



The subcostal-ventral radial strut lies along the low invagination in the lower wing membrane which separates the ventral subcosta and ventral radius (fig. 2). The dorsal subcosta connects to the internal subcostal bulb by bending cuticle along its anterodistal border (figs. 17a and 17b). The internal subcostal bulb is rigid except for this anterior bending cuticle junction. The external subcostal bulb (fig. 17b) which lies at the anterior edge of the wing is flexible. Distal to the dorsal subcosta and separated from it by a furrow of bending cuticle on the upper wing membrane, the costa and subcosta have a common base (figs. 1 and 17b). Tracheae from both veins pass through this area. The lower surface of the wing is membranous in this region.

A ligament, the ventral subcostal-basalar ligament (figs. 2 and 17a), connects the posterior edge of the ventral subcosta and the ventral radial-ventral subcostal ridge to the second basale (fig. 2). The ventral radial-ventral subcostal ridge is a thickening which extends from the internal subcostal bulb across the proximal end of the ventral radius (figs. 2, 17a, and 17b). It may represent the invagination which separates the ventral subcosta and ventral radius. At its posterior end, this ridge fuses with the proximal arm of the ventral ridge (figs. 2 and 16b). From the posterior side of the base of the proximal arm a heavy ligament extends to the pleural wing process, and from the proximal tip of the proximal arm a thinner ligament extends to the second basale (figs. 2 and 16b). The proximal



arm twists on the ventral radius-ventral subcostal ridge which bends about the larger area of bending cuticle that connects it to the more distal region of the ventral radius.

The ventral radius is trough-shaped to its distal end where it narrows to a bending cuticle arch (fig. 2). From the posterior edge of the ventral radius a large dorsal process of the ventral radius extends dorsally close to the dorsal wing membrane (fig. 16b), which carries the ventral wing membrane with it. The anterior edge of the ventral radius and the ventral membrane of the costa-subcosta are separated by a shallow but wide invagination (figs. 2, 17a, and 17b). A membranous notch-like region of the membrane lies in the posterior edge of the ventral radius distal to the dorsal process (fig. 16b). Some bending may occur across the ventral radius at the level of the membrane notch dorsoventral to the plane of the wing. However, the remainder of the ventral radius proximal to the notch and the subcosta form a stiff unit. The portion of the ventral radius distal to the notch is stiff distally to the bending cuticle arch.

The ventral brace of the proximal arm of the dorsal subcosta is continuous with the dorsal subcostal-radial plate ventral ridge, a thickening at the ventral edge of the fused invagination separating the dorsal subcosta, radial plate and costa-subcosta (figs. 16b, 17a, and 25). The section line of fig. 17b lies at the bottom of the open part of the invagination, the fused sides of the lower region have been removed. Only the dorsal regions



of the invagination are bending cuticle (figs. 1, 16b, 17a, and 17b). A large arch, the ventral radius-radial plate connecting arch (fig. 17a), fuses along its anteroproximal and anterodorsal edges to the invagination, and along its posterior edges to the dorsal process of the ventral radius (figs. 16b and 25). A stiff strut, the radial plate strut, extends from the posterior end of the ventral radius-radial plate connecting arch to the proximal end of the bending cuticle arches (fig. 2) at the distal end of the radial plate (figs. 16b, 17a, and 23). These areas join the upper and lower parts of the wing base.

The radial plate lies on the dorsal surface of the wing (fig. 1). Proximally and anteriorly it joins the dorsal subcosta and costa-subcosta by a fold of bending cuticle (figs. 2, 16b, and 17a). Although the anterior edge of the radial plate is bending cuticle, posteriorly its cuticle becomes fully sclerotized (figs. 2). There is a deep strengthening ridge which extends below the posterior margin (fig. 16b), which prevents the radial plate from buckling under the forces placed on it by the radial bridge. The radial bridge connects to the posterior margin of the radial plate by a bending cuticle hinge, which is an extension of the dorsal surface of the radial bridge (figs. 2, 16a, and 18). At its distal end the radial plate joins the radius and second cubitus by two bending cuticle arches (figs. 2, 16b, 17a, and 23). Both arches have a connecting interior proximally, but there is a plate which blocks



the interior of the arch to the second cubitus at the level of the second median plate (figs. 17a and 23). The radial plate strut forms the proximal and common end of both bending cuticle arches (figs. 17a and 23). Posteriorly membrane extends from the radial plate to the scale plate, dorsal second axillary sclerite, first median plate, first and second axillary sclerite, and the dorsal subcosta (figs. 2 and 16a).

The distal end of the radial plate can rotate slightly in the plane of the wing about its junction with the dorsal subcosta, which bends the invagination between the costa-subcosta and radial plate in this plane. However, the dorsal subcosta, radial plate, costa-subcostal margin-radial plate invagination and the bending cuticle arches to the radius and second cubitus form a unit stiff to dorsoventral bending. The bending cuticle arches are stiff to bending in this plane and not in the anteroposterior plane because of their 'U' cross-section. This section is orientated such that the open portion of the 'U' lies on the interior side of the wing membrane. The radial plate twists slightly along its strengthening ridge, between the radial bridge and the radius and second cubitus bending cuticle arches, about the bending cuticle of the costa-subcostal margin-radial plate invagination. There is little rotation of the radial plate about its radial bridge connection in the plane of the wing, but they may bend dorsoventrally on the hinge between them.

Figs. 1 and 15 show the wing venation labelled after Imms (1957). During the upstroke the wing bends towards its concave or lower surface along the proximodistal axis and the wing



camber increases slightly. This may have the effect of reducing the amount of wing bending along this axis. During the down-stroke bending along this axis is minimal because the wing tends to bend towards its convex or upper surface.

#### 4.4.4. *The third axillary sclerite, first median plate, and second median plate*

The cup-shaped proximal end of the first median plate twists ventrally to articulate with the distal edge of the dorsal second axillary which also curves ventrally (figs. 1, 16a, 18, 23, and 24a). Distally the dorsal and ventral edges of the articulating cup of the first median plate twist such that they lie in the dorsal surface of the wing (fig. 23). The invagination between these edges forms a ventral projection to which a ligament from the ventral second axillary sclerite attaches, the ventral second axillary-first median plate ligament (figs. 2 and 23). The first median plate is rigid.

The second median plate articulates with the anterodistal edge of the first median plate along a line of bending cuticle (figs. 1 and 23). This bending cuticle junction is split proximally to permit the rotation of the second median plate on the first median plate in the plane of the wing. The second median plate passes under the second cubitus to articulate with the posterior side of the radius along another line of bending cuticle (figs. 1, 16b, and 23). Although the cuticle of the second median plate is not sclerotized and is more flexible than



the sclerotized cuticle, it remains stiff in flight by its thickness and cross-section (figs. 16a and 16b).

The anterior third axillary sclerite hinges on the posterior edges of the first median plate (figs. 1 and 23). This hinge prevents rotation of the posterior end of the anterior third axillary sclerite further dorsally than approximately the plane of the wing because of the cross-section of the hinge (fig. 24b), and because the second axillary-first median plate hinge prevents this rotation of the first median plate. The pleural-third axillary<sub>a+b</sub> (fig. 9) muscles insert in an involution of the posterior tip of the anterior third axillary sclerite (figs. 23 and 24c). The origin of these muscles is on the anepisternum (fig. 36). The anterior third axillary sclerite is torsionally flexible from its flight position in which it lies in the plane of the wing, to its folded position in which its posterior proximal edge twists ventrally. Along its posterodistal margin the anterior third axillary sclerite articulates with the posterior third axillary sclerite (figs. 1, 23, and 24c). Although the corners of the anterior-posterior third axillary hinge are bending cuticle, thin sclerotized cuticle forms most of the central bending area.

The proximal portion of the posterior third axillary sclerite is trough-shaped. Although it does not bend when compressed, it twists through 180° when the wing unfolds (fig. 23). Hence the membrane from the posterior edge of the posterior



third axillary sclerite at the anterior third axillary sclerite junction, which continues dorsally over the pleural-third axillary<sub>a+b</sub> muscles, is continuous with the membrane from the proximal side of the anterior third axillary sclerite and from the anterior edge of the proximal end of the posterior third axillary (fig. 23).

The posterior third axillary sclerite attaches by a wedge of bending cuticle to the anal area of the wing where the axillary cord tapers into the posterior edge of the wing (figs. 2 and 23). Anteriorly a flange from the posterior third axillary sclerite overlies the base of the anal veins (figs. 2 and 23). Membrane forms the remainder of the flexible third axillary-wing junction (figs. 2 and 23). The proximal tip of the posterior third axillary sclerite attaches to the posterior notal wing process by a thick ligament (figs. 2, 23, and 25). When the wing folds, the proximal tip of the posterior third axillary sclerite twists with the posterior notal wing process. The posterior notal wing process is stiff from its hinge on the scutum (figs. 1 and 29) (sect. 4.2.4.) to the posterior third axillary sclerite, although the region immediately distal to the laterophragma is less sclerotized and more flexible than the more proximal region.

#### 4.4.5. Movement of the first axillary, second axillary, subcosta, radial plate, and the second cubitus

A full understanding of the flight mechanism of the wing



base can only be obtained by a detailed study of the wing base sclerites, the way they hinge upon each other, and by some knowledge of the type of aerodynamic forces developed on the wings. Using conventional aerodynamics, Jensen (1956) shows that the wings of *Schistocerca gregaria* Forskål produce lift throughout the wing beat cycle, but thrust only during the downstroke, both relative to the longitudinal axis of the thorax. The wings produce drag relative to this axis during the upstroke. Baird's (1964) experimental results on the flight aerodynamics of *Galleria mellonella* indicate that the wings produce thrust relative to the longitudinal axis of the thorax during part of the upstroke. He explains that this is due to the small wing supination angles developed during the upstroke, because of the small size of *Galleria mellonella*. *A. orthogonia* supinates its wings at a large angle during the upstroke, and although *A. orthogonia* is smaller than *S. gregaria*, it is much larger than *G. mellonella*. The chord of the wings of *A. orthogonia* is at all times convex dorsally in flight. This indicates that the relative wind acts at an angle below the plane of the wing. Hence, Jensen's (1956) basic analysis probably holds true for *A. orthogonia*. It follows that during the downstroke a dorsal and anteriorly directed aerodynamic force acts about the wing base on the wing, and during the upstroke a dorsal and posteriorly directed aerodynamic force acts about the wing base on the wing. The observed motions of the wing and wing base indicate



that this assumption about the aerodynamic forces is correct.

There are two distinct systems which operate in the wing base. The first axillary, dorsal and ventral axillary sclerites, the radial bridge, radial plate, ventral radius and the dorsal and ventral subcosta (figs. 1 and 2) transfer the power developed on the thorax to the wing, and pronate or, together with the aerodynamic forces, supinate the wing. The anterior and posterior third axillary, first median plate, second median plate, and the bases of the radius and second cubitus (fig. 1), together with the aerodynamic forces, determine the relative retracted or protracted position of the wing. The details of the mechanism of the third axillary system will be considered in section 4.4.6. Only its effects on the wing stroke will be considered here.

There are three distinct hinge systems about which the wing protracts and retracts, elevates and depresses, and pronates and supinates. About 20% of the total angle swept out by the wings in protraction and retraction is due to bending along the primary line of folding which Snodgrass (1935) proposed for a generalized insect. In the generalized insect this line of folding passes between the first axillary and subcostal vein, between the second axillary and radius, and between the first and second median plates. In *A. orthogonia* it passes between the first axillary sclerite and the dorsal subcosta, between the dorsal and ventral second axillary and between the first and second median plates. In the Lepidoptera the ventral second axillary



is thought to be a second piece of the radius annexed to the second axillary complex (Sharplin 1963a). Hence the primary line of folding in *A. orthogonia* does follow Snodgrass' (1935) generalized plan. In addition, the median plates are free to rotate about the first median plate, dorsal second axillary junction in *A. orthogonia*.

In the generalized system the posterior end of the primary line of folding moves up and the wing rotates down and back when the wing folds. In *A. orthogonia* the dorsal second axillary hinges obliquely across the proximal surface of the ventral second axillary. This prevents the primary line of folding from operating as in the generalized system. However, the wing may rotate posteriorly in the anterodistal plane about the dorsal subcosta-first axillary ligament, and the dorsal-ventral second axillary hinge. A third hinge region between the dorsal subcosta and radial plate forms the third apex of a triangular structure which limits this folding rotation (fig. 1). This limit depends upon the stiffness of the sides of the triangle. The dorsal subcosta from the first axillary to the radial plate is heavily braced and rigid. The dorsal second axillary is stiff. It may not move parallel to the axis of its hinge on the first axillary. However, the hinge line may change slightly because the second axillary can rotate in the plane of the wing slightly about the proximal portion of the dorsal second axillary-first axillary hinge. This has little effect on the length of



the sides of the triangle, but rotates the whole triangle which then changes the folding angle limit. The first axillary is rigid and its anterior arm, although composed of bending cuticle, is rigid longitudinally by virtue of its cross-section (fig. 20e) (sect. 4.4.1.).

The stiffness of the last side of the triangle depends on the orientation of the dorsal subcosta-radial plate, and radial plate-bridge hinge. The dorsal subcosta-radial plate hinge will not permit any rotation of these sclerites about each other except that in the plane of the wing, and the radial plate-bridge hinge will not permit any rotation other than that about its axis along the junction between the radial plate and bridge (fig. 1). The radial plate is rigid and a brace extends along the proximal edge of the radial plate. Hence the moment arm formed by the dorsal subcosta and radial plate determines the rotation of the wing about the radial plate-bridge hinge, since the dorsal subcosta-first axillary hinge does not lie on the radial plate-bridge axis. If the radial plate-bridge hinge lies above the dorsal subcosta-first axillary hinge, the wing rotates upward (elevates) and supinates about the radial plate-bridge hinge. If the radial plate-bridge hinge lies below the dorsal subcosta-first axillary hinge, the wing rotates downward (depresses) and pronates about the radial plate-bridge hinge. In flight the supination coincides with the upstroke; pronation, with the downstroke. The ventral wing base membrane extends high on the



ventral second axillary (fig. 18), and thus does not hinder the hinge action. The length of this side of the triangle increases at the top and bottom of the stroke, which decreases the unfolding rotation limit at these times.

The remaining 80% of the total angle swept out by the wing in protraction and retraction is due to bending about a secondary line of folding. This line passes between the dorsal subcosta and the costa-subcostal region, the radial plate and the costa-subcosta region, and across the radial, second cubital and ventral radial bending cuticle arches. The bending cuticle arches form the hinge. When the wing retracts, the bending cuticle between the dorsal subcosta-radial plate and the costa-subcostal region (fig. 1) unfolds, but eventually limits the retraction angle to that permitted by the position of the dorsal subcosta. Contact between the raised portion of the costa-subcostal region (fig. 1), and the dorsal subcosta and radial plate, limits the maximum protraction angle. Hence the position of the dorsal subcosta also limits the protracted angle of the wing. The lower membrane of the wing (fig. 2) also unfolds.

The pleural wing process and lateral margin of the notum apply to the wing bases the major part of the moments which produce the up and downstroke. The wing elevates and depresses on the notum about the hinge formed by the anterior notal wing process-first axillary ligament, and the resilin block which lies between the anterior notal wing process and the first axillary



(fig. 1). The pleural wing process connects to the ventral radius and ventral second axillary by ligaments (fig. 2). The star adjacent to the dorsal second axillary in fig. 1 indicates its approximate position with the wing held horizontally. During the downstroke the anterior notal wing process and median notal wing process move dorsodistally, the latter about twice as far as the former. The pleural wing process moves ventrally. The first axillary moves ventrally at its distal end about its hinge on the anterior notal wing process. Its proximal end moves dorsally with the median notal wing process.

During the downstroke the moments produced by the thorax, which act through the wing brace, must overcome the aerodynamic moment developed on the wing and drive it ventrally. At the beginning of the downstroke the first axillary pushes distally on the top of the dorsal second axillary, and the pleural wing process restrains the lower end of the ventral second axillary (fig. 18). The anterior arm of the first axillary pushes dorso-distally on the dorsal subcosta and the posterior wing process restrains the ventral radius and ventral subcosta. The ventral end of the second axillary complex rotates towards the first axillary about the first axillary-dorsal second axillary hinge, until the anteroproximal portion of the hinge (fig. 20c) limits this rotation. This automatically pronates the wing about the dorsal subcosta-dorsal second axillary hinge. The radial plate-bridge hinge moves ventrally relative to the dorsal subcosta-first



axillary ligament because of the moment placed on it by the first-second axillary system, and the dorsodistally directed force placed on the dorsal subcosta by the first axillary. Hence the wing pronates further about the radial plate-bridge hinge.

The first and second axillary and the rigid subcosta-ventral radius system (sect. 4.4.3.) rotate about the first axillary-anterior notal wing process hinge. The radial bridge transfers the moments from the first and second axillary to the radial plate. The stiff ridge of the posteroproximal edge of the radial plate transfers them to the dorsal subcosta, and to the radial and second cubital bending cuticle arches. The ventral radius also transfers the moments developed on it to these arches through the ventral radius-radial plate connecting arch (fig. 17a). The dorsal subcosta, ventral subcosta, radial plate and ventral radius rotate ventrodistally as a unit. The bending cuticle arches transmit the depression and pronation moments to the wing.

Contraction of the subalar musculature during the downstroke pulls the ventral second axillary proximally and ventrally, and pulls the pleural wing process proximally by the tension developed in the subalar-pleural wing process ligament (fig. 2). This increases the moment which produces the downstroke, and increases the moment which pronates the wing, since the ventral second axillary-subalar ligaments connect to the second axillary below the ventral second axillary-pleural wing process ligament (figs. 16a and 18).



The dorsal and the ventral second axillary sclerites rotate posteriorly at their posterodistal ends about the ventral second axillary-pleural wing process ligament. The posterior portion of the dorsal second axillary-first axillary hinge pushes closely together, and the whole wing base rotates slightly posterior at its distal end, the secondary line of wing folding. At the same time the wing rotates anteriorly at its distal end about the secondary line of wing folding because of the thrust forces developed on the wing. The first median plate is free to rotate in the plane of the wing about its hinge on the dorsal second axillary. However, a large ligament extends from the distal end of the first median plate to the ventral second axillary (figs. 2, 5, and 23). Hence, the ventral second axillary limits the anterior rotation of the first median plate. The second median plate hinges between the distal end of the first median plate and the invagination between the radius and second cubitus. When the wing rotates anteriorly the tension developed between the second axillary complex and the invagination between the radius and second cubitus transfers a moment directly from the second axillary complex to the wing. Hence a second system transfers the downstroke moments to the wing.

Contraction of the subalar musculature cannot supinate the wing by rotating the posterior edge of the second axillary and the first axillary ventrally about the median notal wing process, because the median notal wing process overlaps the first axillary



anteriorly and connects very closely to the first axillary posteriorly (figs. 20a and 20b). The median notal wing process also constantly pushes the first axillary dorsodistally during the downstroke. Only a small contribution to supination can be effected by the subalar system. This, by compressing the ligaments anterior to the pleural wing process dorsally, and stretching the ligaments posterior to the pleural wing process. Kammer's (1967) conclusion, based on her electrophysiological studies and possibly on Wilson's (1962) study of the locust, that the subalar muscles are supinators, is wrong.

The ventral subcosta-basalar ligament inserts on the ventral subcosta slightly ventral to the ventral radius-pleural wing process ligament. At the beginning of the downstroke, when the aerodynamic thrust forces protract the wing rapidly, the dorsal subcosta-radial plate limits this protraction. The moment, which produces the protraction, then also rotates the wing base posteriorly at the secondary line of folding about the primary line of folding. Thus the ventral subcosta-basalar ligament is stretched, and the anteriorly directed component of tension produced by the basalar system rotates the wing base anteriorly at its distal end about the primary line of wing folding during the downstroke (fig. 44). If the ventral subcosta-basalar ligament is cut the wing unfolds incompletely during less vigorous flight. Vigorous flight always results in full wing unfolding.



The force produced by the contraction of the basalar musculature in the downstroke also contributes to the moment which produces the downstroke. At the beginning of the downstroke the ventral subcosta lies approximately distally to the dorsal subcosta-, dorsal second axillary-first axillary hinge and the first axillary-anterior notal wing process hinge. Contraction of the basalar muscles produces a ventral component of force on the ventral subcosta, which produces a moment, which contributes to the moment which pronates and depresses the wing. However, as the wing rotates ventrally the ventral subcosta lies increasingly ventral and decreasingly distal to the dorsal subcosta-, dorsal second axillary hinge. The projection of the path of the ventral subcosta-basalar ligament on the anterodistal plane is approximately colinear with the dorsal subcosta-, dorsal second axillary-first axillary hinge. Since a proximally directed force would be required to produce a pronating moment when the wing rotates ventrally, the basalar system cannot pronate the wing about the dorsal subcosta-, dorsal second axillary-first axillary hinge but it does continue to depress the wing. It may pronate the wing by its ventrally directed component of force, which would stretch the ligaments anterior to the pleural wing process ventrally and compress those posterior to this dorsally. Only a small part of the total pronation can be effected in this way.

The ventral radial-second basalar ligament probably transfers little power to the wing for four reasons. First, the proximal arm of the ventral radius twists in and out of the plane



of the wing about the proximal end of the ventral radius. Second, the distal process of the second basalare bends laterally readily although it is stiffer to dorsoventral bending. Third, the ventral radial-second basalare ligament is thin. Fourth, the ventral radial-second basalar ligament leaves the second basalare at a level close to the resilin ligament which attaches the proximal process of the second basalare to the pleural ridge. Hence, little of the forces developed by the basalar muscles can be applied to the ventral radial-second basalar ligament. Rather than power transfer, the distal process of the second basalare, the ventral radial-second basalar ligament, and the proximal arm of the ventral radius with the tegula form a mechanical part of a proprioceptive system. The anterior pleural membrane suspends the tegula (fig. 13b) (see tg. tear, figs. 1 and 2). The tegula forks over and under the wing base, and the distal process of the second basalare fits closely to the ventral side of the tegula (fig. 42). Hence, the second basalare influences the lateral and to a small extent the dorso-ventral position of the tegula in flight. The tegula rubs on the scale plate (fig. 1) dorsally, and the ventral sensory process of the tegula with sensory hairs at its tip extends into the region between the ventral subcosta and ventral radius (fig. 42) ventrally.

During the upstroke the moments produced by the thorax, which act through the wing base, provide the principle part of the moment which drives the wing dorsally. The aerodynamic moment developed



on the wing, although it acts in the same sense as the thoracic moment, probably contributes little to the upstroke movement of the wing. The thoracic upstroke moment is produced when the margin of the notum moves ventroproximally carrying with it the first axillary-notal hinge, and the pleural wing process moves dorsoproximally carrying with it its ligaments to the ventral subcosta and the ventral second axillary (sect. 4.3.4.). The first axillary rotates inward about the anterior notal wing process from its position in the anterodistal plane at the bottom of the stroke, to lie approximately dorsoventrally at the top of the stroke.

The pleural wing process applies a dorsally directed force to the ventral radius and the ventral second axillary through the subcostal and ventral second axillary-pleural wing process ligaments. The notum pulls the first axillary ventroproximally, and the first axillary pulls proximally on the dorsal subcosta and the top of the dorsal second axillary. These forces, together with the aerodynamic lift force, supinate the wing about the dorsal subcosta-, dorsal second axillary-first axillary hinge until the posterior portion of the dorsal second axillary-first axillary hinge limits this motion. The dorsal subcosta moves ventroproximally at its articulation with the first axillary and the second axillary complex rotates the radial bridge dorsally. The radial plate-bridge hinge lies dorsal to the dorsal subcosta - first axillary articulation, hence the wing further supinates



about the radial plate-bridge hinge. Then the wing rotates upwards about the first axillary-notal hinge.

The wing, distal to the secondary line of folding, because of the drag forces developed on it, rotates slightly posterior about the secondary line of folding during the upstroke. The third axillary complex rotates the first median plate anteriorly about its articulation with the dorsal second axillary (sect. 4.4.6.), and pushes the second median plate anteriorly to stop the wing from retracting. Thus the moment applied between the first median plate and the radial-second cubital invagination limits the posterior rotation of the wing during the upstroke (fig. 44). The anterior third axillary also pushes distally on the base of the anal veins. This produces a second moment about the stiff anal vein-second cubital area to limit the posterior rotation of the wing. At the posterior rotation limit of the wing the secondary line of folding moves slightly anterior and the wing base rotates anteriorly about the primary line of bending. This slackens the ventral subcosta-basalar ligament during the upstroke. Two other factors contribute to this rotation. First, the posterior portion of the dorsal second axillary-first axillary hinge pulls apart slightly on its articulating ligament (fig. 20d), when the first axillary places this hinge in tension. Since the ligament of the more anterior portion of this hinge holds the anterior part of it close to the first axillary at all times, the dorsal second axillary rotates at its



posterodistal end about the more anterior ligament. Second, since the third axillary system pushes the distal end of the first median plate anteriorly about its articulation with the dorsal second axillary (sect. 4.4.6.), the ventral second axillary is pulled anteriorly at its distal end by the ventral second axillary-first median plate ligament. This tends to rotate the wing base anteriorly about the primary line of folding. The triangular structure between the dorsal subcosta-first axillary ligament, the dorsal-ventral second axillary, and the dorsal subcosta-radial plate hinge limit the anterior rotation of the wing base on the primary line of folding.

Contraction of the pleural-subtegular muscle pulls the posterior wing process anteriorly relative to the notum. This increases the supination and decreases the pronation of the wing. This change does not alter pronation or supination about the dorsal subcosta-, dorsal second axillary-first axillary hinge but supinates the wing base on any slack in the notal-wing base ligaments.

To test some of the hypothetical movements of the wing base sclerites, I used the data tabulated in table 3. Fig. 43 shows the projections of the first and second axillary sclerites at the top and bottom of the stroke on the frontal plane. I arbitrarily let the first axillary extremities be the posterior first axillary-median notal wing process ligament, and the proximal portion of the dorsal second axillary-first axillary hinge.



The second axillary arbitrarily extends from the proximal portion of the dorsal second axillary-first axillary hinge to the posterior end of the ventral second axillary-pleural wing process ligament. I assume that the pleural wing process remains in its top of the stroke position during the wing stroke. Therefore I subtract the total actual movement of the pleural wing process from the bottom of the stroke positions of the first and second axillary. If I make the following four assumptions, the positions of the ventral end of the second axillary coincide with the top and bottom of the stroke positions which I measured, and these points lie at a distance less than the length of the ventral second axillary-pleural wing process ligament from the pleural wing process. First, the first axillary makes an angle of  $84^\circ$  to the anterodistal plane of the insect at the top of the stroke. Second, the second axillary, with the wing in a supinated position, makes an angle of  $115^\circ$  with the first axillary at the top of the stroke. Third, the first axillary makes an angle of  $20^\circ$  to the horizontal at the bottom of the stroke. Fourth, the second axillary makes an angle of  $45^\circ$  to the first axillary at the bottom of the stroke with the wing in a pronated position. The paths traced out by the intermediate positions of the sclerites are estimated.

#### 4.4.6. *Movements of the third axillary and median plate, and wing pronation and retraction*

During the downstroke the thrust produced by the wings is



greater than the total drag on the insect. Thus the wing rotates as far anteriorly on the thorax as possible. In this position the walls of the costa-subcostal margin and the subcosta contact those of the radial plate and the dorsal subcosta (fig. 1). The slow anterior rotation of the distal end of the wing base about the first axillary-dorsal subcosta ligament (sect. 4.4.5.), during the downstroke, permits the whole wing to rotate anteriorly (fig. 44). However, at the bottom and top of the stroke, and probably during the upstroke, the wing must be held against the drag forces on the wing to remain open.

Kammer (1967) shows that the lateral oblique dorsal longitudinal muscle is electrophysiologically active during the upstroke. The contraction of the muscle rotates the distal end of the posterior notal wing process dorsally (sect. 4.3.4.). The distal end of the posterior notal wing process pushes the proximal end of the posterior third axillary with it. The posterior third axillary hinges on the anterior third axillary (figs. 23 and 24c). As the distal end of the posterior third axillary moves dorsally, it rotates the posterior-anterior third axillary hinge and the anterior third axillary anterodistally in the plane of the wing. The anterior third axillary cannot rotate dorsally out of the plane of the wing because the anterior third axillary-first median plate hinge limits the dorsal rotation of the anterior third axillary to that of the first median plate (fig. 24c). The first median plate is torsionally rigid, and hinges on the dorsal second



axillary and is held from its ventral side by the ventral second axillary-first median plate ligament (figs. 16a, 18, and 23), such that it may only rotate in the plane of the wing. Hence, the posterior third axillary rotates the anterior third axillary and first median plate anterodistally about the dorsal second axillary. The second median plate hinges on the distal end of the first median plate, passes below the second cubitus, and hinges on the radius-second cubitus invagination (figs. 1 and 23). The antero-distal rotation of the first median plate and the anterior third axillary about the dorsal second axillary pushes the second median plate ventroanteriorly at its posterior end, and dorsoanteriorly at its anterior end. The second median plate pushes the radius-second cubitus invagination dorsoanteriorly. The thickness and cross-section of the second median plate prevent it from buckling under this compressive load. The radius-second cubitus invagination and the bases of the costa, subcosta, radius, first cubitus, second cubitus and first anal vein form an anteroposteriorally stiff region in the plane of the wing (fig. 1). The dorsoanterior movement of the radius-second cubitus invagination and the anterior third axillary therefore rotates the entire wing anteriorly about the secondary line of bending. A split in the first median plate-second median plate hinge permits the anterior second median plate and the first median plate to rotate about unequal radii by opening as the wing rotates anteriorly, and closing as the wing rotates posteriorly.



The ventral second axillary-first median plate ligament and dorsal second axillary-first median plate hinge both prevent excessive dorsal travel of the distal end of the first median plate in the plane of the wing. However, during the upstroke when the second axillary rotates further anteriorly than it does in the downstroke, and the anterior third axillary places a dorsally directed component of force on the first median plate, the first median plate and second median plate both move dorsally. This raises the radius-second cubitus invagination and the distal end of the radial plate which increases the camber of the wing slightly.

Many authors describe the laterophragma and the lateral oblique dorsal longitudinal muscle but none their true function in Lepidoptera. Erlich and Davidson (1961) indicate that the lateral dorsal longitudinal muscle extends from the mesoscutum to the anterior apodeme of the postalar portion of the mesothoracic epimeron in *D. plexippus*; to the phragma (Snodgrass 1935), and to the postnotum or phragma, "postalare", in *E. imperialis* (Michener 1952), and the "preclavicolae" in *H. convoluli* (Berlese 1909), and the "laterophragma" in all lepidopterans (Sharplin 1963b). Kammer (1967) shows the lateral oblique dorsal longitudinal muscle to be active electrophysiologically in the upstroke in *Mimas tiliae* L. She then concludes incorrectly that this muscle is solely a wing elevator in all Lepidoptera. It probably provides only a small contribution to wing elevation in *A. orthogonia*.



Pringle (1968) considers the lateral oblique dorsal longitudinal muscle to be absent or reduced in Lepidoptera.

The lateral oblique dorsal longitudinal muscle of *P. americana* extends between the tergum and the second phragma (Carbonell 1948). Tiegs (1955) concludes that this muscle is a depressor of the wing in *B. germanica* on the basis of anatomical studies, but Kammer (1967) shows this muscle to be active electrophysiologically during the upstroke in *P. americana*. Ewer and Mayler (1967) note that this muscle is well developed in the flightless female of *D. erythrocephala*, another Dictyopteran. On this basis he concludes that it must function in some system other than the flight system.

Snodgrass (1935), Tiegs (1955), and Smart (1959) assume, by the anatomical position of the lateral oblique dorsal longitudinal muscle in Diptera, that this muscle is one of the main elevators of the wing. This was predicted earlier by the mechanics of the dipteran thorax by Ritter (1911). Nachtigall and Wilson (1967) show electrophysiologically that the sternobasalar muscle or abductor muscle protracts the wing in Diptera.

Tiegs (1955) suggests on the basis of anatomical studies that the lateral oblique dorsal longitudinal muscle in a number of Homopterans is a main wing elevator. The muscle extends between the scutum and the phragma. Parsons (1960) indicates that this muscle extends between the lateral surface of the ventral process of the second phragma and the anterodorsal region of the



mesoscutum in the heteropteran *Gelastocoris oculatus* (Fabricius).

On this basis she suggests that the muscle is an indirect up-stroke muscle. Barber and Pringle (1966) indicate that this muscle extends between the anterior dorsolateral corners of the tergum and the ventrolateral extensions of the post-phragma. They believe this muscle to be mainly a wing supinator but also show electrophysiologically that it displays motor activity during the wing protraction. They suggest that the lateral oblique dorsal longitudinal muscle is partly responsible for the unlocking effect and another two sets of muscles contribute to wing protraction.

The wing of *A. orthogonia* protracts when the lateral oblique dorsal longitudinal muscle contracts. The mechanism is identical to that which holds the wing anteriorly during the upstroke. Tension in the ventral second axillary-posterior third axillary ligament prevents the proximal travel of the anterior third axillary when the protraction begins.

Sharplin (1964) describes wing retraction in the Lepidoptera. There are no differences here except in detail. Wing retraction unfolds the deep costa-subcosta and radial plate invaginations, which do not require the distal end of the subcosta to rotate posteriorly except when the wings are close to the body. The posterior-third axillary<sub>a+b</sub> muscle pulls the anterior third axillary proximally at its posterior end which rotates the first median plate posteriorly about the dorsal second axillary (fig. 23).



The second median plate pulls the radius-second cubitus invagination posteriorly about the bending cuticle arches. The split in the proximal edge of the first median plate-second median plate closes, and the plates buckle dorsally. The posterior notal wing process-posterior third axillary hinge moves ventrally into the impression in the subalare. When the longitudinal axis of the wing has moved to within about  $15^{\circ}$  of the longitudinal axis of the thorax, tension on the ventral second axillary-posterior third axillary and ventral second axillary-first median plate ligaments, due to the travel of the first median plate and third axillary, rotate the end of the ventral second axillary posteriorly about the dorsal second axillary-ventral second axillary hinge. The tension placed on the costa-subcosta invagination cuticle rotates the distal end of the subcosta posteriorly about the first axillary-dorsal subcosta ligament, which carries the ventral radius and to a small extent the radial plate with it. Hence the wing base rotates about the primary line of folding. The dorsal process of the ventral radius contacts the dorsal arm of the central second axillary, and pushes it posteriorly. The median notal wing process moves to a ventroproximal position and the first axillary lies with its distal end much further dorsal than its posterior end, and displaced slightly posterior. The radial plate twists dorsally at its anterodistal end and the costa-subcostal margin bends ventrally about the anterior edge of the radial plate.



## 5. Discussion

Observation of the flight structures of preserved specimens was sufficient to determine and describe the basic flight structures of *A. orthogonia*. However, a large number of problems became apparent when I attempted to observe and measure the movements of the flight structures in flying specimens. I could readily induce an intact mounted specimen to fly for periods of about two minutes by removal of tarsal support or by directing a small wind at its head. Occasionally, dissected specimens flew nearly as well as intact insects; however, because of the dissection required to permit observation of the various structures in living insects, flight was more often reduced to flutters of about five seconds duration. Such flight varied in frequency and thus reduced the effectiveness of the stroboscope for observation. The stimuli required to initiate these flutters included burning the tarsi, genitalia and antennae with a hot wire and holding acetic acid near or brushing it on these structures. Such stimuli produced maximal responses from the insect. Flight under these conditions is different from normal flight. Therefore, I used only data obtained from animals which were minimally dissected (table 3).

Russenberger and Russenberger (1959) claim that the flight mechanism of a fresh dragonfly could be moved through its flight positions, and that such movements were largely identical to those of the freely flying individual. Similar treatment of *A. orthogonia*



was instructive, but, in part because of the wing folding mechanism the basic flight mechanism never operated in exactly the same way as that of the flying specimens observed. The posture of the flying animal was different because of the contraction of the tonic musculature, particularly the furcopleural muscle. In addition the wing base of *A. orthogonia* is more complex and less heavily sclerotized than that of the dragonfly.

Russenberger and Russenberger embedded dragonfly specimens in Araldite and obtained sections of them by milling successive 0.1mm layers from the Araldite. Photographs of each section produced in this way showed the serial sections of the specimens. They removed the muscles of these specimens with potassium hydroxide solution before embedding. The potassium hydroxide treatment of *A. orthogonia* left the posture of the thorax very different from the flight posture, and softened the sclerites. Thus embedding would be of no more value than simple observation of potassium hydroxide treated specimens. Specimens preserved in ethanol exhibit a wide range of thoracic postures due to variation in contraction of the flight muscles. None of such specimens are suitable for determining flight postures. One method by which the flight postures could be studied is by freezing flying specimens with liquid air. Such a specimen would have to be dissected while frozen.

It is tempting to draw an analogy between the mechanism of the thorax and wing base of *A. orthogonia*, and the 'click mechanism'



of the dipteran thorax first proposed by Boettiger and Furshpan (1952), and later explained by Pringle (1957). A major difference exists between dipterans and *A. orthogonia*; the anterior parascutum (the lateral shelf of the scutum which supports the anterior notal wing process) hinges on the scutum in Diptera, but fuses to the scutum to form a rigid structure in *A. orthogonia* (sect. 4.2.2.). Although this immediately removes the possibility of a 'click mechanism' in *A. orthogonia* like that of the dipterans, there remains the possibility that the mechanism of *A. orthogonia* may be bistable.

The first axillary sclerite pivots about the resilin pad which lies between the first axillary sclerite and the anterior notal wing process (sect. 4.4.1. and 4.4.5.). Since this pivot lies centrally on the first axillary sclerite, if this sclerite rotates through the anterodistal plane the distal end of it would move first distally then proximally, the proximal end first proximally and then distally. The area of the scutum between the anterior notal wing process and the median notal wing process or the thorax between the distal end of the first axillary sclerite and the pleural wing process might form a spring by which energy stored from an earlier part of the wing stroke cycle could be supplied to a later part of the wing stroke cycle. This cannot happen since the first axillary sclerite rotates to a position approximately in the anterodistal plane, but no further (sect. 4.4.5.).



Sharplin (pers. comm.) finds that when live specimens of *Pieris rapae* L. were rapidly frozen on dry ice and allowed to thaw, the wing takes up a fully up or down position. The wing may be moved freely, but is stable only in either of the extreme positions. The first and second axillary sclerites form a stiff, although differently orientated, unit during the up and downstrokes (sect. 4.4.5.). During the up and downstroke the wing base pushes the pleural wing process distally initially. As the median notal wing process passes the level of the pleural wing process-wing base ligaments the pleural wing process moves proximally, which releases any energy stored earlier in the stroke cycle. However, this movement is small. Storage of energy by the subtegular apodeme-pleural wing process unit may take the place by an increase in tension on the furcopleural muscle or its apodeme, by twisting the cuticle of the pleural ridge, or by stretching the prescutal-subtegular apodeme resilin ligament.

The resonant properties of the thorax and wing are important in many insects which possess a click action wing base (Pringle 1968). Since the wing beat frequency of *A. orthogonia* varies by as much as two times during the experimental period (about 20 minutes), the thorax-wing system resonance must be extremely variable, or of less importance to the flight of this species because the effective click action is small.

Supination and pronation in insects with myogenic flight muscles, such as Diptera and Hymenoptera, must be automatic



because the basalar and subalar musculature cannot contract rapidly enough to effectively pronate or supinate the wing during the flight cycle (Pringle 1957). Probably automatic pronation and supination is a feature of a large number of insects in addition to those with myogenic flight muscles. In a number of specimens of Zeugloptera, Monotrysia, and Ditrysia the articulation between the first axillary and second axillary of both fore and hind wings lies in the plane of the wing at an oblique angle to the longitudinal axis of the wing. The second axillary extends below the surface of the wing to the pleural wing process as does the ventral radius. Probably in all Lepidoptera during the downstroke the indirect as well as the direct muscles pronate the wing. During the upstroke the indirect muscles and aerodynamic forces on the wing supinate it about the first axillary-second axillary hinge, as in *A. orthogonia*.

The pronation and supination system described here for *A. orthogonia* can probably be extended beyond the Lepidoptera. Snodgrass (1929) described the wing base of *Dissosteria carolina* L. The first axillary-second axillary articulation again lies in the plane of the wing at an oblique angle to the longitudinal axis of the wing. The second axillary again connects to the posterior wing process below the surface of the wing. In the flight of *S. gregaria*, the notum moves dorsodistally and the posterior wing process resists the distal displacement of the lower end of the second axillary, which results in a 'click'



mechanism (Pringle 1957, from unpublished data of Weis-Fogh).

The pronation, supination system is probably much the same as that of *A. orthogonia*, although Snodgrass (1927, 1929) and Wilson (1962) proposed that the subalar musculature supinates, and the basalar musculature pronates the wing during the down-stroke.

Wilson and Weis-Fogh (1962) showed electrophysiologically that the subalar muscles of the fore wing only of *S. gregaria* were most active in the downstroke when the body angle was close to horizontal. This activity reduced as the body angle increased. The wings thus pronated more and supinated less, and in this way produced approximately the same lift at all body angles. It is possible that the mesothoracic subalar muscles of locusts and grasshoppers are a special case, and that the more general function of the subalar muscles is to pronate the wings together with the basalar muscles. Wilson and Weis-Fogh (1962) showed electrophysiologically that both the subalar and the indirect downstroke muscle fired before the top of the stroke in *S. gregaria* and that pronation occurred before the basalar muscles fired. Certainly the basalar muscles do not pronate the wing alone. The aerodynamic forces (Pringle 1957) and the mechanical structure of the wing base (Wilson and Weis-Fogh 1962) pronate the wing during the upstroke, probably about the first axillary-second axillary articulation as in *A. orthogonia*.



Pringle (1957) describes the general wing base structure of Coleoptera. During the downstroke the basalare pulls the pleural wing process proximally and the notum moves dorsodistally. Pringle (1957) suggests that the basalar muscles pronate and depress the wing, but that the subalar simply depresses the wing along with the indirect muscles. The first axillary-second axillary articulation lies in the plane of the wing at an oblique angle to the longitudinal axis of the wing, and the second axillary joins the posterior wing process below the surface of the wing. The indirect, subalar, and basalar muscles probably all pronate the wing during the downstroke. The first axillary-subcostal junction lies distal to the line of action of the first axillary-second axillary hinge, hence, ventral rotation of the distal end of the first axillary accompanies pronation about the first axillary-second axillary hinge. The first axillary attaches close to the anterior extremity of the notum. Hence it is held ventrally while the posterior end of the first axillary rotates dorsally during the downstroke. The hind wing of Lepidoptera operates in a very similar way. The aerodynamic force probably supinates the wing in the upstroke about the same hinge axes.

In Pringle's (1957) investigation of the function of the wing base of Hymenoptera (*Apis mellifera* L. and *Xylocopa tenuiscapa* Westwood), he concludes that pronation and supination are automatic. The first axillary of *A. mellifera* has a long anterior



extension which lies far distal to the first axillary-second axillary hinge. Pringle (1957) believes that the notum places a twisting moment on the first axillary which pronates and depresses the wing in the downstroke and supinates and elevates the wing in the upstroke. Probably the wing base of the Hymenoptera functions much the same as the wing base of the Coleoptera. When the scutellar arm moves forward it moves the first axillary forward, which in turn pushes forward on the top of the second axillary. The posterior wing process restrains the bottom of the second axillary. When the first and second axillary hinge limits the rotation of these sclerites about each other, the wing has been pronated about the first-second axillary hinge. The first and second axillaries then rotate as described by Pringle (1957) to depress the wing about the first-second axillary hinge. The wing supinates about the first-second axillary hinge and then elevates when the scutellar arm moves posteriorly on the first axillary.

Pringle (1957) shows that the pronation and supination of the wings of Diptera is due to the limited rotation of the first axillary on the anterior end of the scutellar lever. However, again the first-second axillary junction lies in the plane of the wing at an oblique angle to the longitudinal axis of the wing. The second axillary articulates with the posterior wing process below the wing. Some additional pronation and supination may take place about the first-second axillary hinge. Pronation



about this hinge would take place at the beginning of both up and downstrokes; supination, in the latter part of both up and downstrokes.

Barber and Pringle (1966) suggest that pronation and supination of the wings of belostomatid bugs is automatic. They indicate that there are four sets of fibrillar flight muscles which produce the wing elevation, depression, pronation, and supination. The dorsal longitudinal and basalar muscles pronate and depress the wing, the dorsoventral and lateral oblique dorsal longitudinal muscles supinate and elevate the wing. The first-second axillary hinge of *G. oculatus*, another Heteropteran, lies in the plane of the wing, and at an oblique angle to the longitudinal axis of the wing (Parsons 1960). As in *A. orthogonia* pronation and supination probably take place about this hinge in Heteroptera.

The lateral oblique dorsal longitudinal muscle is active at flight initiation and during the upstroke (Barber and Pringle 1966). Since the distal end of the phragma is lever-like and the fourth and third axillary system of *G. oculatus* (Parsons 1969) appears to be somewhat like that of *A. orthogonia*, it is possible that the lateral oblique dorsal longitudinal muscle may protract the wing at flight initiation, and hold the wing protracted during the upstroke, as in *A. orthogonia*.

The wings of the Odonata and Ephemeroptera do not pronate or supinate about the first-second axillary hinge. However,



insects of neopterous origin probably all exhibit some tendency to pronate and supinate their wings about this hinge.



## 6. Conclusion .

The notum and pleuron function as a diamond shaped structure. The region of bending in the notum and the central hinge of the pleuron, although not obvious, are important to the function of this structure. Both of these hinges and the anterior hinge probably store energy from one part of the stroke cycle to be used in a following part of the cycle.

The posterior hinge, the region of the laterophragma, functions with the lateral oblique dorsal longitudinal muscle to protract the wing through the third axillary complex. This system is probably common to all Lepidoptera. The Heteroptera may also have a similar system for wing protraction.

The dorsal longitudinal, basalar, and subalar muscles all pronate the wing about the first-second axillary hinge, and depress the wing about the wing base notal articulations. This system is common to the fore and hind wings of all Lepidoptera. This system probably forms the bases for pronation and depression in a large number of other insects, and is probably present to some extent in all insects of neopterous origin. The insects with high wing beat frequencies have developed a mechanical means of supination during the upstroke. The Lepidoptera and many other insects with slower wing beat frequencies depend upon aerodynamic forces as well as mechanical means to supinate the wing. This supination takes place about the first-second axillary hinge.



## 7. Tables and Figures

Table 1. Abbreviations of terms used in the figures for the flight structures of *A. orthogonia*

[Nouns begin with a capital letter, adjectives with a lower case letter. Full stops follow abbreviated words.]

A. - Anal vein	Fu. - Furca
a. - anterior	Fus. - Furcasternum
Ad. - Apodeme	I. - Insertion
Aeps. - Anepisternum	In. - Incision
an. - anal	int. - internal
Art. - Articulation	Iv. - Invagination
Ax. - Axillary sclerite	Keps. - Katepisternum
ax. - axillary	l. - longitudinal (lateral in Sharplin 1963a,b)
B. - Bridge	lat. - lateral
Ba. - Basalare	Lig. - Ligament (Li in Sharplin 1963a,b)
ba. - basalar	Lph. - Laterophragma
Bc. - Basicosta	M. - Media
bd. - bending	m. - median
B1. - Blade	Mb. - Membrane
C. - Costa	Mer. - Meron
Cd. - Cord	Mu. - Muscle
Ct. - Cuticle	N. - Notum
Cu. - Cubitus	obl. - oblique
Cx. - Coxa	P. - Pleuron
d. - dorsal	Peps. - Pre-episternum
dl. - dorsal longitudinal	Ph. - Phragma
di. - distal	Pl. - Plate
Epm. - Epimeron	po. - posterior
Eps. - Episternum	Pr. - Process
ex. - external	
F. - Frenulum (fold in Sharplin 1963a)	



Table 1 (Cont'd)

Ps. - Presternum  
 Psc. - Prescutum  
 px. - proximal  
 R. - Radius  
 r. - radial  
 Re. - Retinaculum  
 Ri. - Ridge  
 S. - Sternum  
 Sa. - Subalare  
 sa. - subalar  
 Sc. - Subcosta  
 Scl. - Scutellum  
 Sct. - Scutum  
 Sl. - Scale  
 Sp. - Spiracle  
 Ss. - Spinasternum  
 Stcx. - Sternocoxale  
 Stg. - Subtegula (Subtg. in Sharplin 1963a)  
 Su. - Suture  
 T. - Tergum  
 Te. - Tendon cap  
 Tg. - Tegula  
 Tr. - Trochanter  
 Tra. - Trachea  
 v. - ventral  
 W. - Wing



Table 2. Abbreviations of terms used for the flight muscles of  
*A. orthogonia*, and the equivalent abbreviated terms  
used for the flight muscles of *T. polyphemus* by Nüesch  
(1953)

[all muscles tabulated are represented in both meso- and metathorax except for those indicated (§, †). The prefixes I, II, and III indicate muscles of the pro-, meso-, and metathorax respectively.]

Muscle	Abbreviation	Nüesch
<i>Large Indirect Acting Muscles</i>		
<i>Longitudinals</i>		
first dorsal longitudinal	d.l <sub>1a-e</sub>	d <sub>11</sub>
lateral oblique dorsal longitudinal	lat.obl.d.1.	d <sub>12</sub>
<i>Dorsoventrals</i>		
anterior tergosternal	a.t.-s.	d <sub>v1a</sub>
posterior tergosternal	po.t.-s.	d <sub>v1b</sub>
tergosternal	t.-s.	d <sub>v1</sub>
anterior tergocostral	a.t.-cx.	d <sub>v2</sub>
tergotrochanteral	t.-tr.	d <sub>v3a+b</sub>
posterior tergocostral <sub>a</sub>	po.t.-cxa	d <sub>v5</sub>
posterior tergocostral <sub>b</sub>	po.t.-cx <sub>b</sub>	d <sub>v4</sub>
<i>Large Direct Acting Muscles</i>		
sternobasalar	s.-ba.	p <sub>v1</sub>
coxobasalar	cx.-ba.	p <sub>v2</sub>
trochanterobasalar	tr.-ba.	p <sub>v3</sub>
coxosubalar <sub>a</sub>	cx.-saa	p <sub>v5</sub>
coxosubalar <sub>b</sub>	cx.-sab	p <sub>v4</sub>
pleurosubalar	p.-sa	p <sub>1</sub>



Table 2 (Cont'd)

*Small Muscles*

third dorsal longitudinal	d1 <sub>3</sub>	d1 <sub>3</sub>	§
first ventral longitudinal	v.1 <sub>1</sub>	v1 <sub>1</sub>	
second ventral longitudinal	v.1 <sub>2</sub>	v1 <sub>2</sub>	++
tergobasalar	t.-ba.	pd <sub>5</sub>	
prescutal-basalar	psc.-ba.	pd <sub>1</sub>	§
furcupleural	fu.-p.	pv <sub>7</sub>	
furcobasalar	fu.ba.	pv <sub>8</sub>	+
pleuroprescutal apodeme	p.-psc.ad.	p <sub>2</sub>	† *
pleurosutegular	p.-stg.	pd <sub>4</sub>	§
pleural-third axillary <sub>a+b</sub>	p.-3ax <sub>a+b</sub>	pd <sub>2a,b,c</sub>	§
pleural-third axillary <sub>a+b+c</sub>	p.-3ax <sub>a+b+c</sub>	pd <sub>a,b,c</sub>	†
pleural-first axillary	p.-lax.	pd <sub>3</sub>	
Pleurocoxal	p.-cx.	pv <sub>6</sub>	

\*This must be Sharplin's (1963b) 3t.-p. muscle, not the spiracular dilator muscle of Nüesch (1953) as suggested by Sharplin (1963b).

Legend: § mesothorax only  
† metathorax only  
++ not illustrated for the metathorax



Table 3. The limits of movement of the right side of the mesothoracic notum of *A. orthogonia* and the associated sclerites of its wing base.

[The arrow head indicates the maximum downstroke position, the tail indicates the maximum upstroke position.]

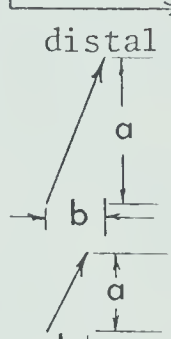
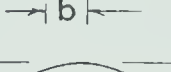
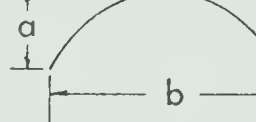
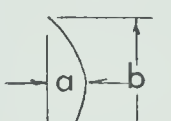
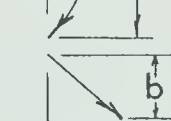
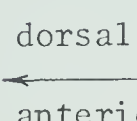
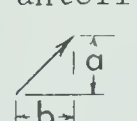
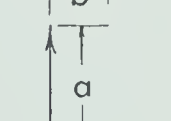
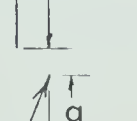
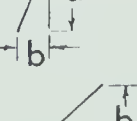
Structure	Movement (mm)	Orientation	Mutilation required to observe movements
<u>FRONTAL PLANE</u>			
m.n.w.pr.-lax. hinge	a=0.37 b=0.15		tegula removed
a.n.w.pr.-lax. hinge	a=0.20 b=0.11		tegula removed
lax.-2ax. articulation	a=0.21 b=0.58 c=0.21		the Sc. and tegula removed
v.2x.-p.w.pr. lig. at its base on 2 ax.	a=0.10 b=0.36		the Sc. and tegula removed
p.w.pr. tip	a=0.19 b=0.16		the Sc. and tegula removed
Ba.	See fig. 39a,b,c		tegula removed
<u>SIDE PLANE</u>			
mesoprescutum	a=0.15 b=0.15		tegula removed
m.n.w.pr.-lax. hinge	a=0.37		tegula removed
a.n.w.pr.-lax. hinge	a=0.20 b=0.09		tegula removed
Sa.	a=0.22 b=0.20		tegula removed
Ba.	See fig. 39a,b,c		tegula removed

Fig. 1. Semi-diagrammatic dorsal view of the right fore wing base. In this illustration the epimeron and laterophragma have been flattened into the plane of the wing. The tegula is not illustrated. The star adjacent to the dorsal second axillary indicates the approximate position of the pleural wing process when the wing is horizontal.

Fig. 2. Semi-diagrammatic side view of the left mesothoracic pleural and notal region and ventral region of the fore wing. The wing is in an elevated position. The tegula is not illustrated. The preepisternal region has been folded into the plane of the illustration.

Note: Black indicates a thick sclerite; diagonal lines, a thin sclerite; cross hatching, the scale plate; close stipple, bending cuticle; scattered stipple, membrane; clear areas, ligaments.



Fig. 3. Semi-diagrammatic dorsal view of the right hind wing base.

Fig. 4. Semi-diagrammatic side view of the left metathoracic pleural region and ventral region of the hind wing. The hind wing is in an elevated position.

Note: Black indicates a thick sclerite; diagonal lines, a thin sclerite; cross hatching, the scale plate; close stipple, bending cuticle; scattered stipple, membrane; clear areas, ligaments.

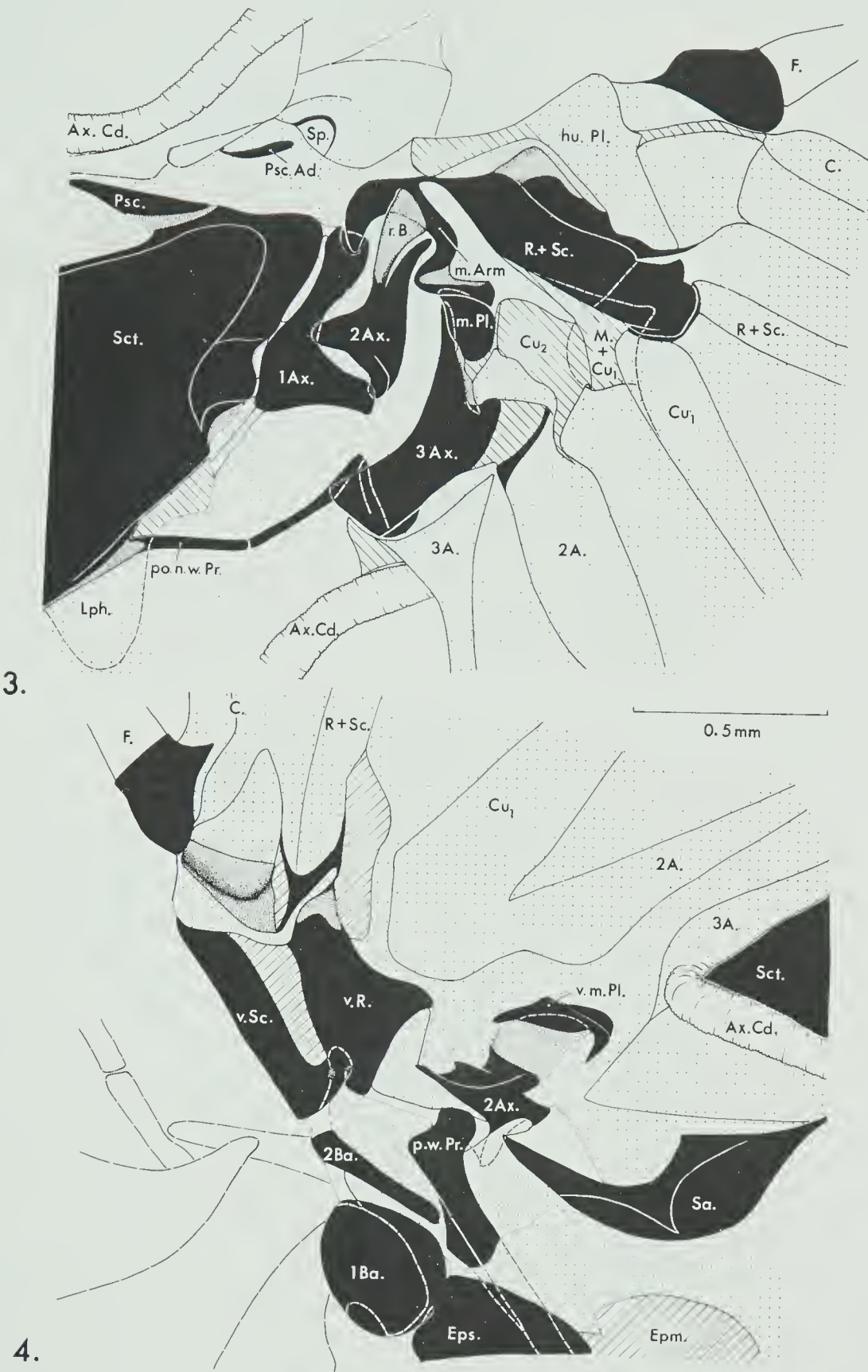
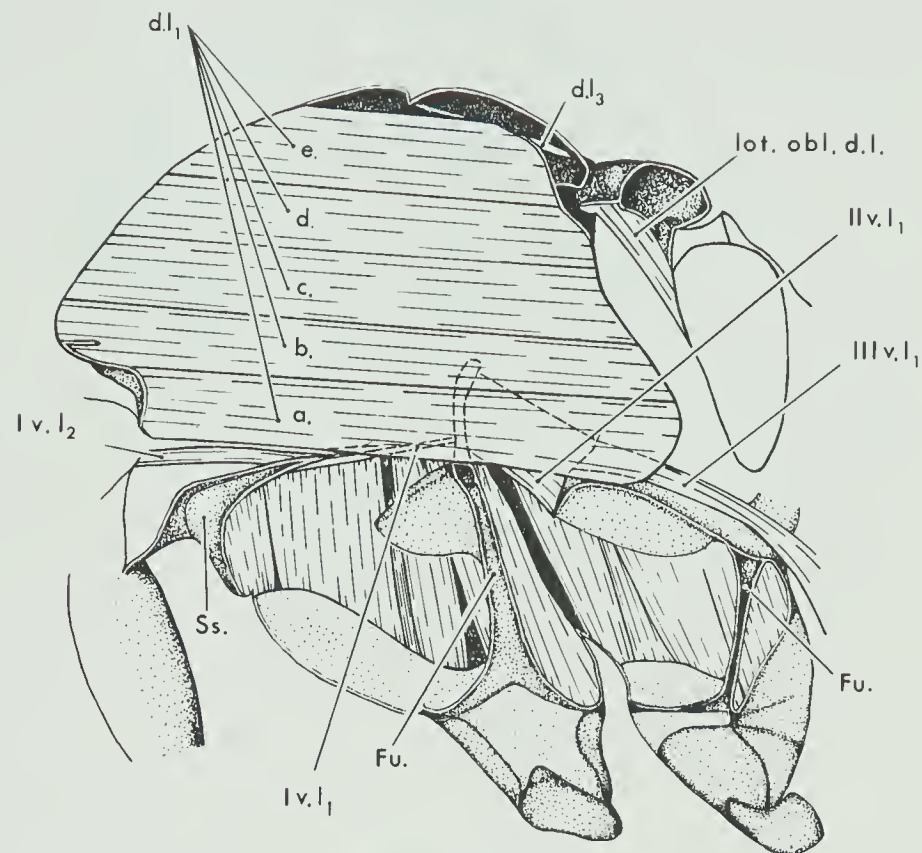
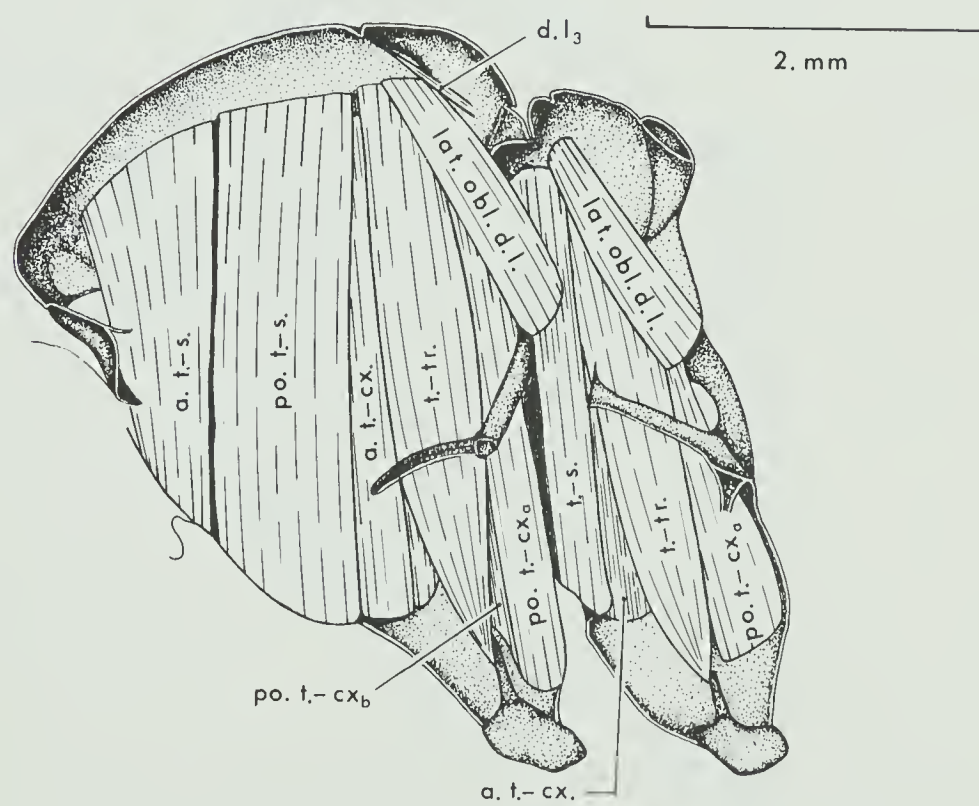


Fig. 5. Lateral inside view of the right side of a sagittal section of the pterothroax.

Fig. 6. Lateral inside view of the right side of a sagittal section of the pterothorax with the longitudinal muscles and the phragma removed.



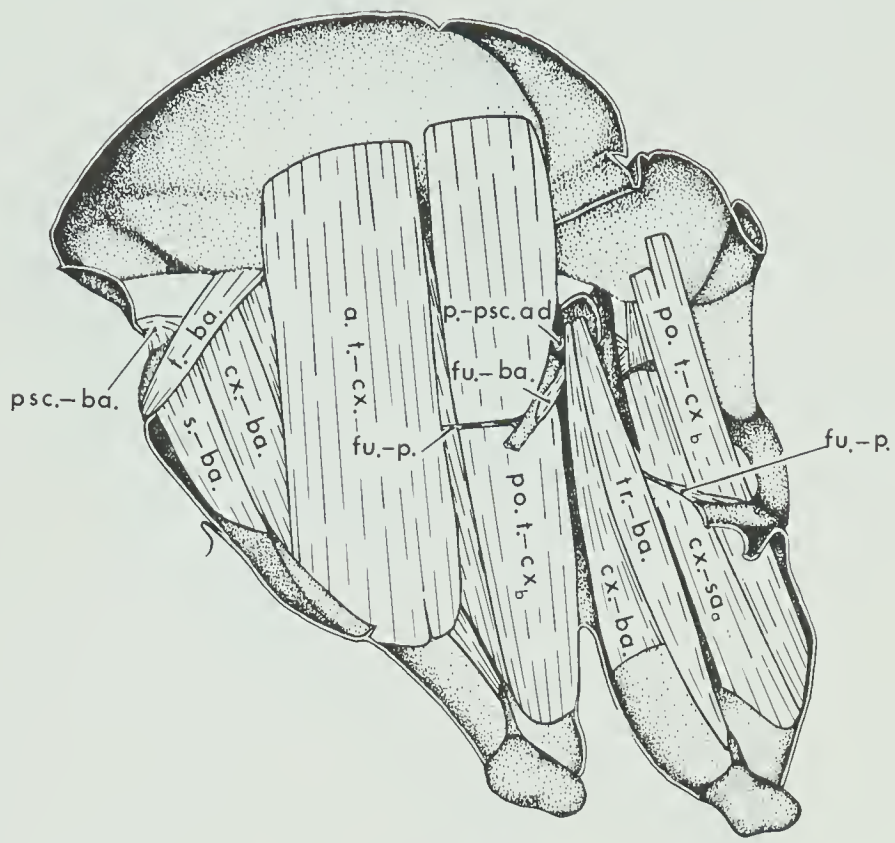
5.



6.

Fig. 7. Lateral inside view of the right side of a sagittal section of the pterothorax with the longitudinal and proximal dorsoventral muscles, and the phragma removed.

Fig. 8. Lateral inside view of the right side of a sagittal section of the pterothorax with the longitudinal and dorsoventral muscles, and the phragma removed.



2. mm

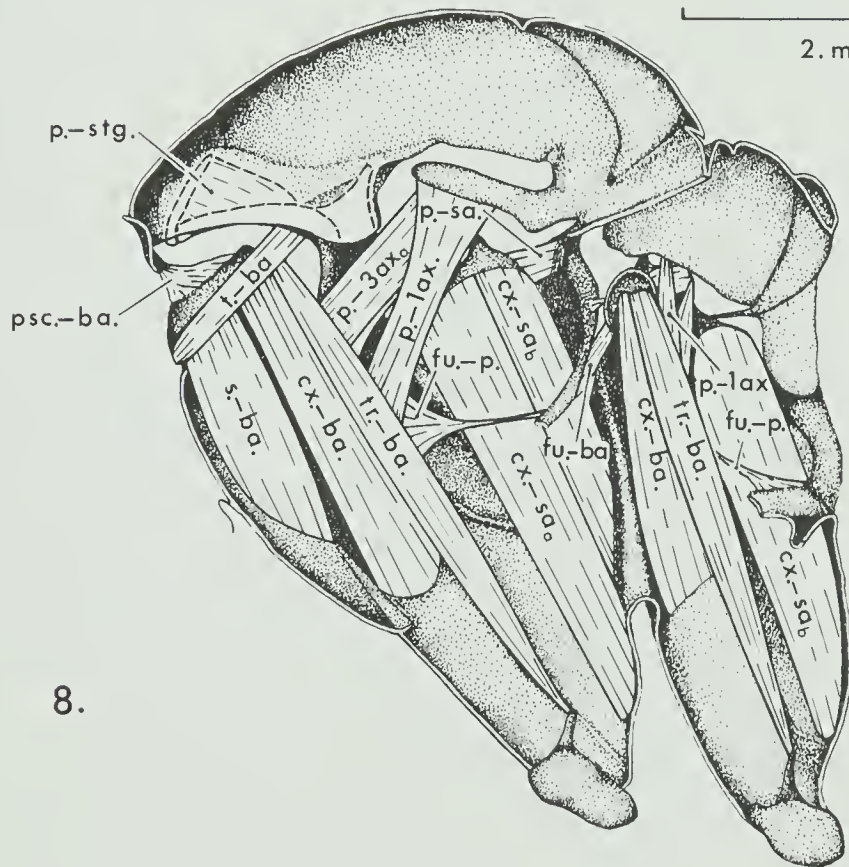


Fig. 9. Lateral inside view of a sagittal section of the pterothorax with all the longitudinal, indirect acting dorsoventral, and most of the large direct acting muscles, and the phragma removed.

Fig. 10. Left side view of the pterothorax with the wing, wing base, and tegula removed.

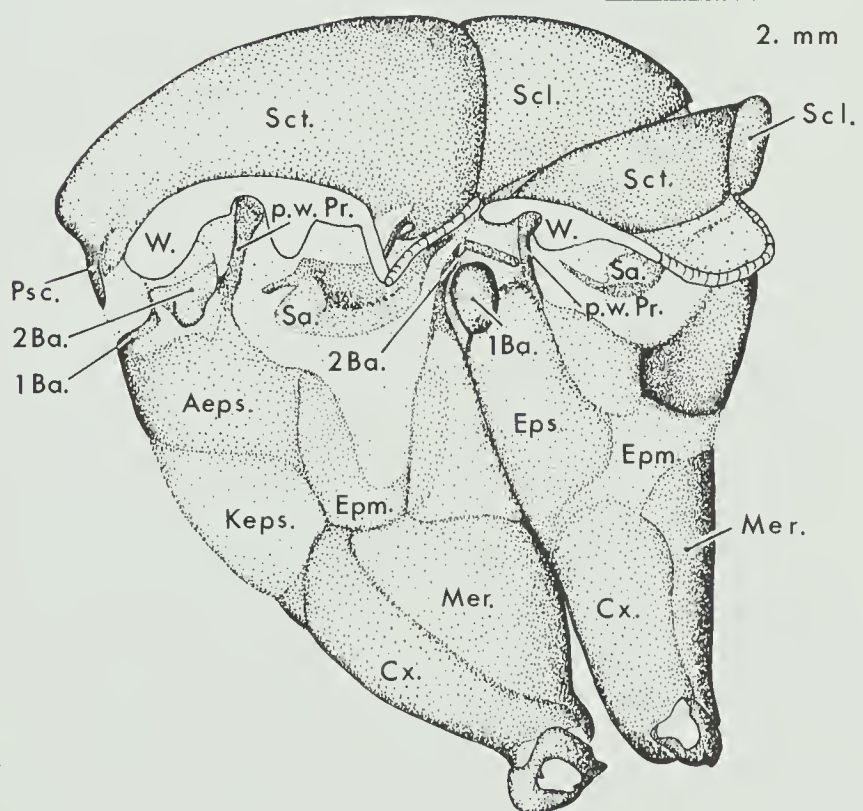
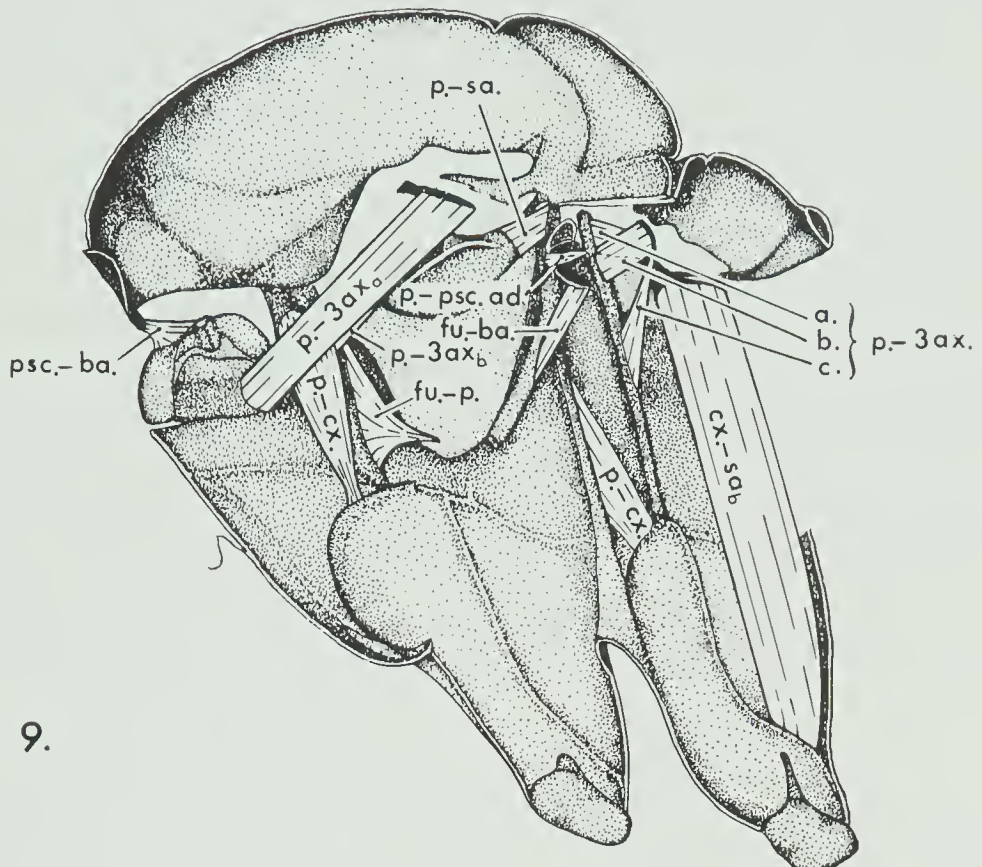


Fig. 11. Side view of the left pterothorax with the levels and orientations of sections 11a, 11b, and 11c indicated.

Fig. 11a. Cross-section of the mesothoracic dorsal longitudinal muscles.

Fig. 11b. Cross-section of the mesothoracic dorso-ventral muscles.

Fig. 11c. Cross-section of the metathoracic dorso-ventral muscles.

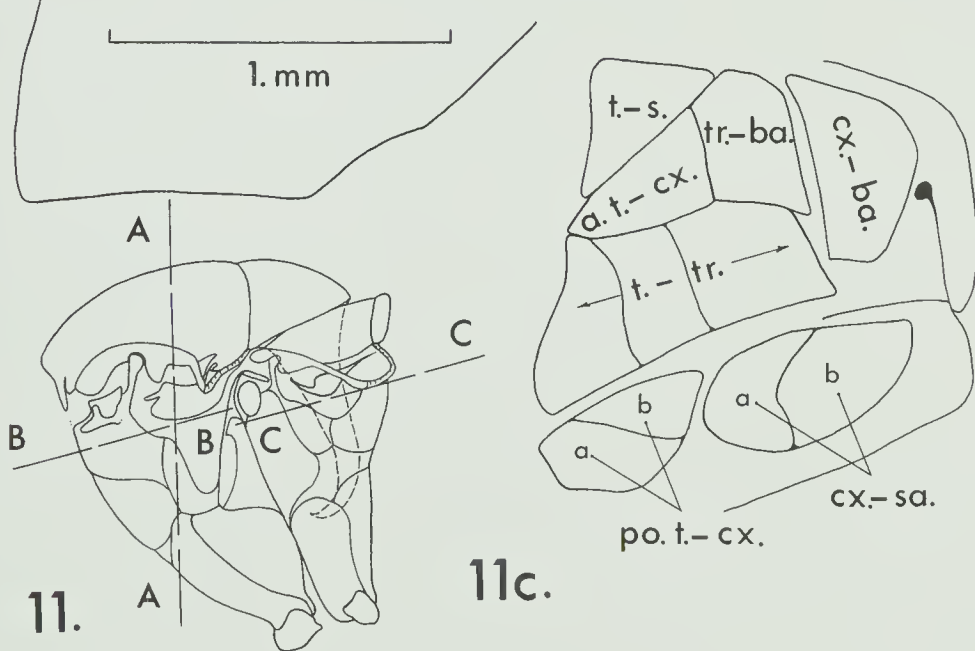
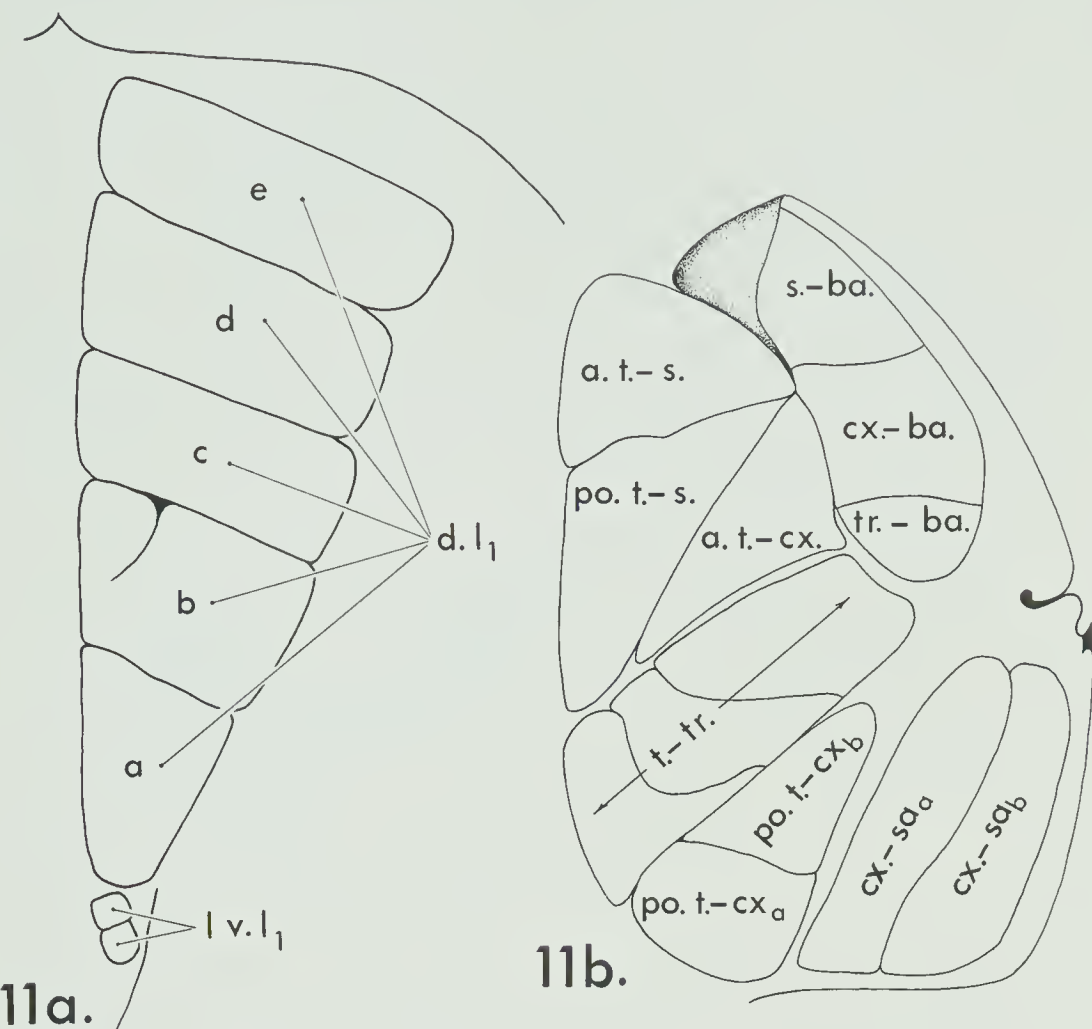
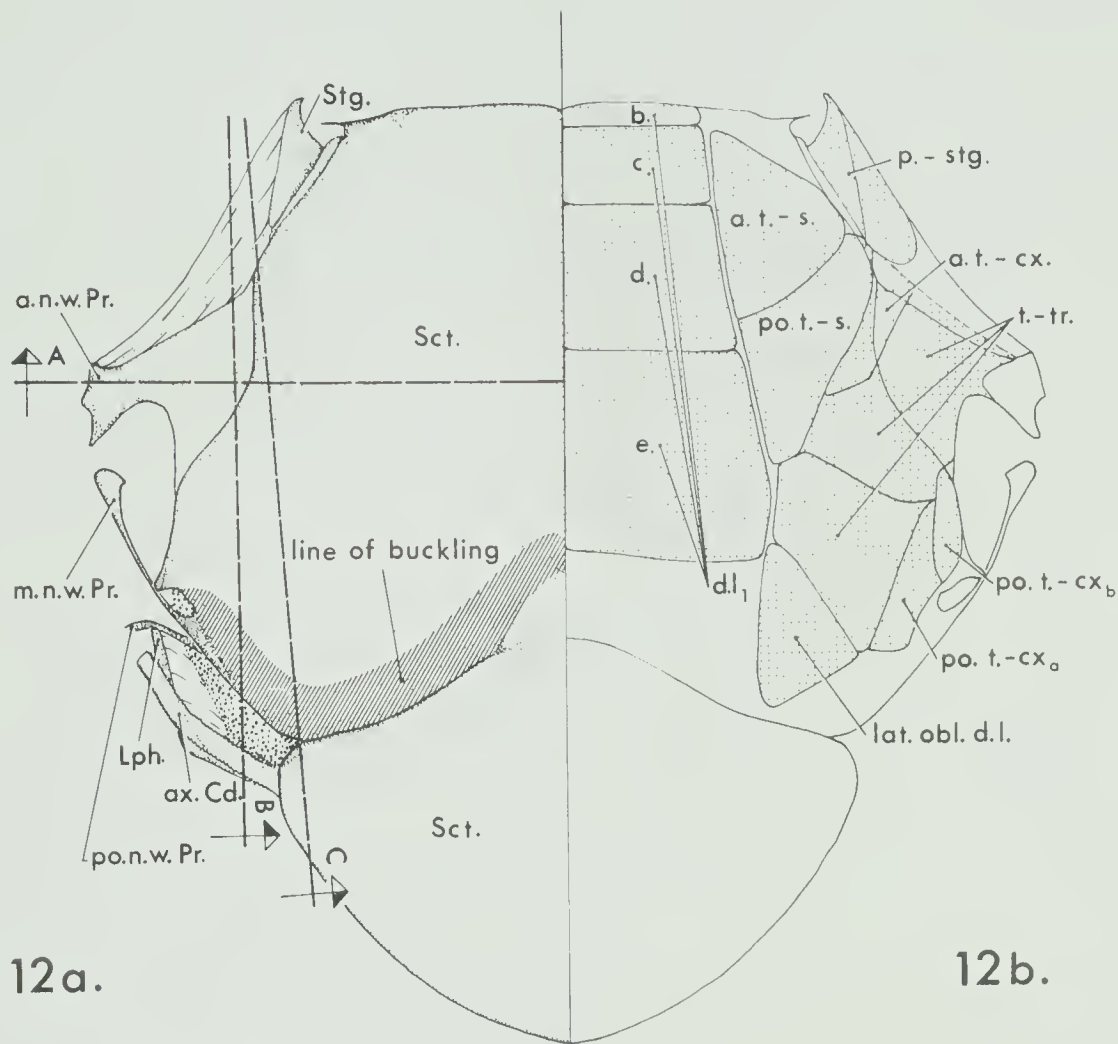


Fig. 12a. Top view of the left half of the mesonotum with  
the line of buckling indicated (cross hatched).

Fig. 12b. Top view of the right half of the mesonotum  
with the insertions of the flight muscles  
indicated.



12a.

12b.

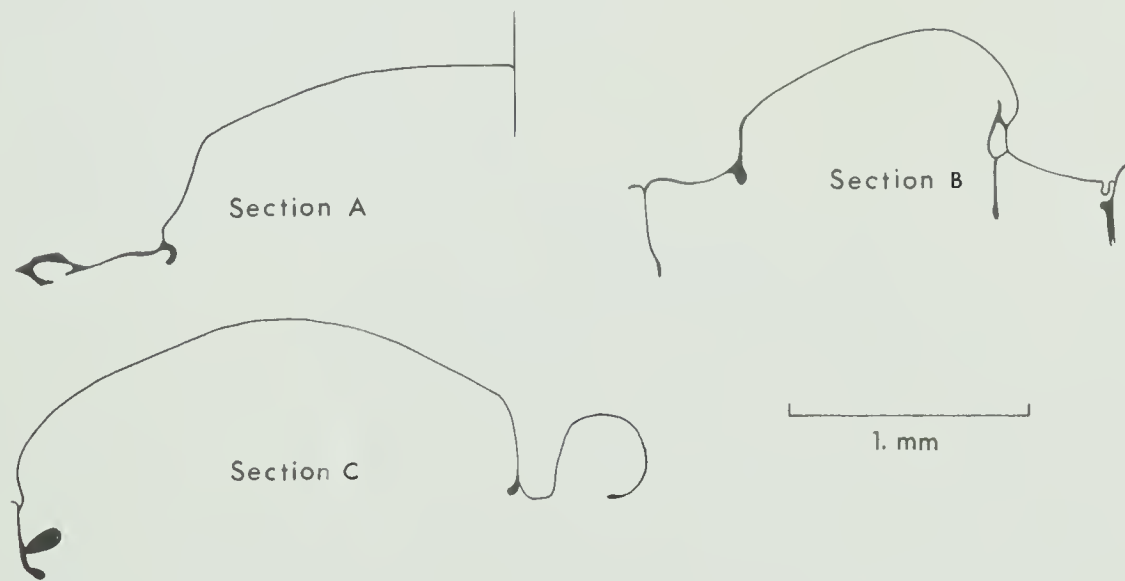
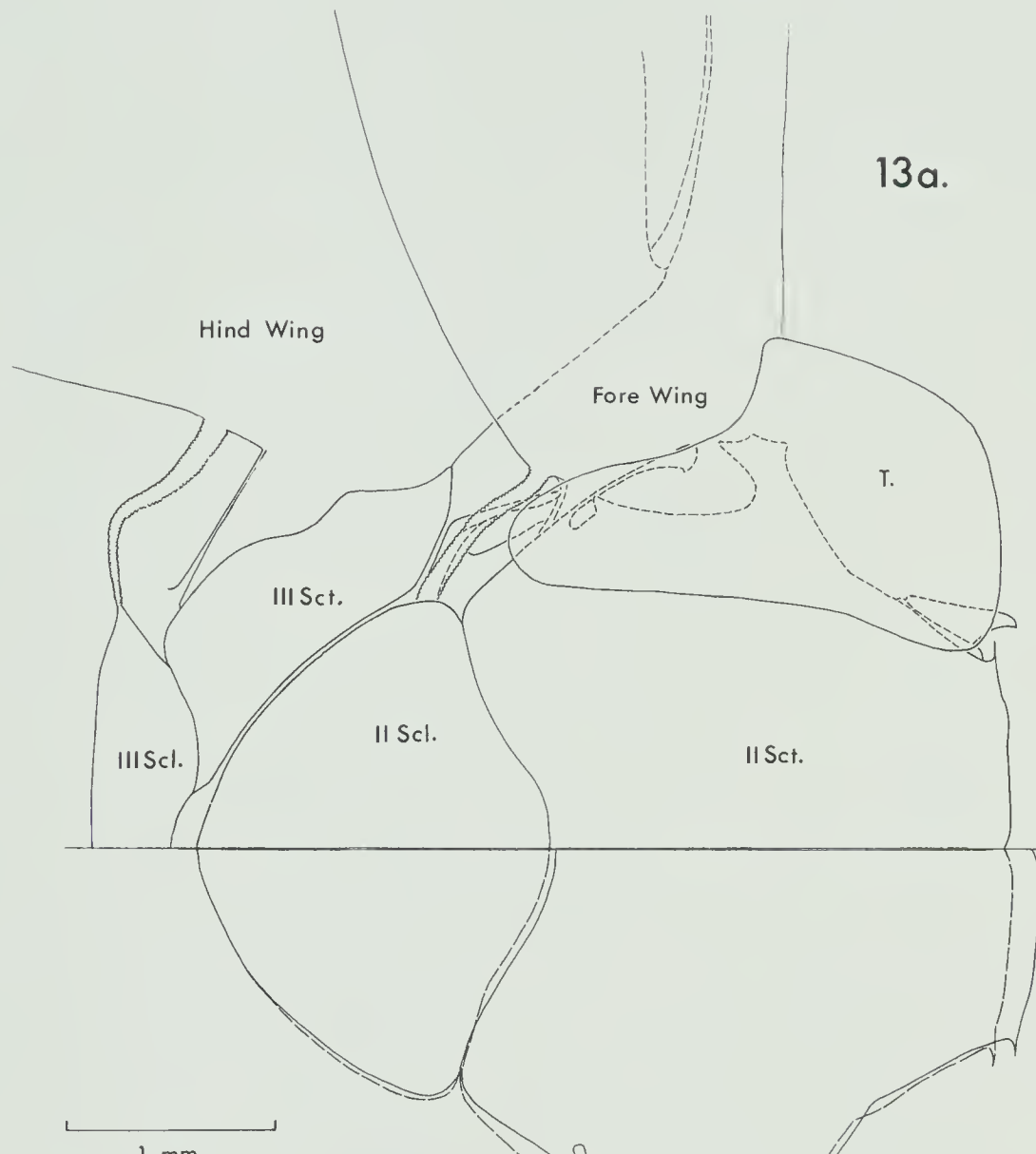


Fig. 13a. Top view of the left side of the pterothorax.

Fig. 13b. Top view of the right side of the mesothorax  
with the maximum upstroke positions indicated  
by solid lines, and the maximum downstroke  
positions indicated by broken lines.

13a.



13b.

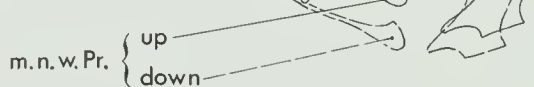
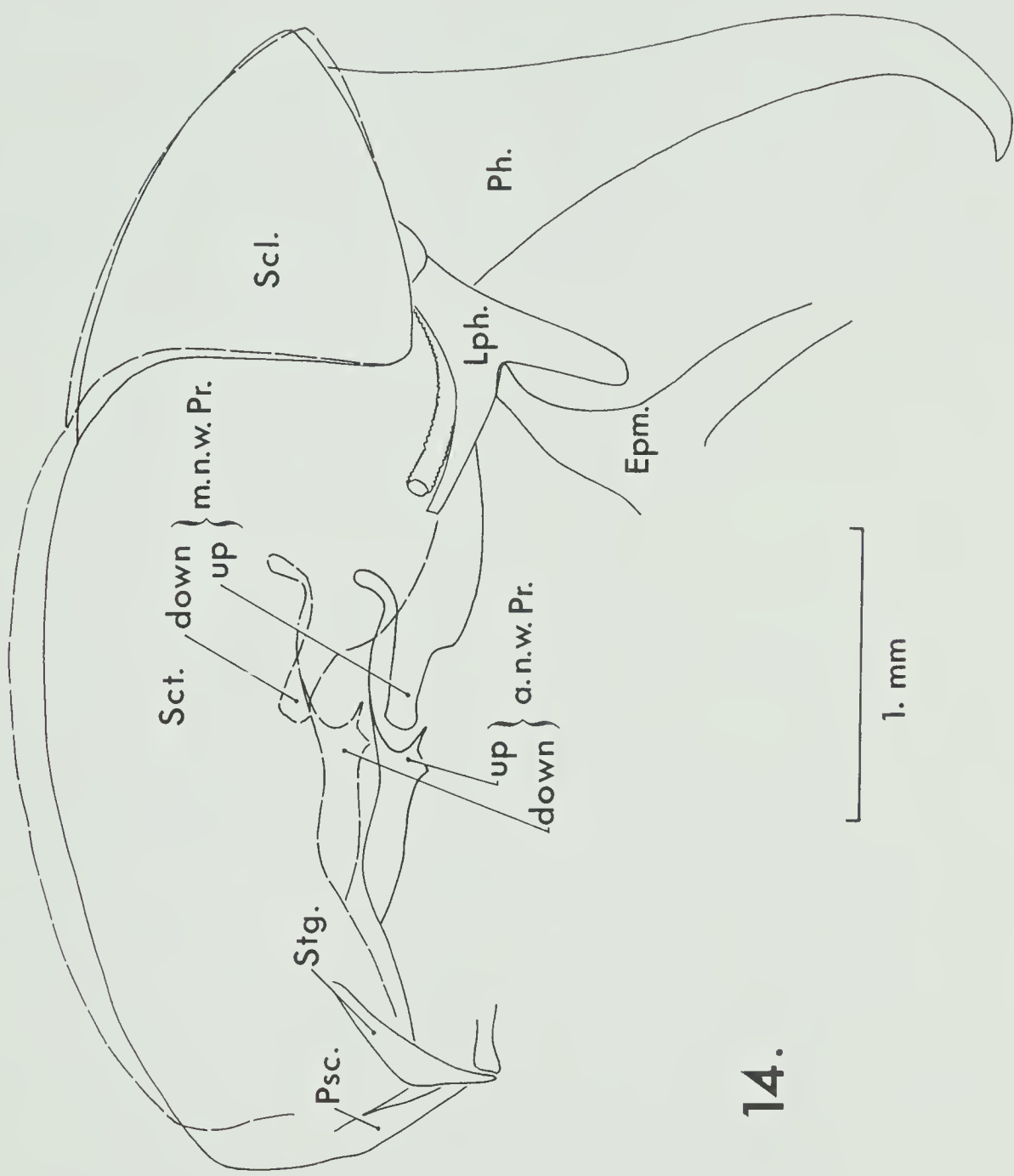


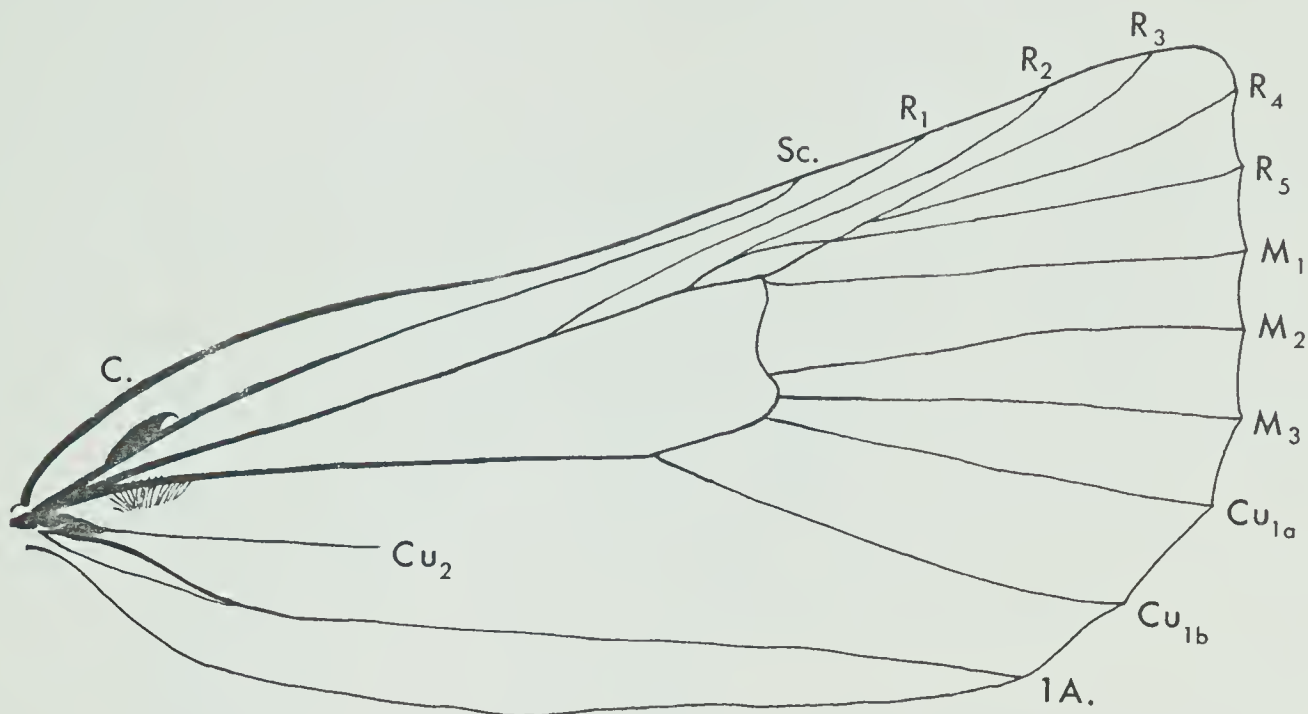
Fig. 14. Side view of the left side of the mesothorax  
with the maximum upstroke positions indicated  
by solid lines, and the maximum downstroke  
positions indicated by broken lines.



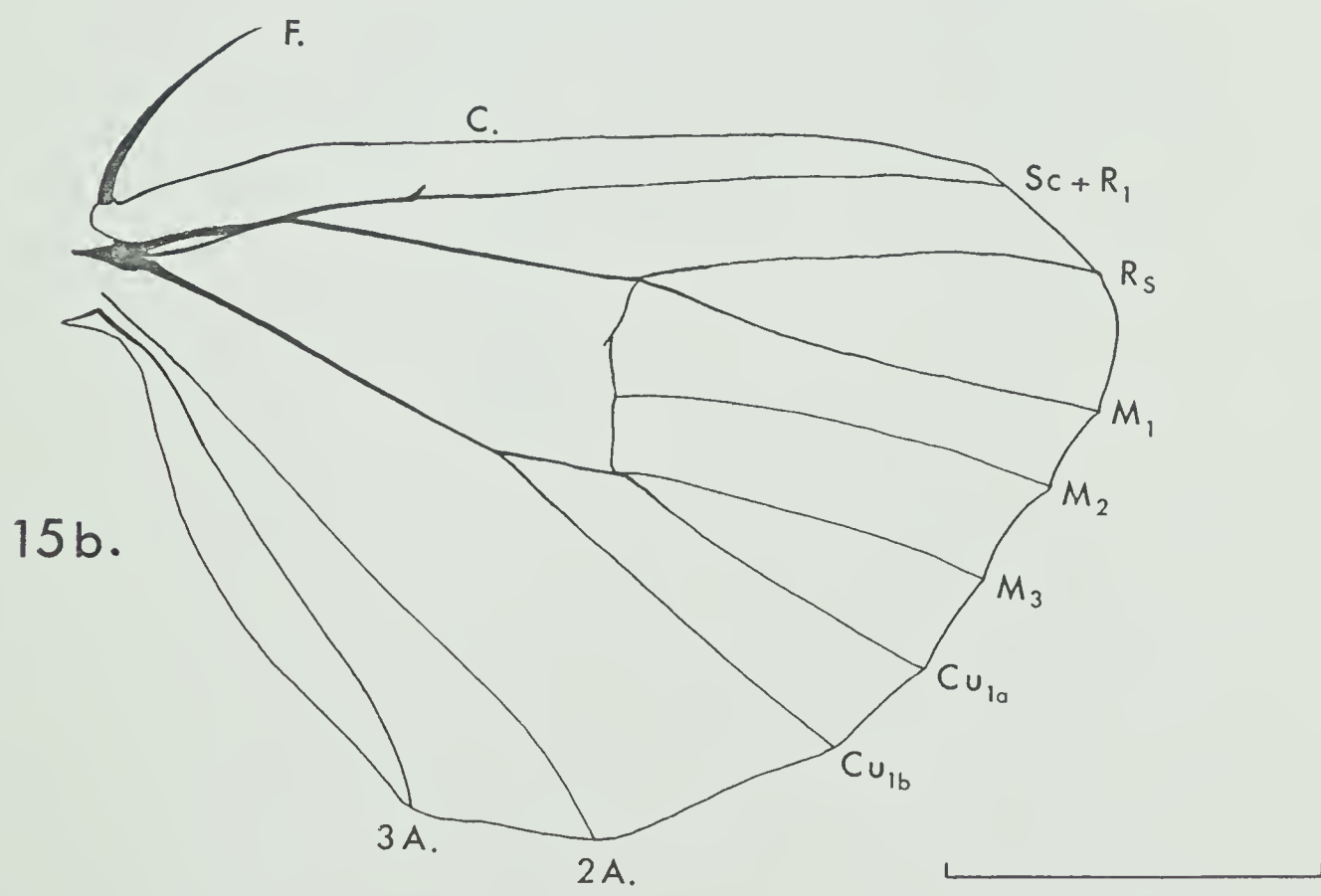
14.

Fig. 15a. Top view of the right fore wing.

Fig. 15b. Top view of the right hind wing.



15a.



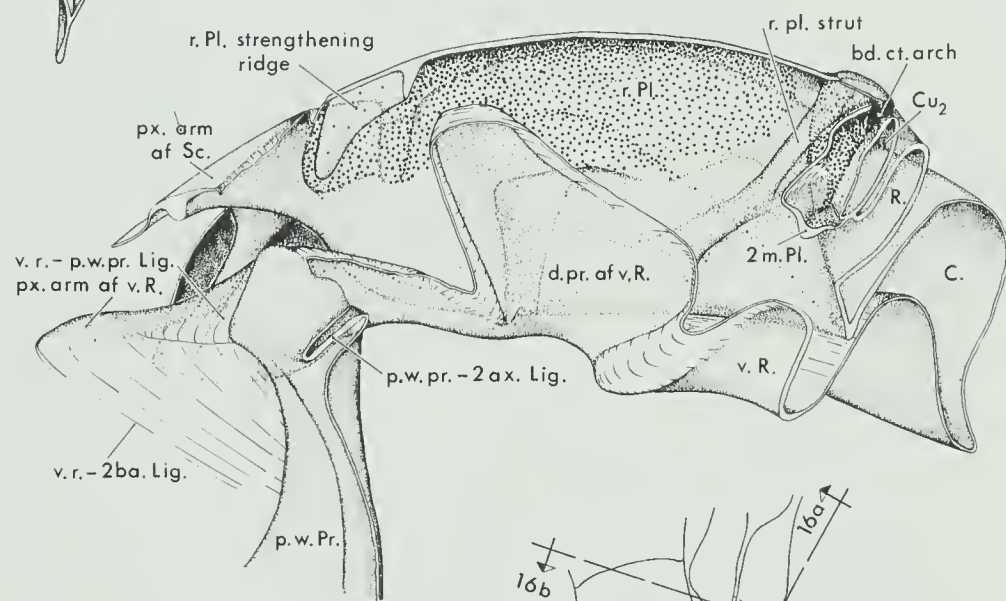
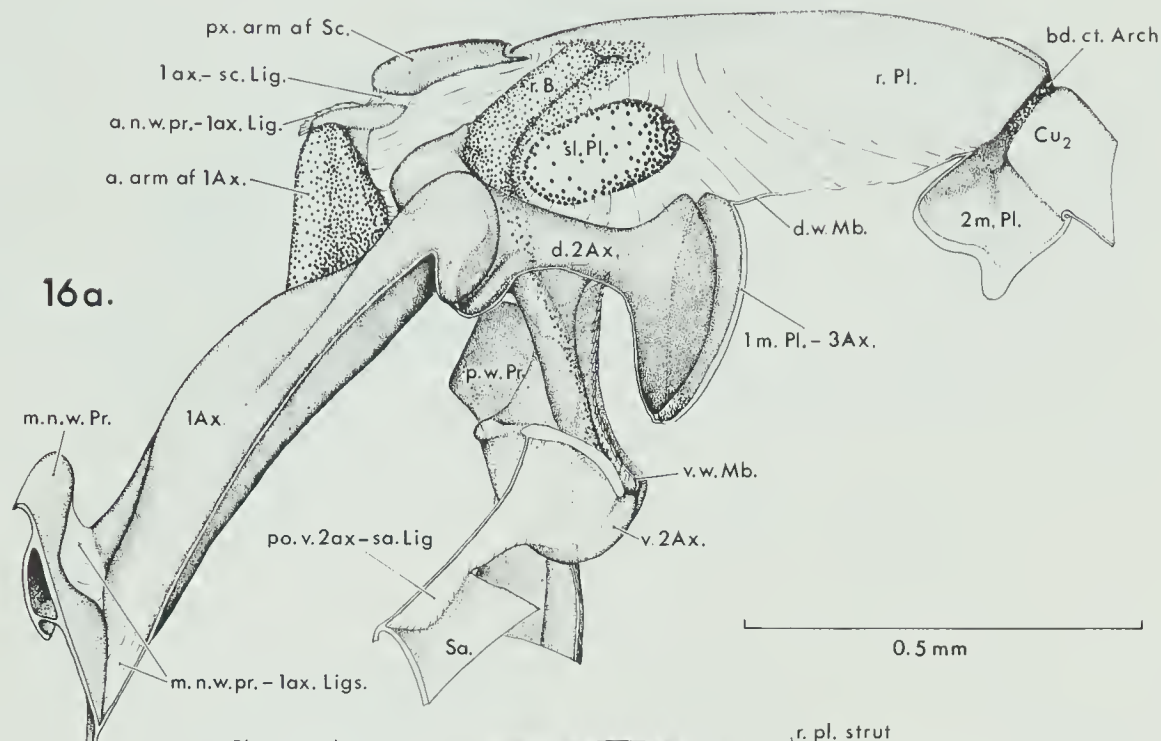
15b.

5. mm

Fig. 16. Top view of the right fore wing base with the levels and orientations of sections 16a and 16b indicated.

Fig. 16a. Dorsoposterior view of a section through the right fore wing base just posterior to the first and second axillaries, and the radial plate.

Fig. 16b. Posterior view of a section through the right fore wing dorsal subcosta, radial plate, ventral radius, and second median plate.



**16b.**

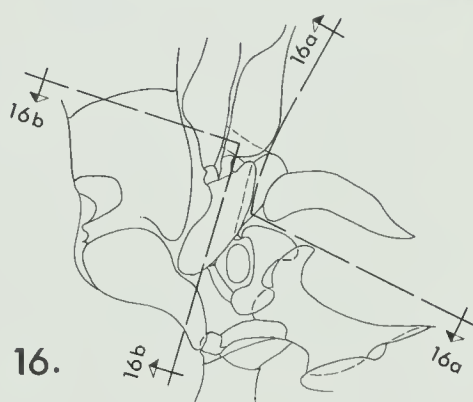
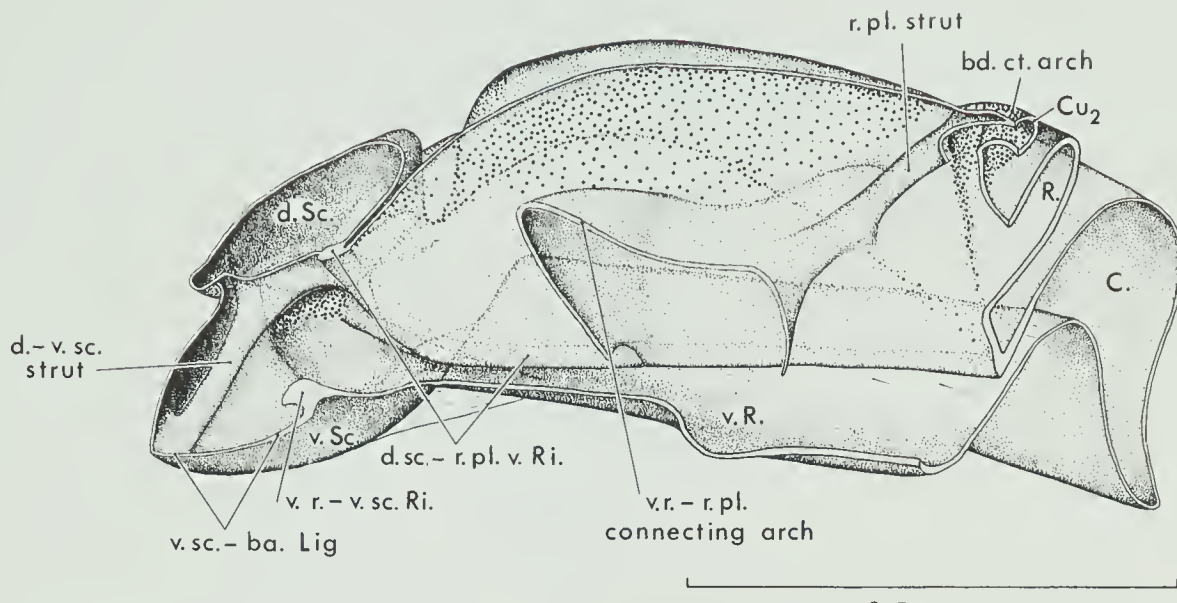


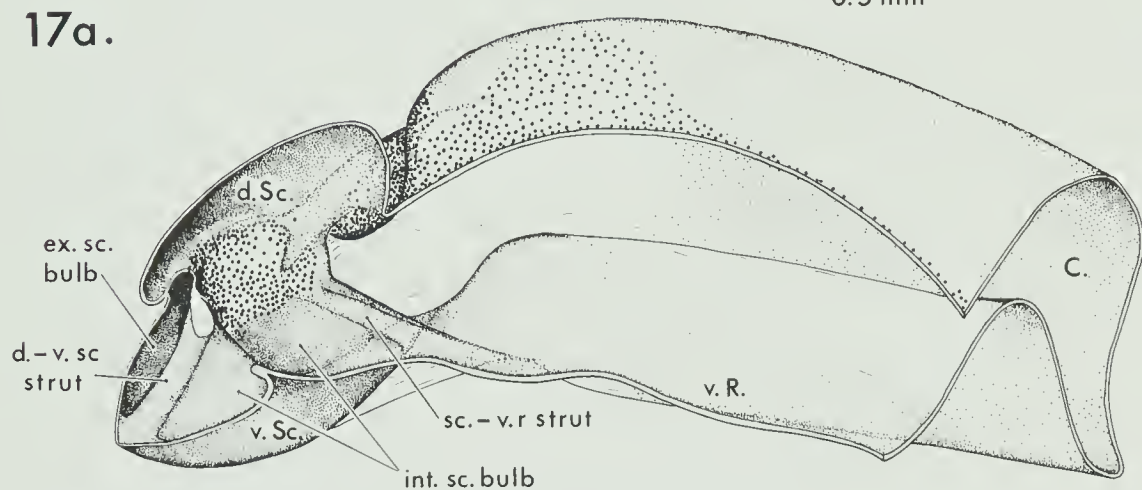
Fig. 17. Top view of the right fore wing base with the levels and orientations of sections 17a and 17b indicated.

Fig. 17a. Posterior view of a section through the right fore wing ventral subcosta, dorsal subcosta, ventral radius, and radial plate.

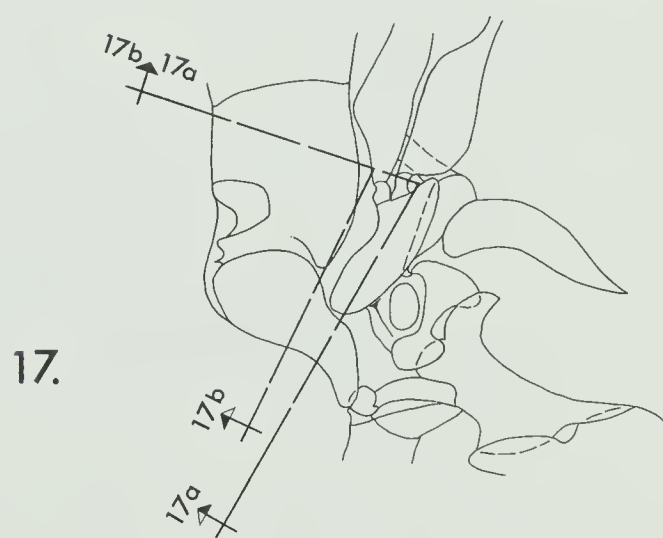
Fig. 17b. Posterior view of a section through the right fore wing ventral subcosta, dorsal subcosta, ventral radius, and costal-subcostal margin.



17a.



17b.



17.

Fig. 18. Side view of the second axillary complex of  
the right fore wing.

Fig. 19. Side view of the left mesothoracic basalar  
complex.

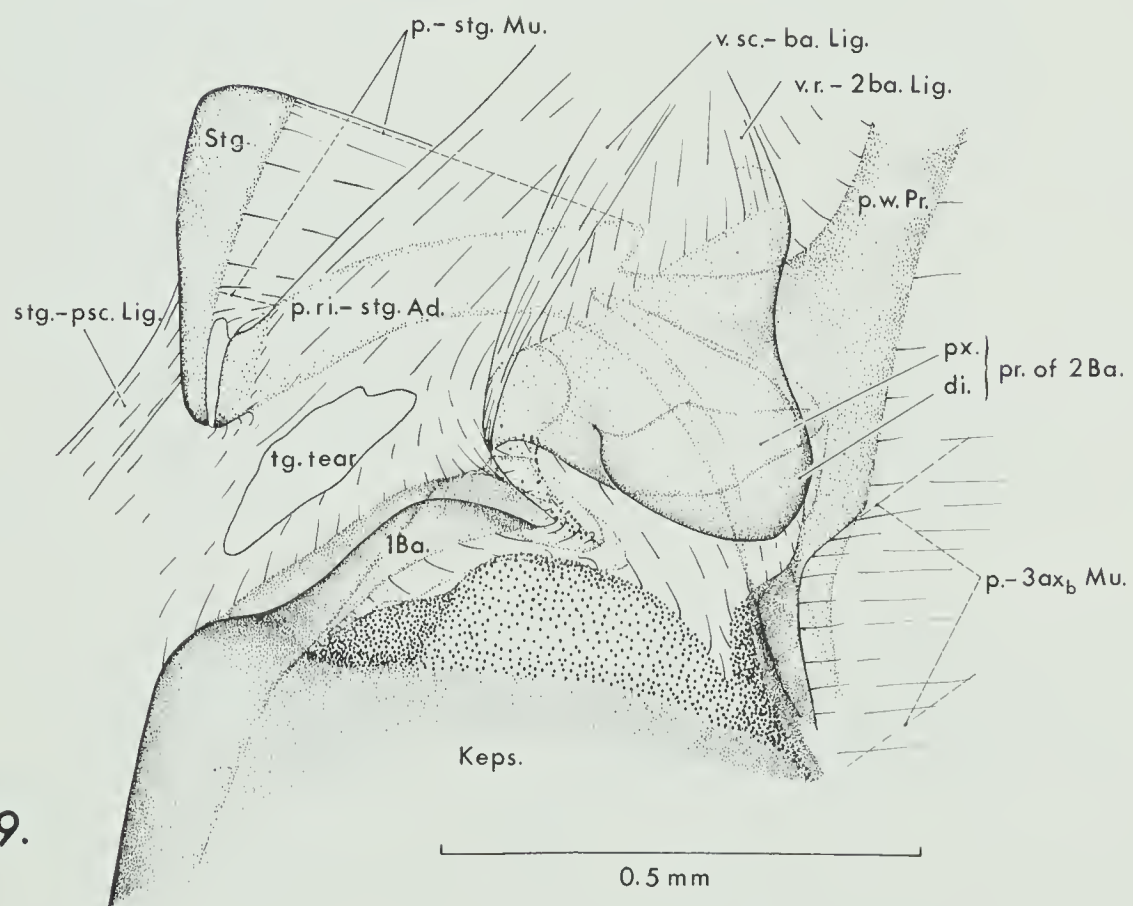
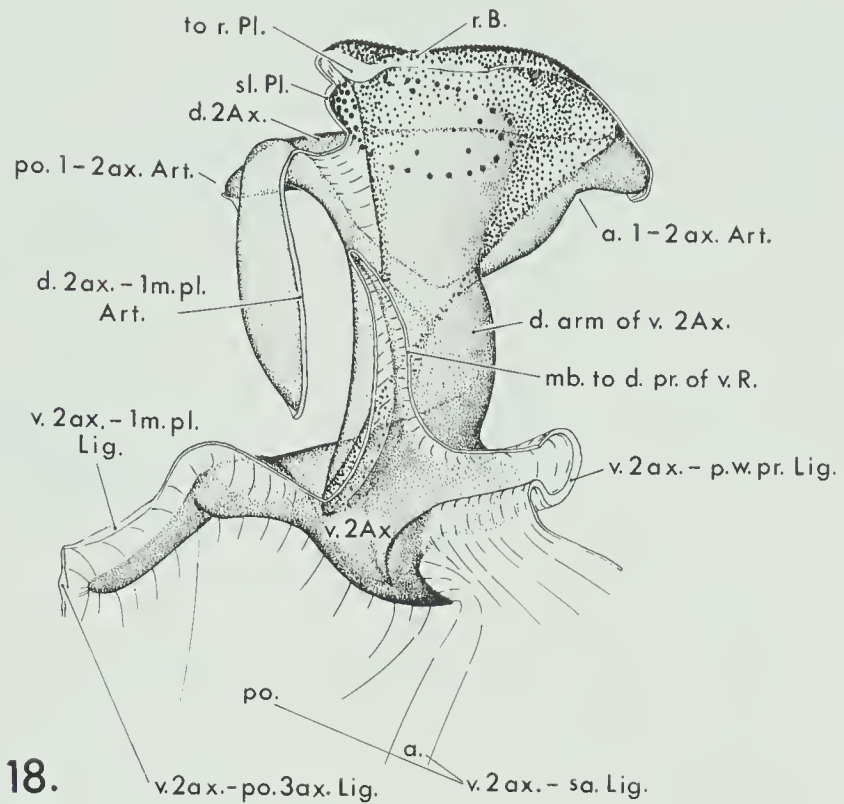


Fig. 20. Dorsal view of the left mesothoracic first axillary and adjacent sclerites with the levels and orientations of sections 20a to 20e indicated.

Fig. 20a. Section through the anterior median notal wing process-first axillary ligament.

Fig. 20b. Section through the posterior median notal wing process-first axillary ligament.

Fig. 20c. Section through the anterior first-second axillary ligament.

Fig. 20d. Section through the posterior first-second axillary ligament.

Fig. 20e. Section through the anterior arm of the first axillary.

Fig. 21. Side view of the left mesothoracic scutum and basalar complex with the level and orientation of section 21a indicated.

Fig. 21a. Section through the left mesothoracic scutum and basalar complex.

Fig. 22. Dorsolateral view of the left mesothoracic first-second basalar hinge with the level and orientation of section 22a indicated.

Fig. 22a. Section through the left mesothoracic first-second basalar hinge.

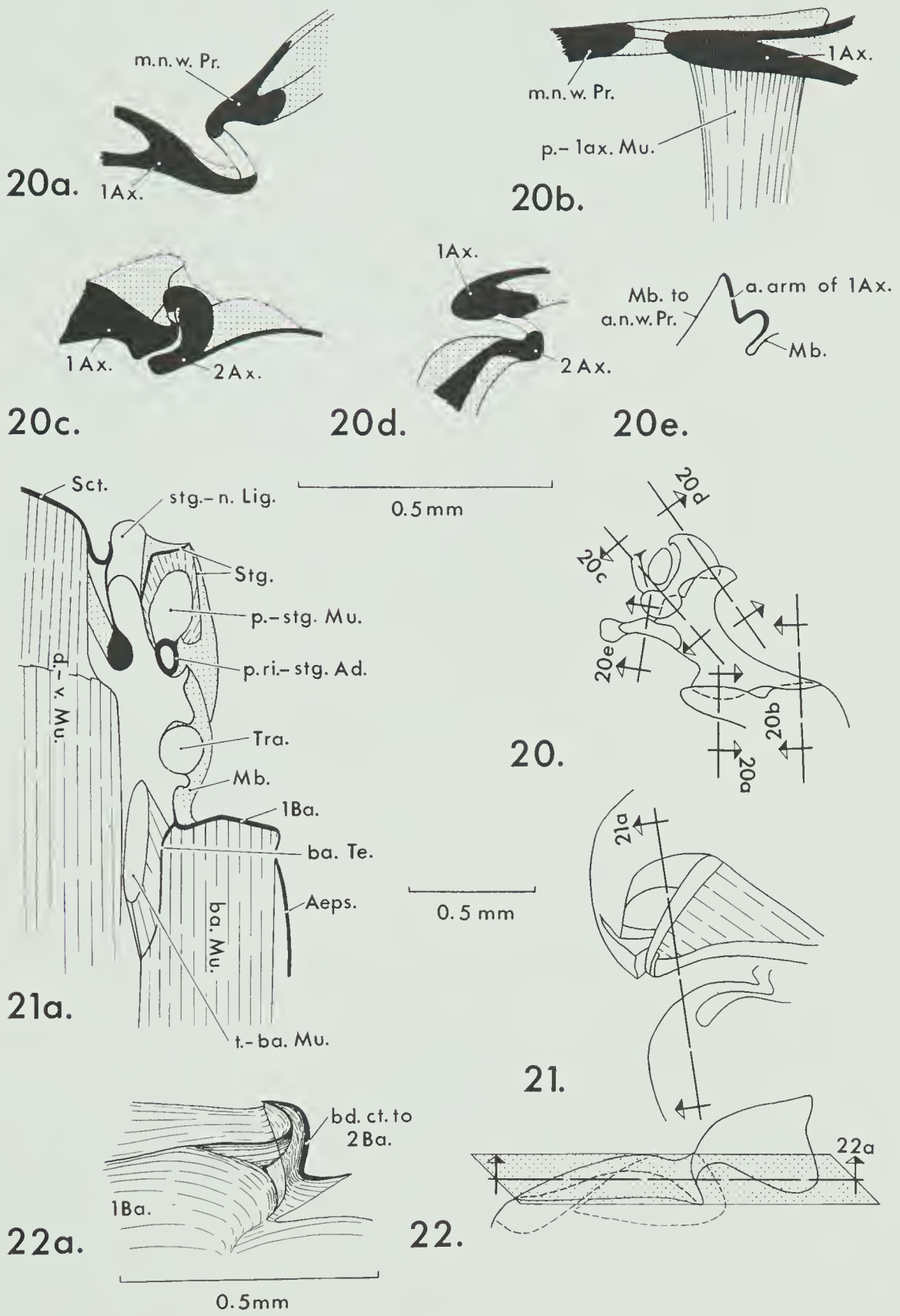


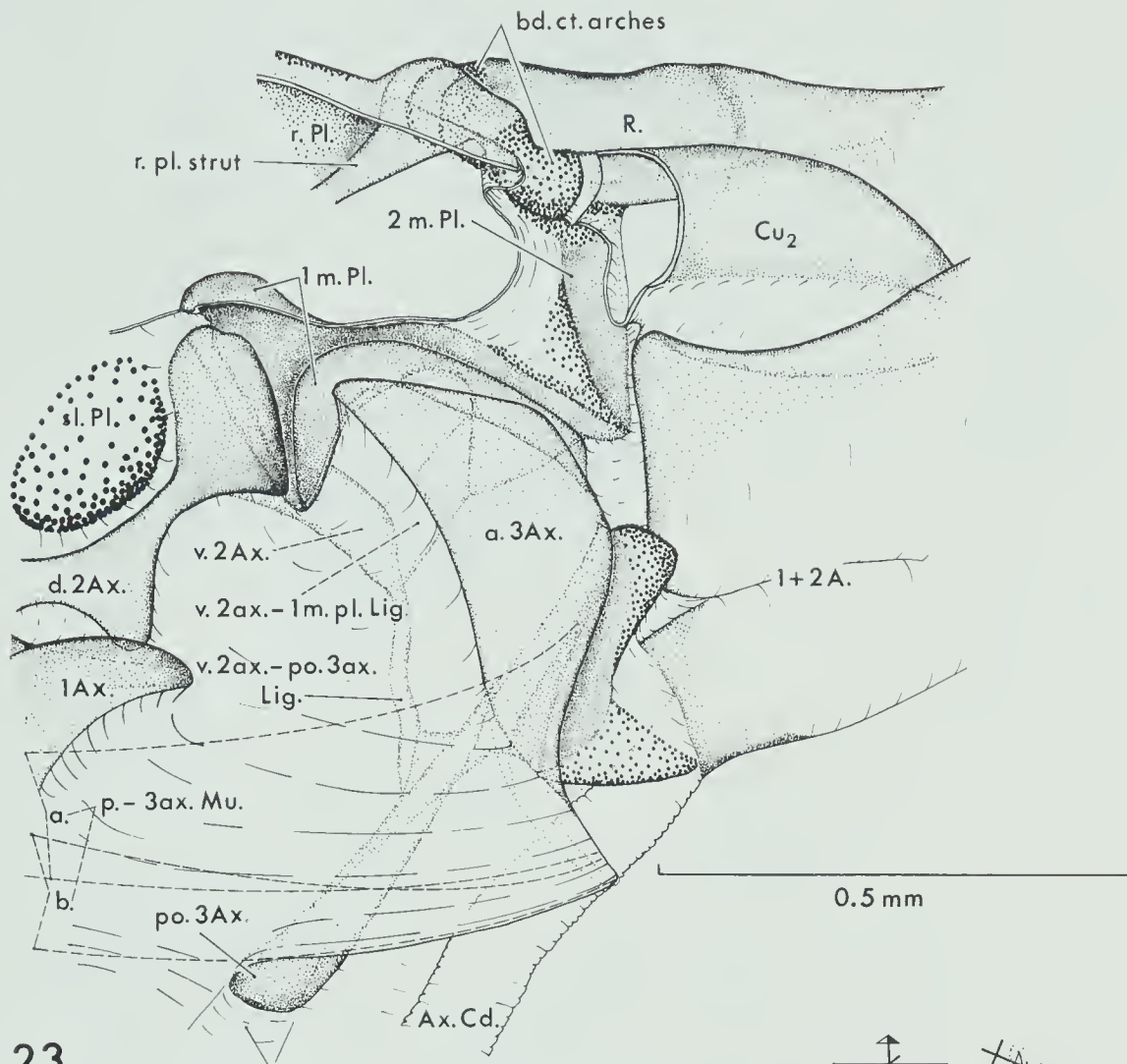
Fig. 23. Posterodorsal view of the dorsal side of the third axillary complex of the right fore wing. Part of the radial plate and second cubitus have been removed to expose the second median plate.

Fig. 24. Dorsal view of the third axillary complex with the levels and orientations of sections 24a to 24c indicated.

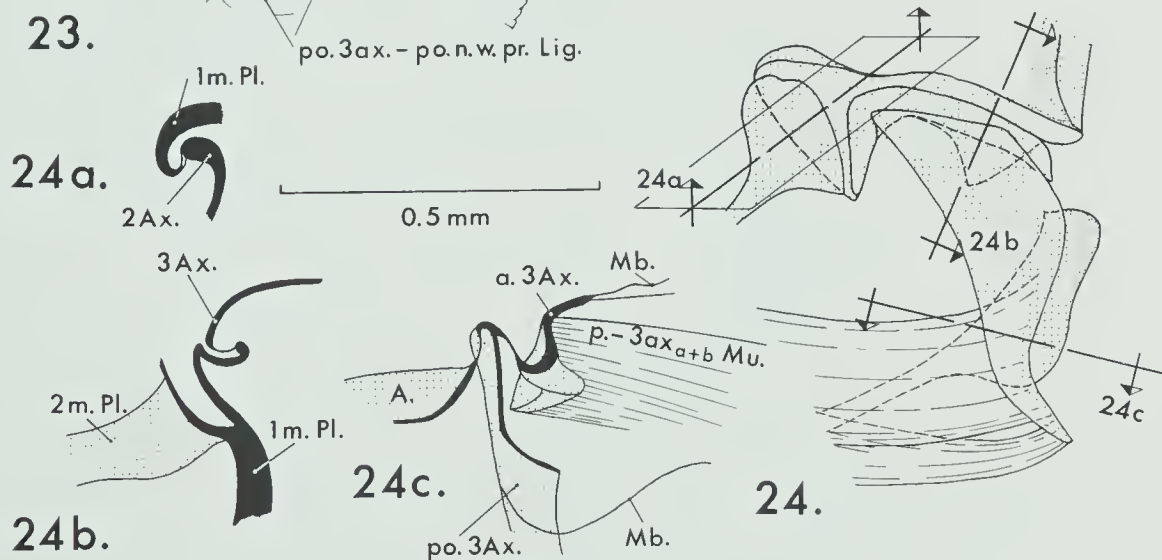
Fig. 24a. Section through the dorsal second axillary-first median plate ligament.

Fig. 24b. Section through the first median plate-anterior third axillary articulation.

Fig. 24c. Section through the anterior-posterior third axillary articulation.



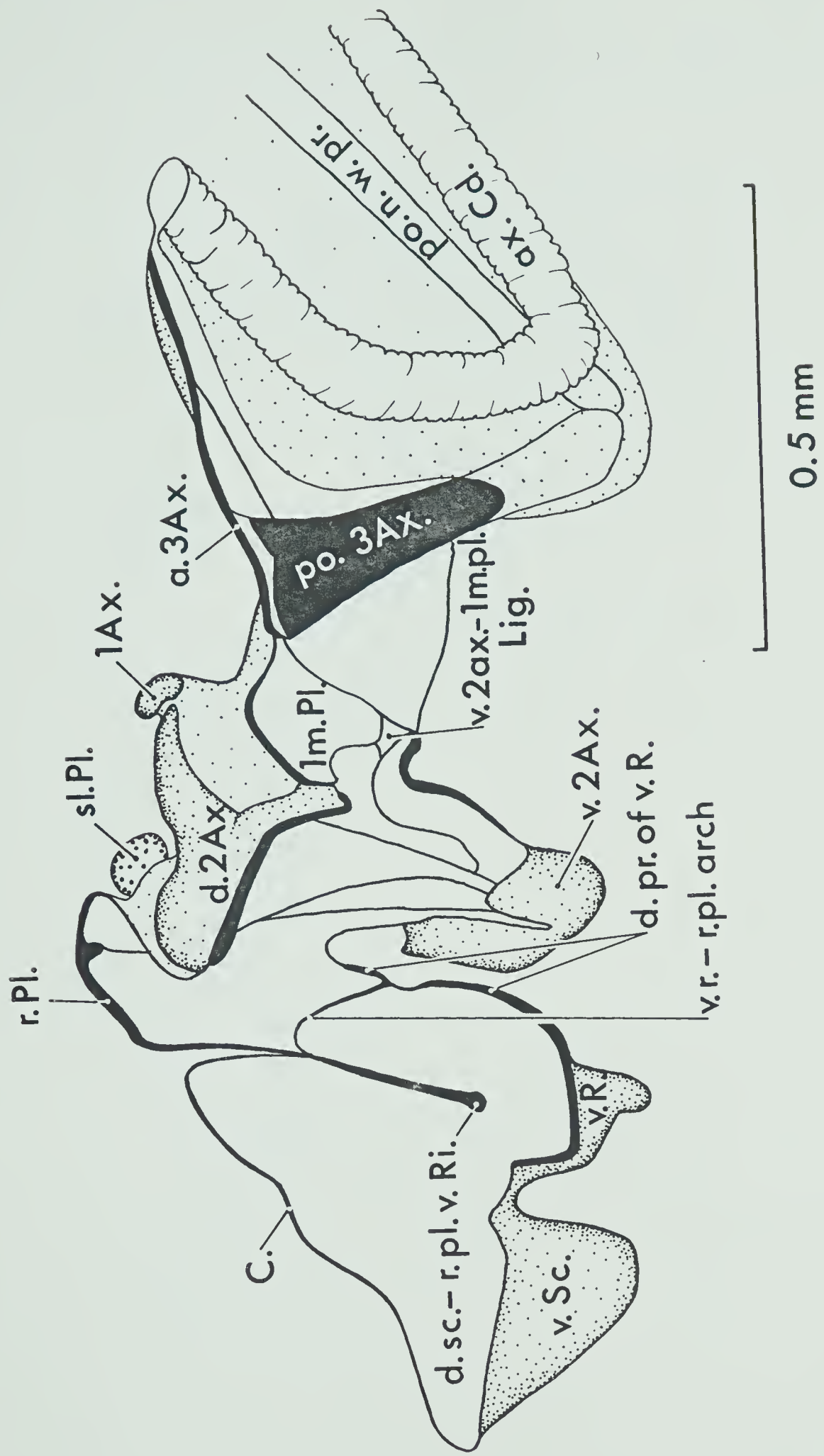
23.



24b.

24.

Fig. 25. Section parallel to the longitudinal axis of the insect through the left mesothoracic wing base.



25.

Fig. 26. Dorsal view of the right mesonotum with the level and orientation of section 26a indicated.

Fig. 26a. Inside ventrolateral view of the right side of the mesonotum. The anterior end of the notum has been folded distally. Broken lines indicate the muscle insertions.

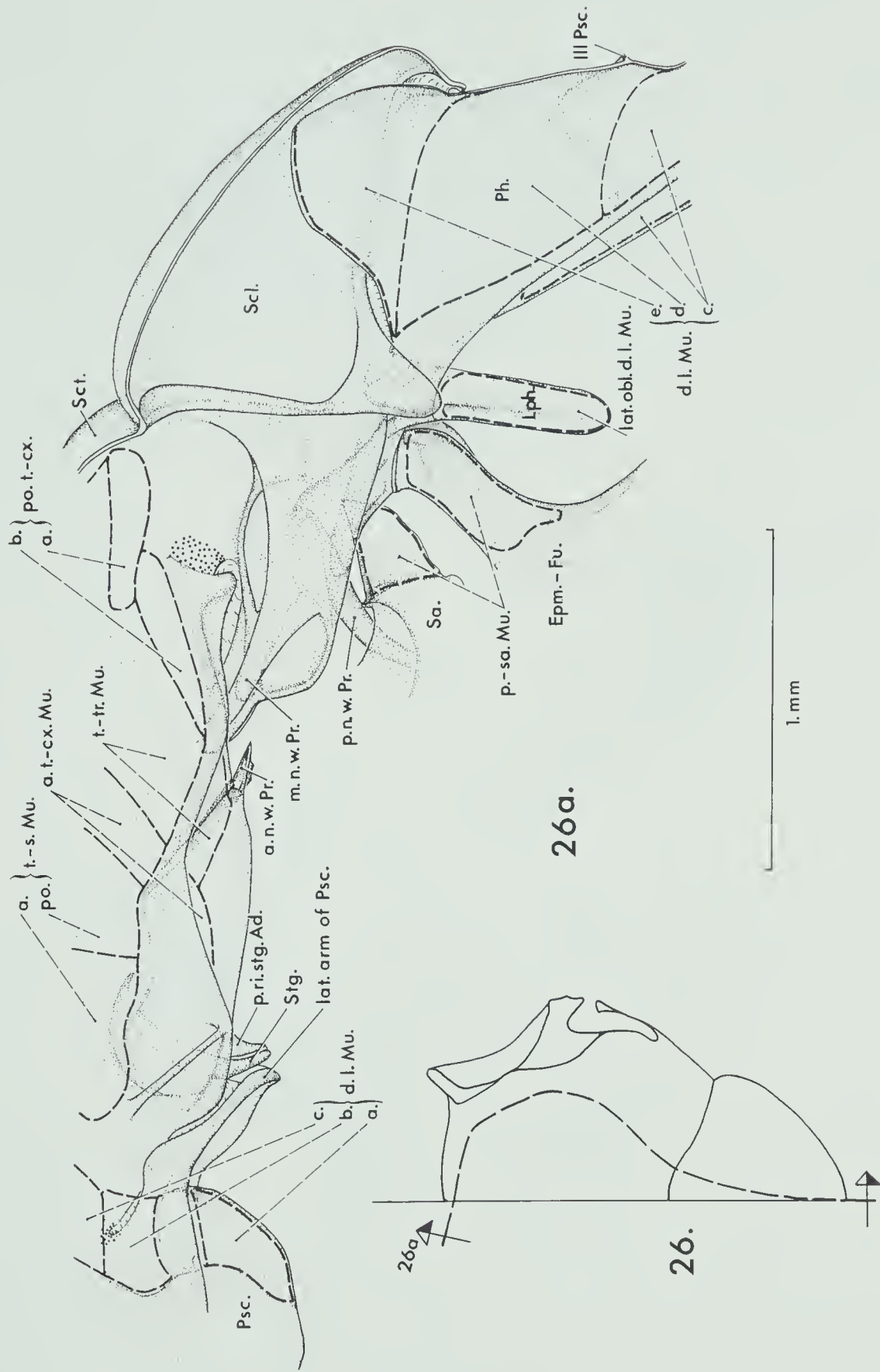
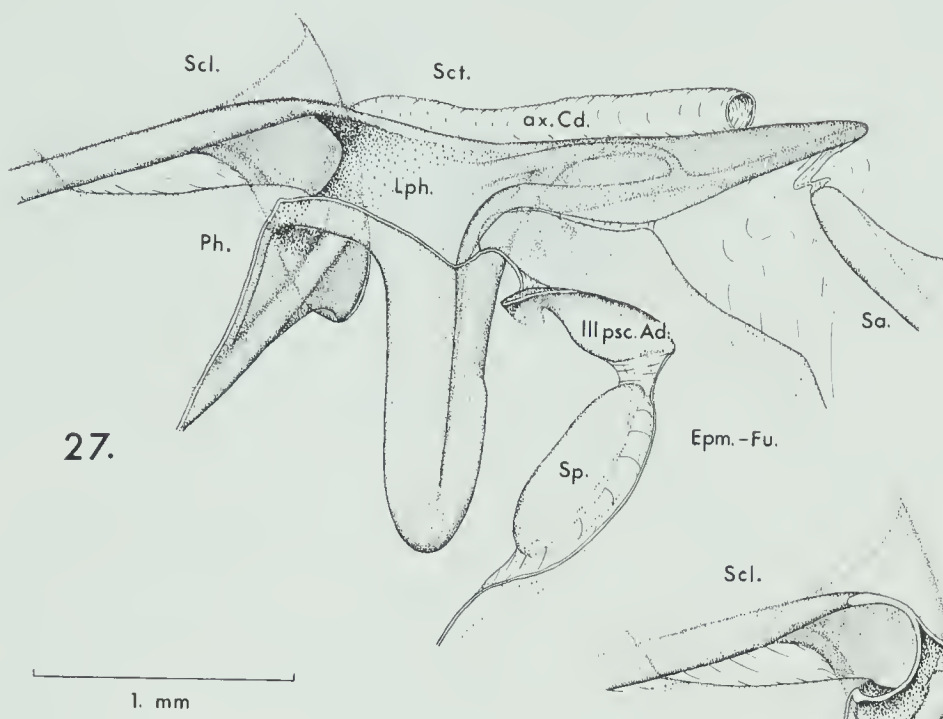


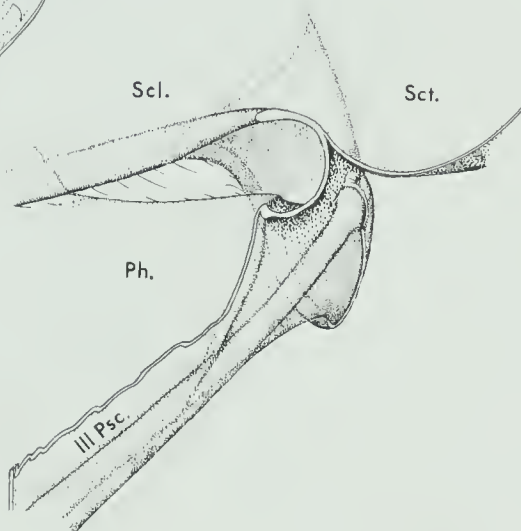
Fig. 27. Side view of the right mesothoracic laterophragma.

Fig. 28. Side view of the right mesothoracic phragma with the laterophragma removed.

Fig. 29. Dorsolateral view of the right mesothoracic laterophragma.



28.



29.

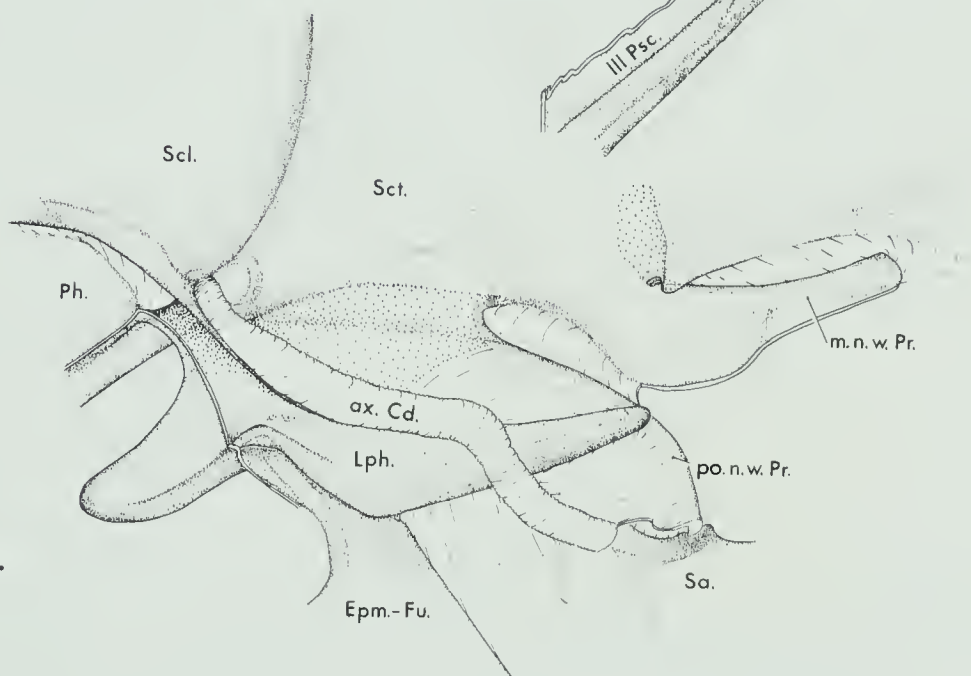


Fig. 30. Mesothoracic right first axillary, dorsal subcosta, and anterior notal wing process viewed from a position above and towards the midline of the insect.

Fig. 31. Top view of the right mesothoracic anterior notal wing process.

Fig. 32. Cross-section through the mesothoracic first axillary-anterior notal wing process junction at the level of the resilin block.

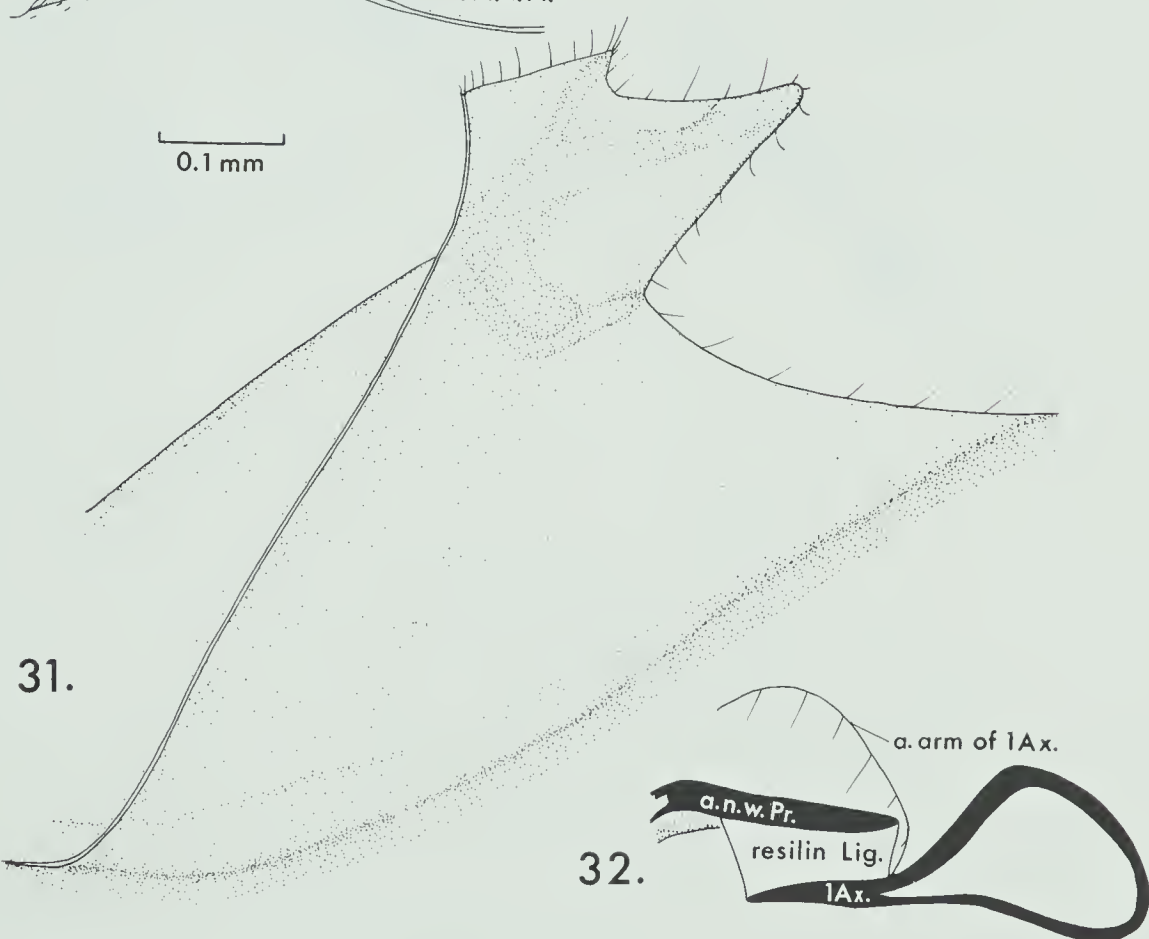
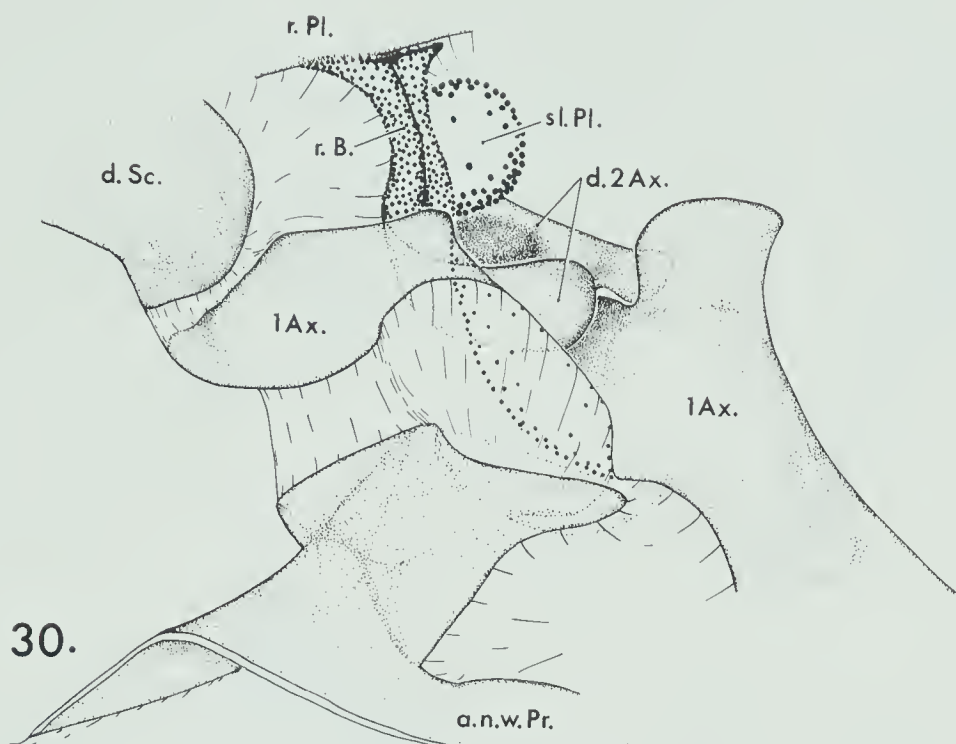


Fig. 33. Side view of the left mesothoracic notum and phragma with the levels and orientations of sections 33a to 33d indicated.

Fig. 33a. Cross-section of the mesothoracic scutal-scutellar suture at a level about half way between the central axis and the lateral margin of the insect.

Fig. 33b. Section through the left mesothoracic epimeral-laterophragmal articulation.

Fig. 33c. Section through the dorsal end of the left mesothoracic phragma-scutal-scutellar articulation.

Fig. 33d. Section through the ventral end of the left mesothoracic phragma-scutal-scutellar articulation.

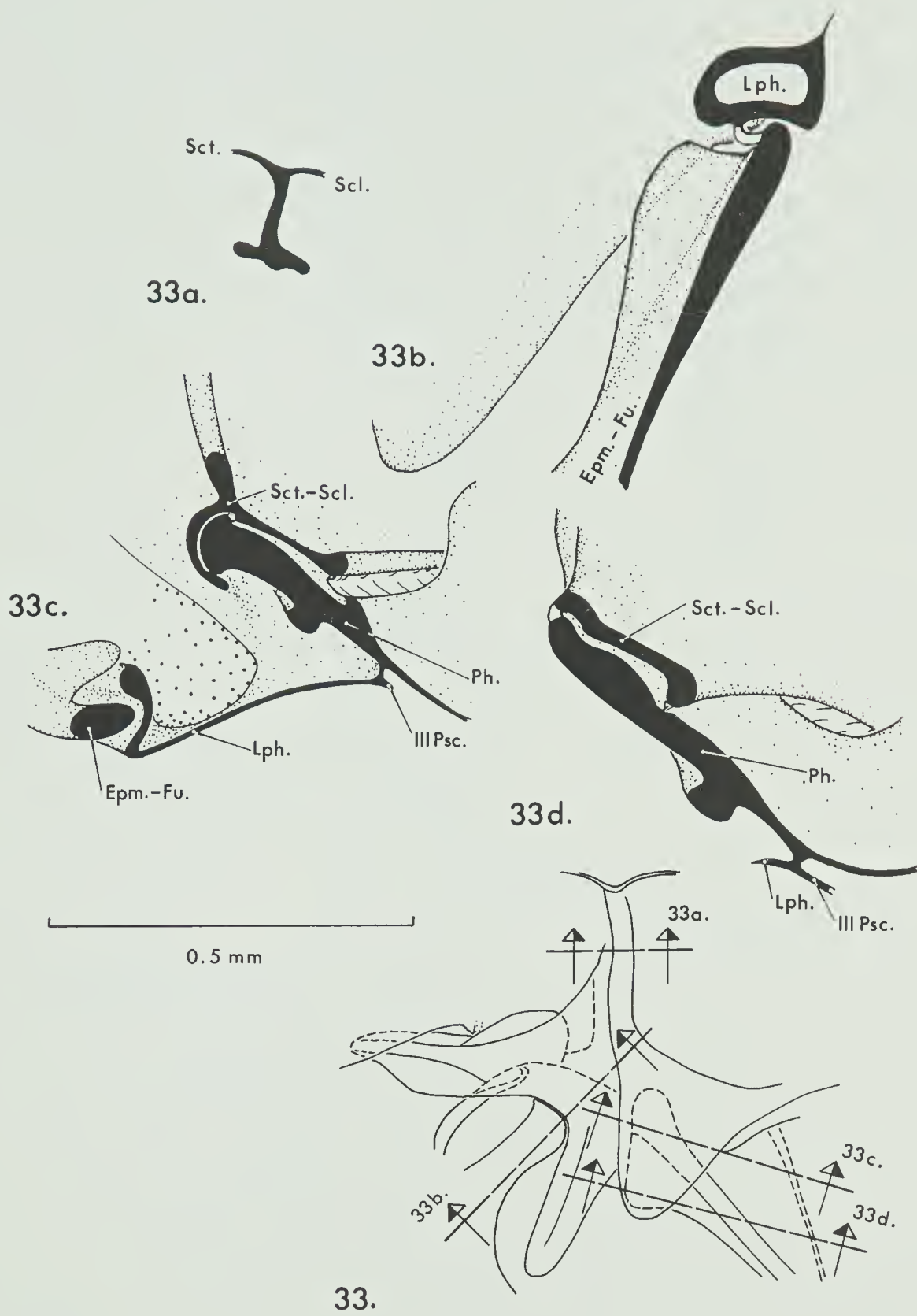


Fig. 34. Lateral inside view of the right mesonotum with the levels and orientations of sections 34a and 34b indicated.

Fig. 34a. Section through the right mesonotum at the level of the base of the anterior arm of the laterophragma.

Fig. 34b. Section through the right mesonotum at the level of the anterior tip of the anterior arm of the laterophragma.

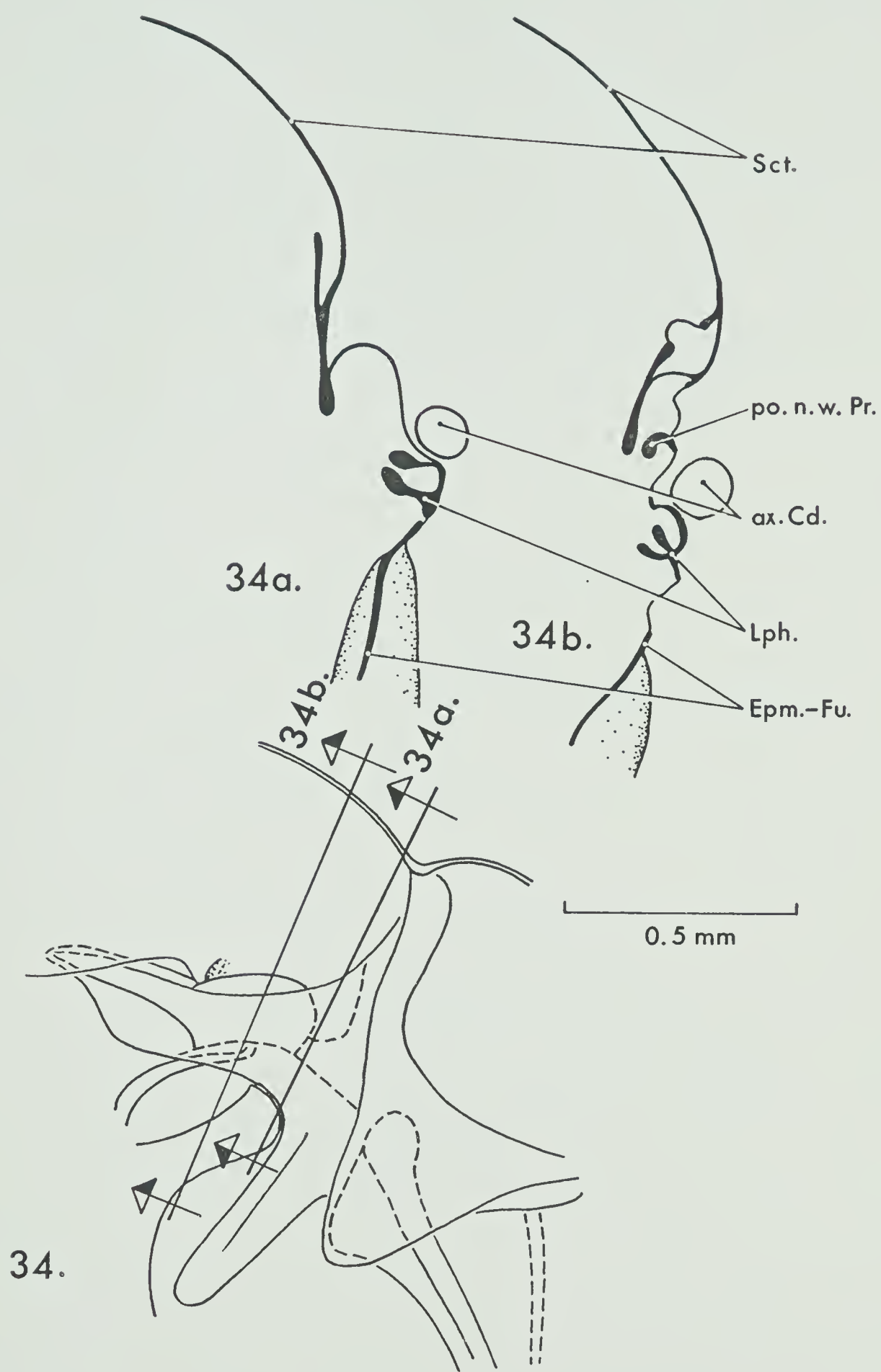
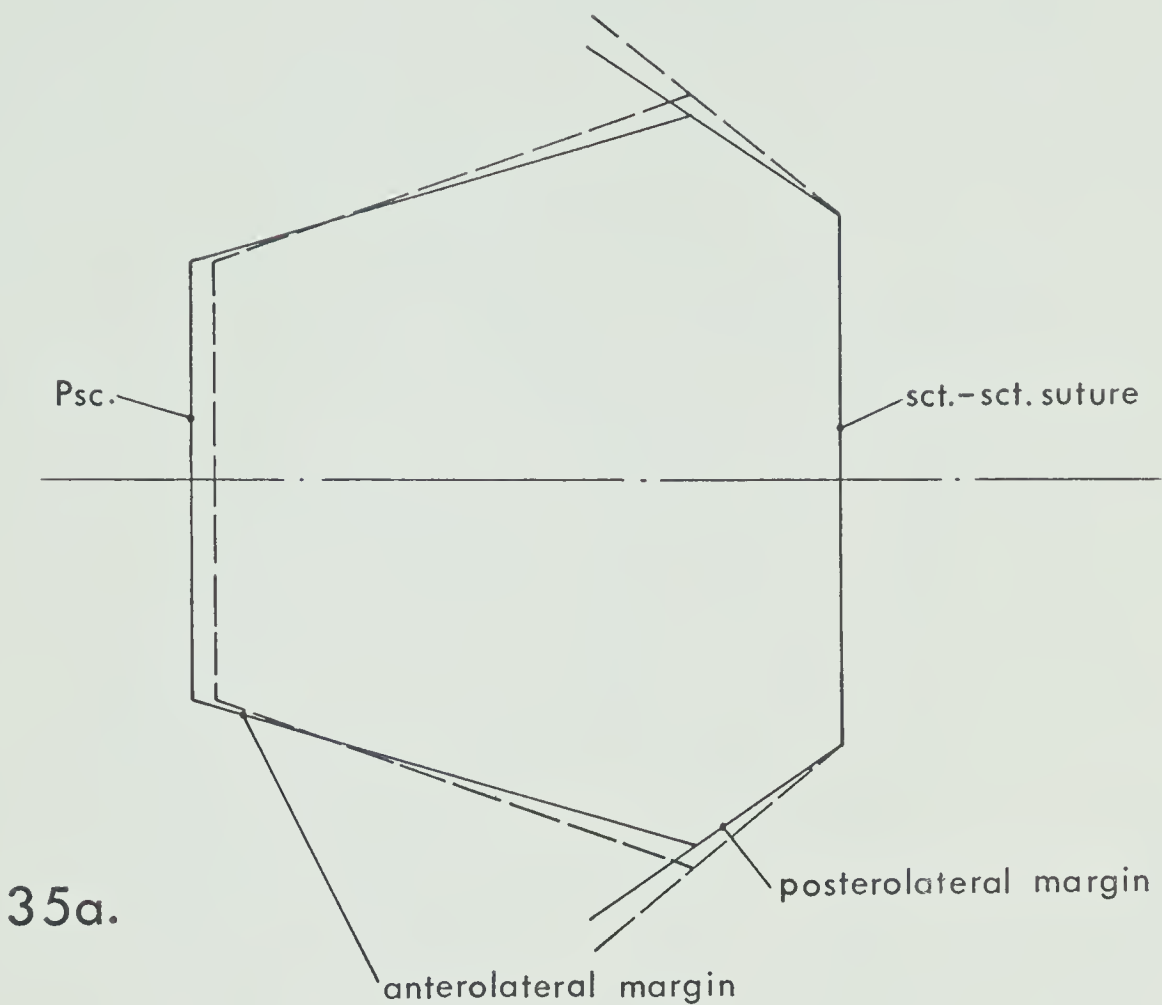
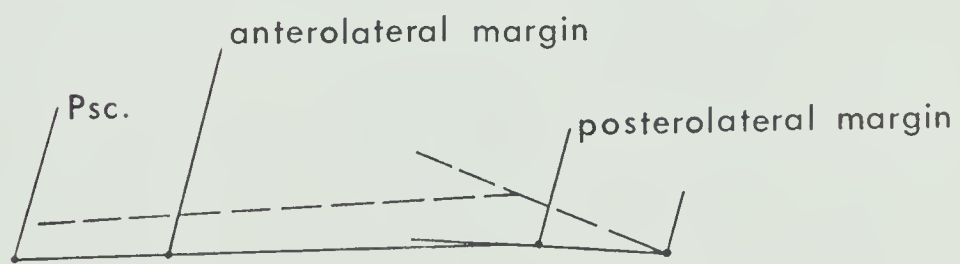


Fig. 35a. Diagrammatic top view of the mechanism of the mesonotum. Broken lines indicate maximum downstroke positions; solid lines, upstroke positions.

Fig. 35b. Diagrammatic side view of the mechanism of the right side of the mesonotum. Broken lines indicate maximum downstroke positions; solid lines, upstroke positions.



1. mm



35b.

Fig. 36. Inside lateral view of the right mesothoracic pleuron and sternum. The pre-episternal region has been deflected distally.

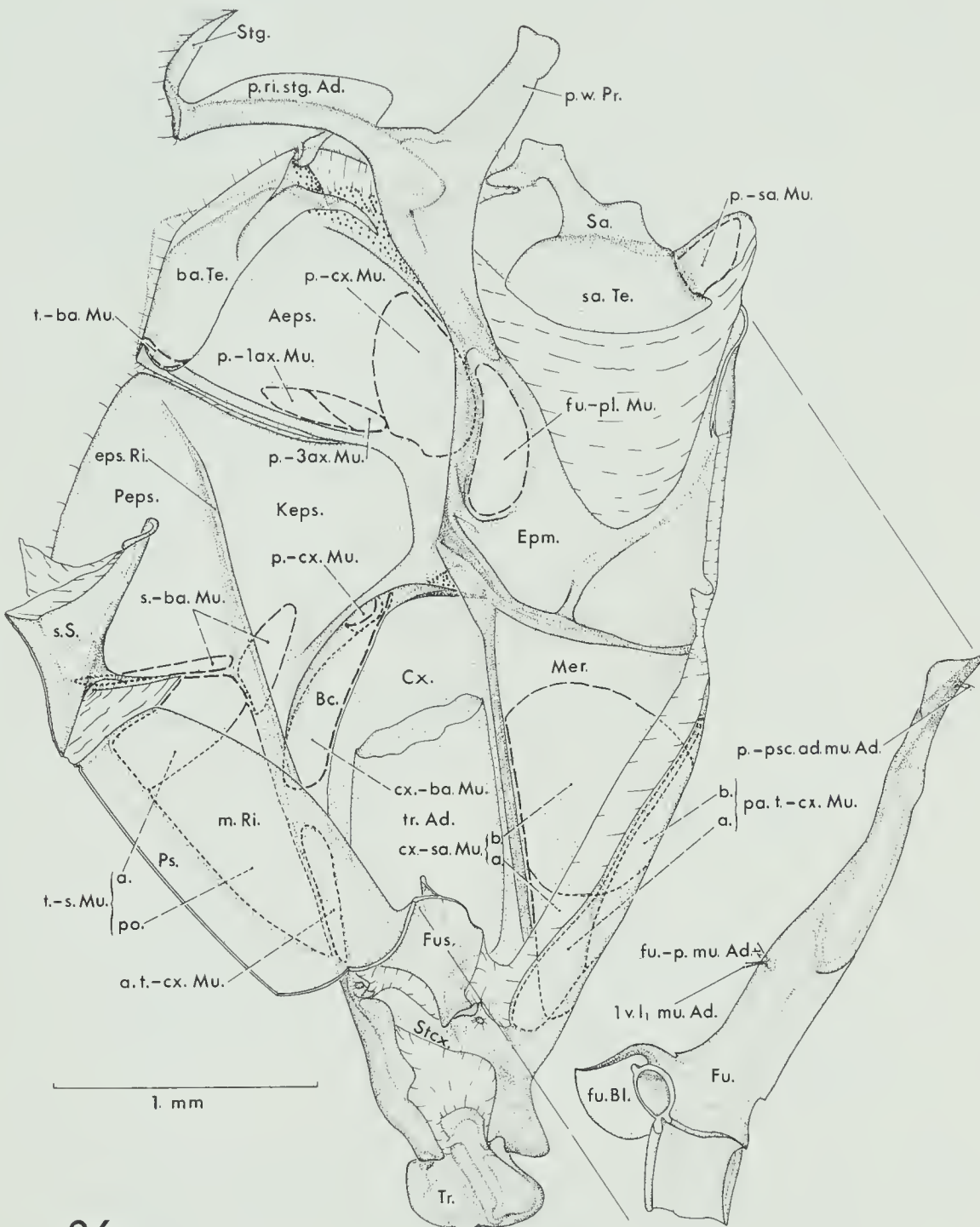


Fig. 37. Side view of the right mesothoracic pleuron with the levels and orientations of sections 37a to 37f indicated.

Fig. 37a. Section through the right mesothoracic pleural region at the level of the furcopleural muscle.

Fig. 37b. Section through the right mesothoracic pleural region at the level of the origin of the pleural-third axillary muscle.

Fig. 37c. Section through the right mesothoracic pleural region at the level of the dorsal end of the origin of the pleural-third axillary muscle.

Fig. 37d. Section through the right mesothoracic pleural region at the level of the proximal process of the second basalare.

Fig. 37e. Section through the right mesothoracic pleural region at the level of the distal process of the second basalare.

Fig. 37f. Section through the right mesothoracic pleural region at the level of the pleural wing process.

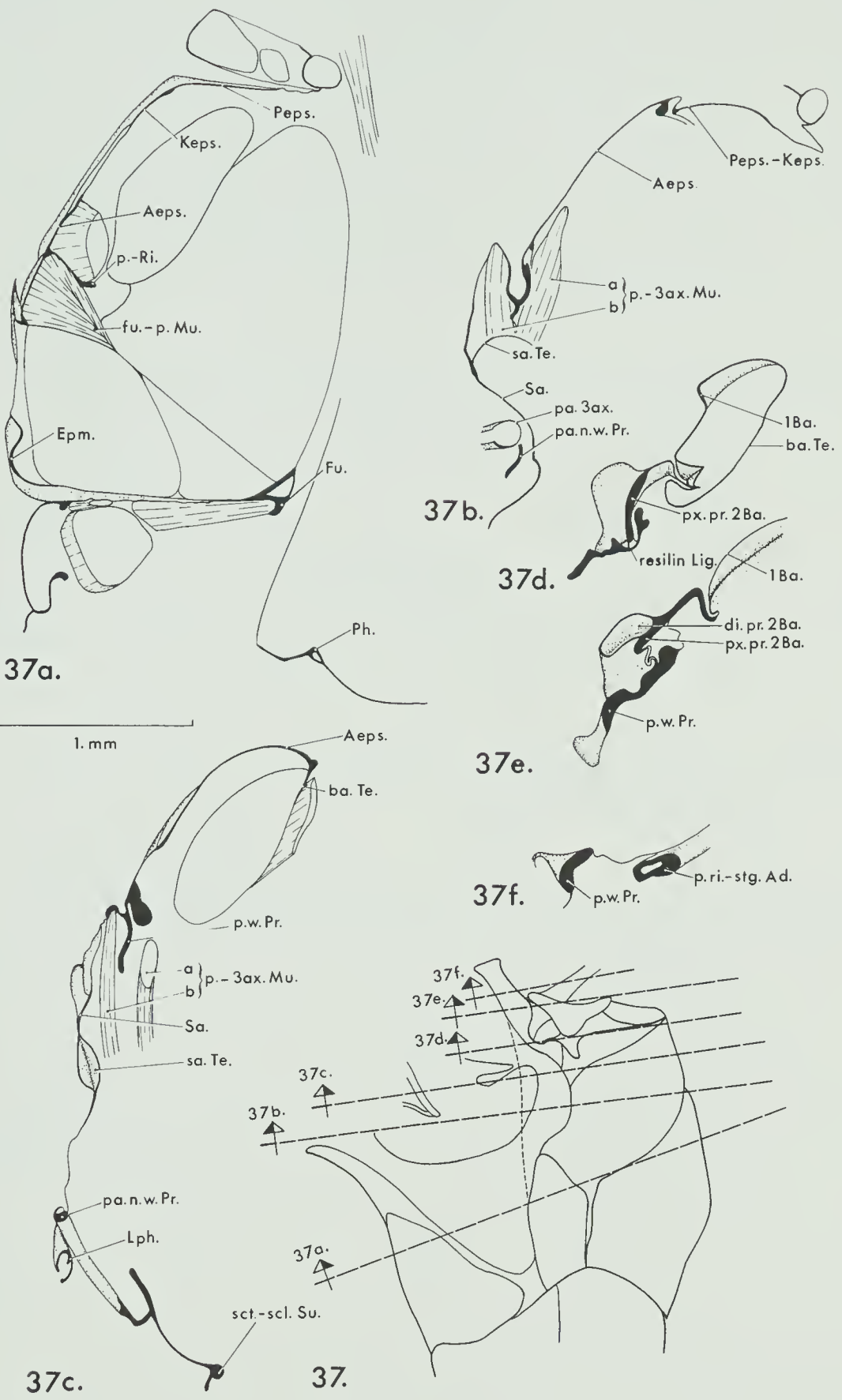


Fig. 38. Inside lateral view of the right mesothoracic pleuron and sternum with the levels and orientations of sections 38a to 38e indicated.

Fig. 38a. Section through the mesothoracic furcasternal region at a level immediately ventral to the pre sternum.

Fig. 38b. Section through the mesothoracic furcasternal region at a level immediately ventral to the furcal blade.

Fig. 38c. Section through the ventral region of the right mesothoracic furca.

Fig. 38d. Section through the dorsal region of the right mesothoracic furca.

Fig. 38e. Section through the right mesothoracic furcal-epimeral junction.

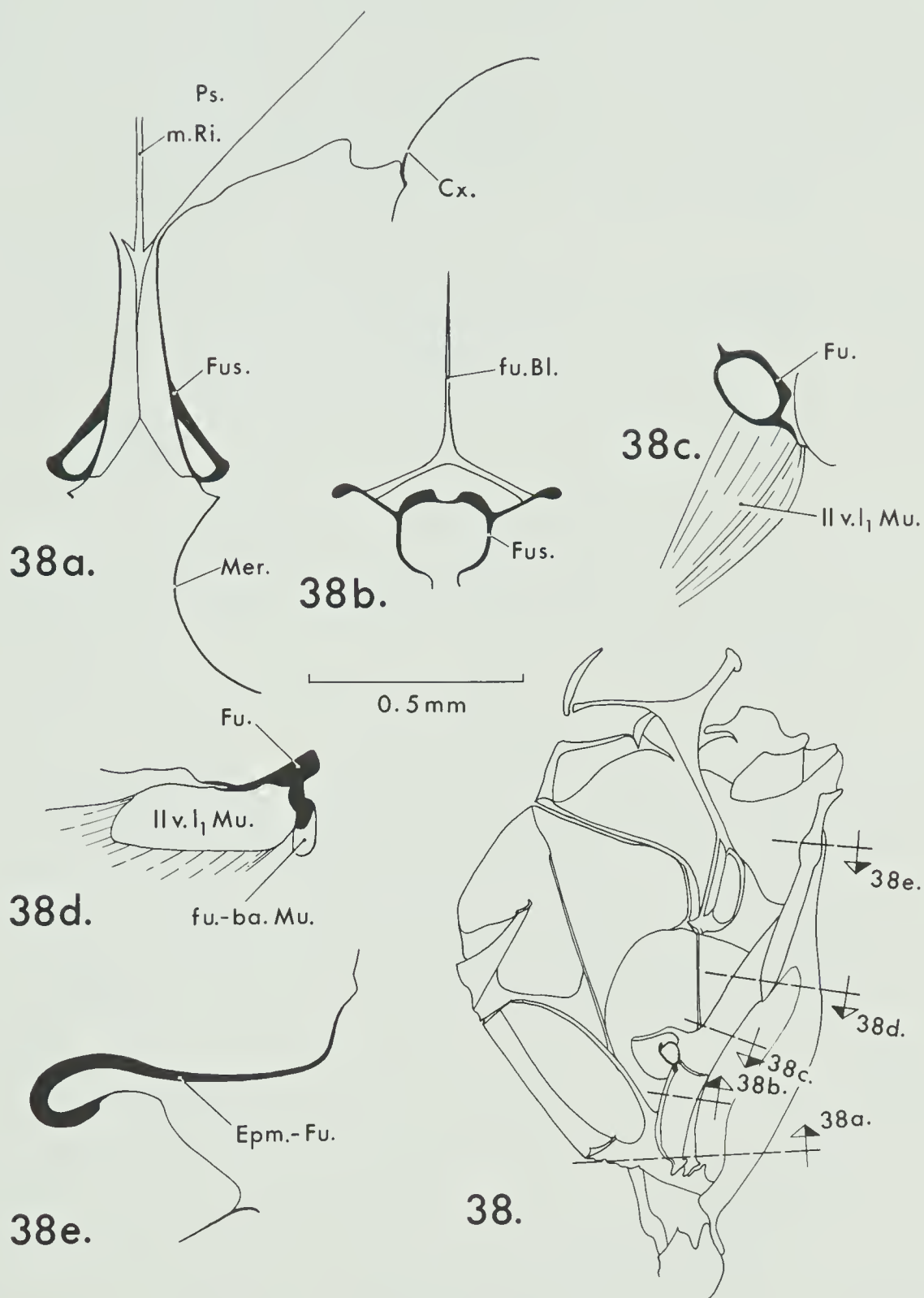


Fig. 39. Side view of the left mesothoracic basalar complex and anepisternum with the hinge points of figs. 39a to 39c indicated.

Fig. 39a. Diagrammatic representation of the side view of the left mesothoracic basalar complex and anepisternum.

Fig. 39b. Diagrammatic representation of the front view of the left mesothoracic basalar complex and anepisternum.

Fig. 39c. Diagrammatic representation of the top view of the left mesothoracic basalar complex and anepisternum.

Note: Broken lines and primed letters, which indicate the hinges, indicate the maximum downstroke positions. Solid lines and unprimed letters indicate the maximum upstroke positions.

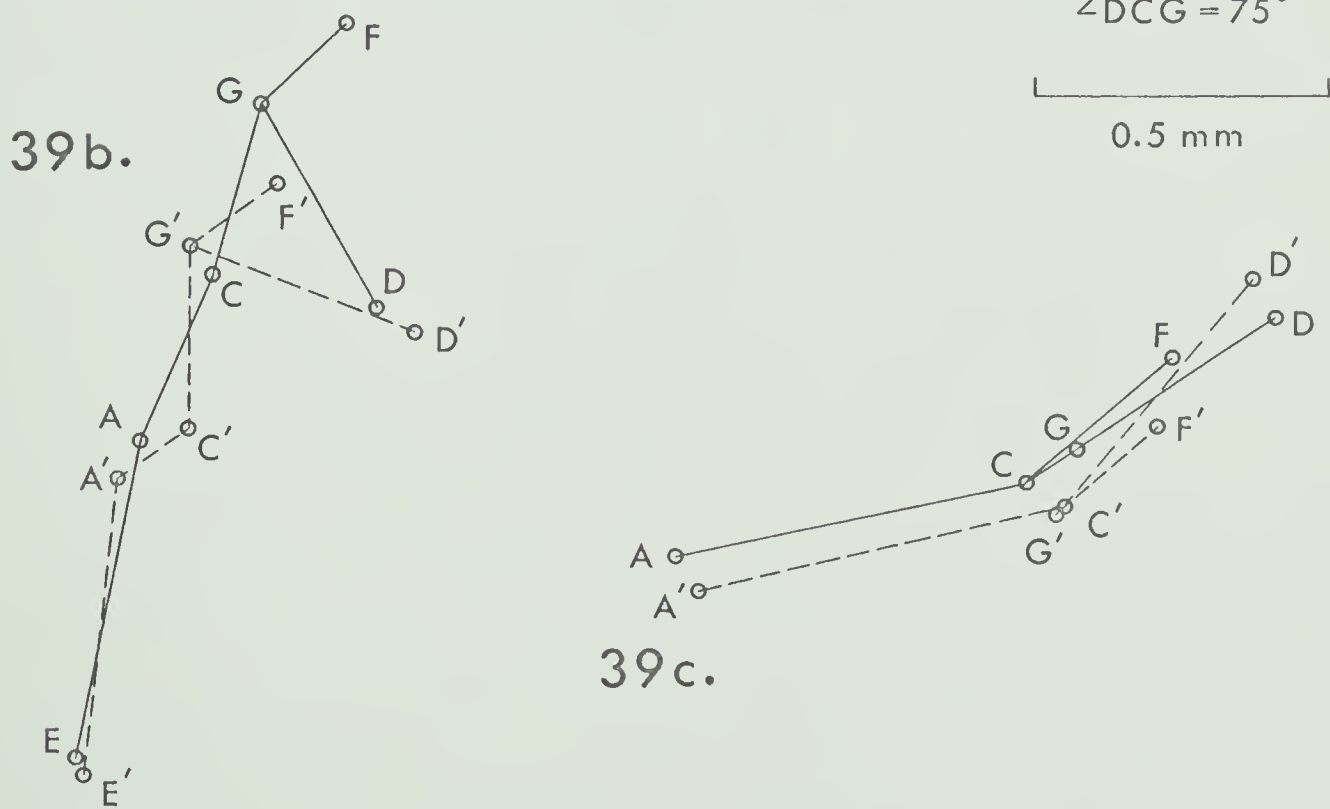
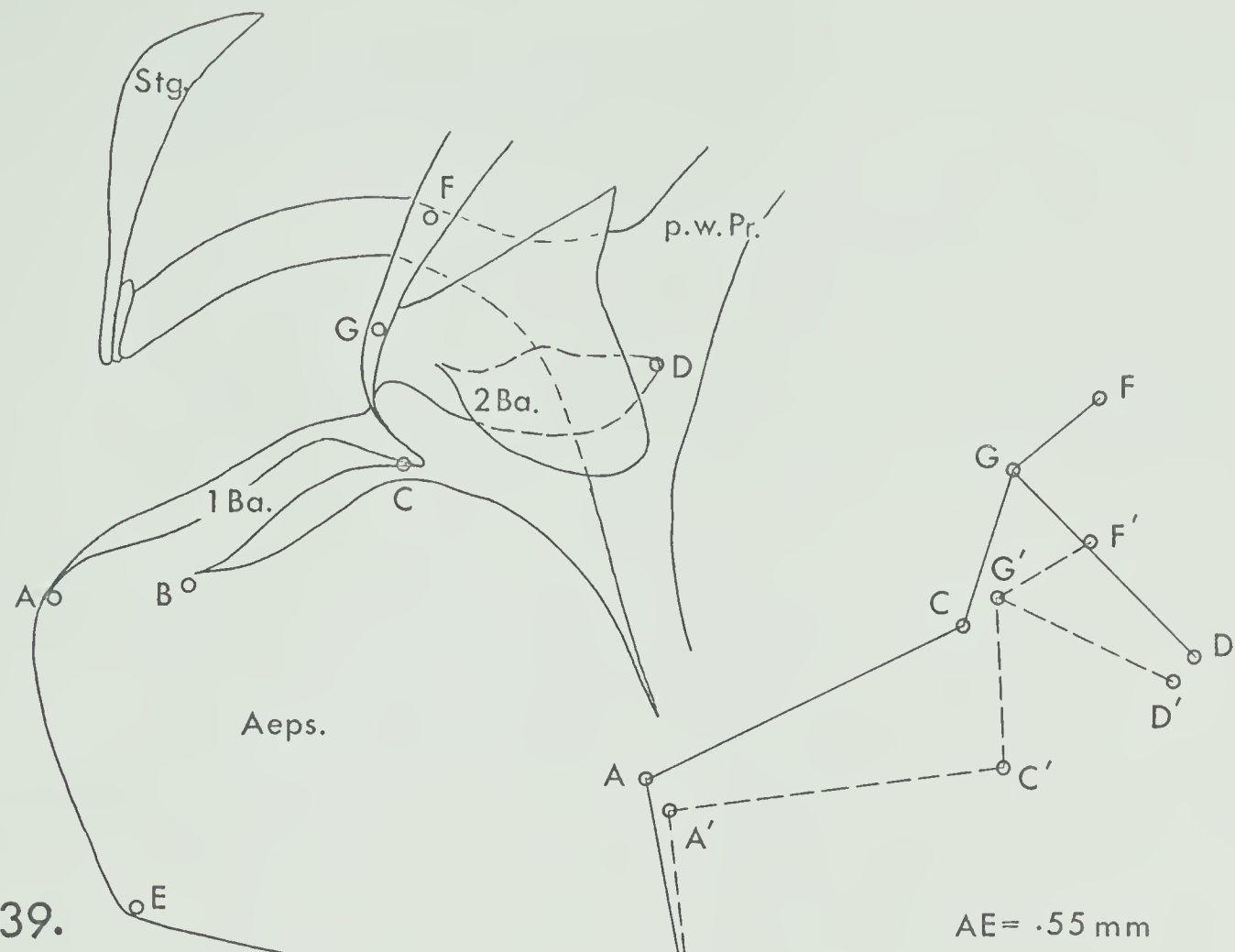


Fig. 40a. Diagrammatic representation of the left side of the mesothorax during the downstroke. The arrows indicate the indirect muscle tensions.

Fig. 40b. Diagrammatic representation of the left side of the mesothorax during the upstroke. The arrows indicate the indirect muscle tensions.

Note: AB represents the anterolateral margin of the scutum, C represents the posterolateral margin of the scutum, CD represents the pleuron and sternum except for the pleural wing process and the pleural ridge-subtegular apodeme, ADE represents the pleural wing process and the pleural ridge-subtegular apodeme, and F represents the point of attachment of the basalar and subalar ligaments to the wing base.

Points ABCD lie in the plane of the page, E and F lie above the page.

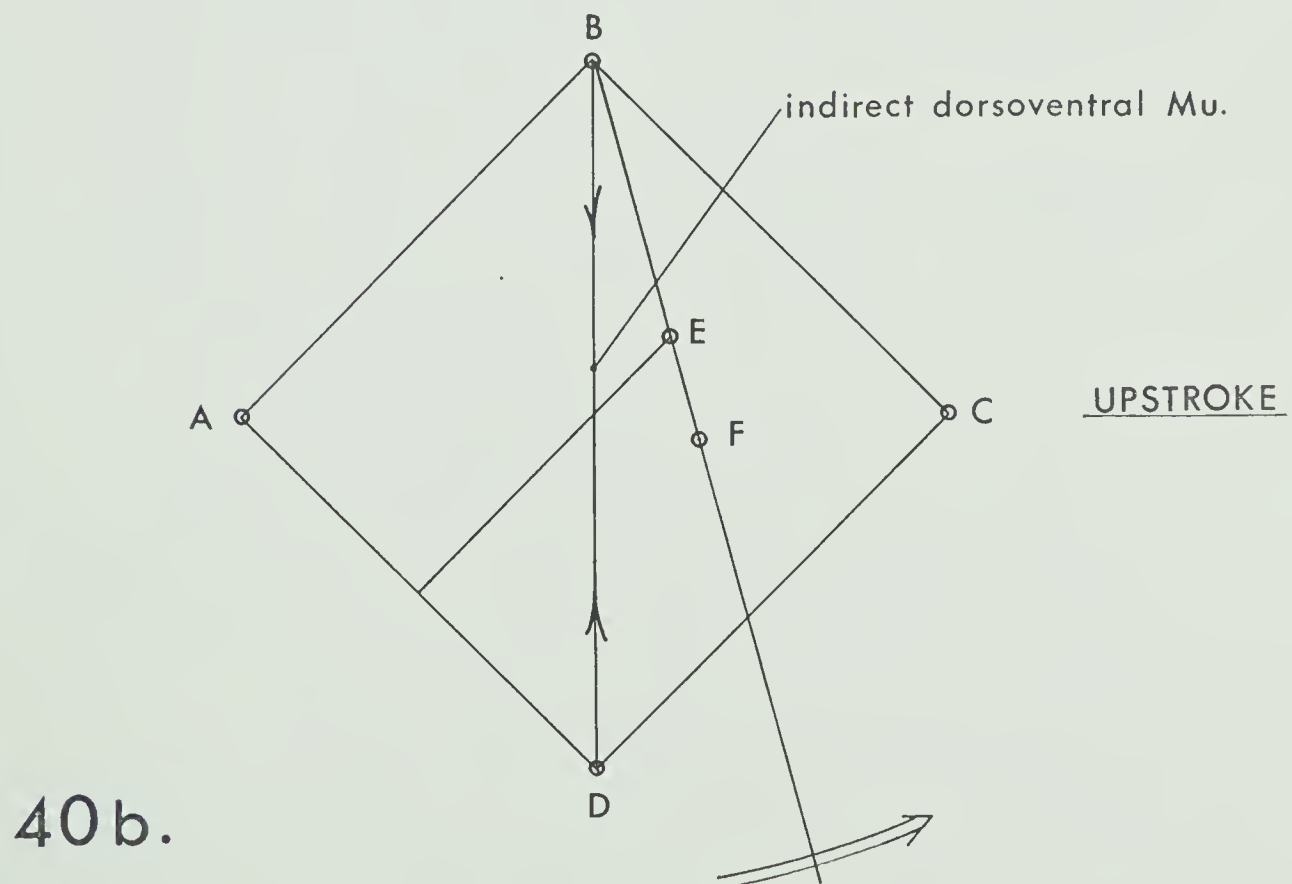
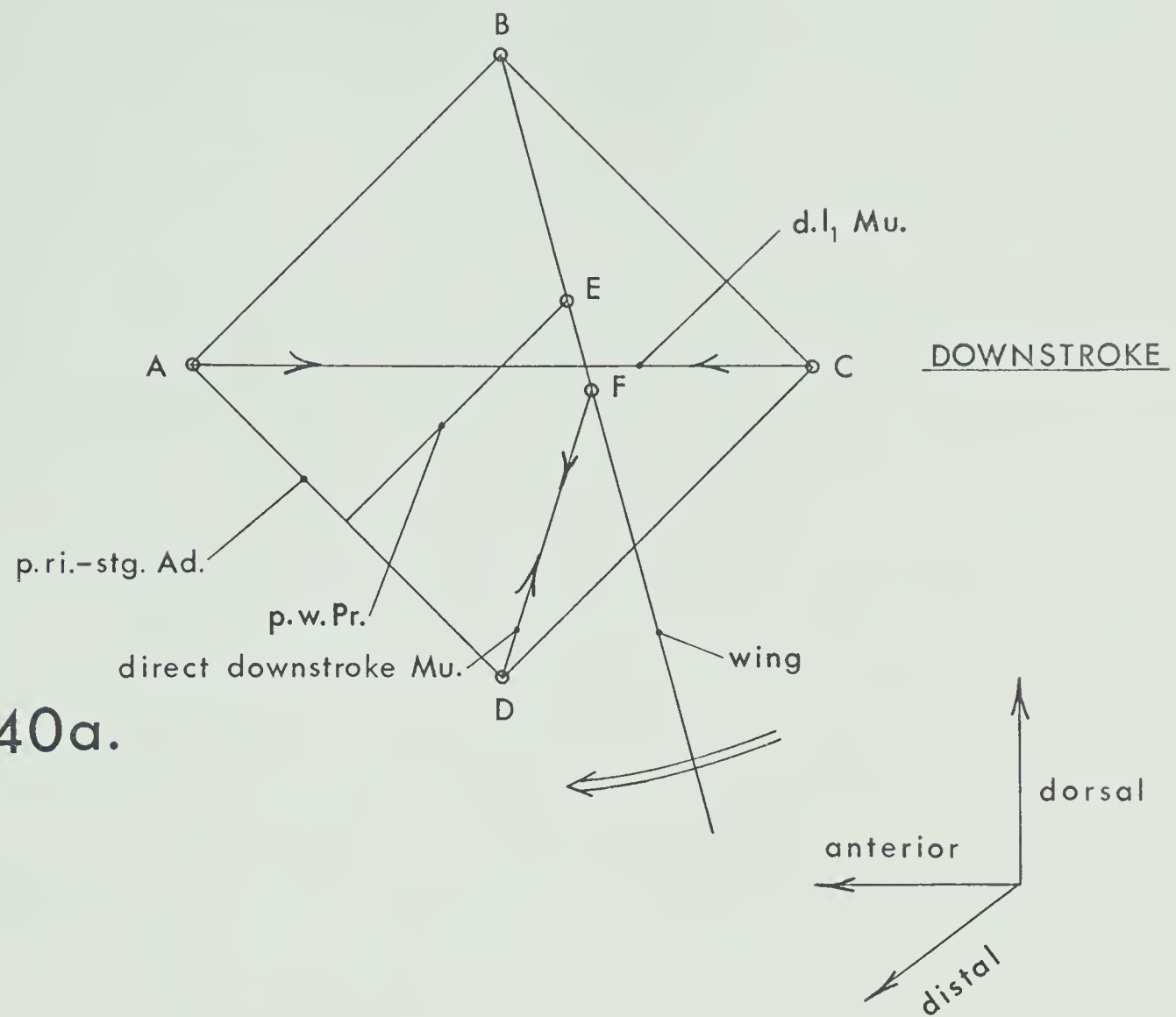


Fig. 41a. Diagrammatic representation of the left side of the mesothorax at the beginning of the downstroke. The arrows indicate muscle tensions.

Fig. 41b. Diagrammatic representation of the left side of the mesothorax at the beginning of the upstroke. The arrows indicate muscle tensions.

Note: AB represents the anterolateral margin of the scutum, BC represents the posterolateral margin of the notum. Between C and D lie the epimeron, furca, furcasternum, presternum, episternal ridge, katepisternum, coxa, and meron. DE represents the pleural wing process, DZ represents the pleural ridge-subtegular apodeme, EF represents the connections of the subalar and basalar musculature to the wing base, and ZA represents the subtegula.

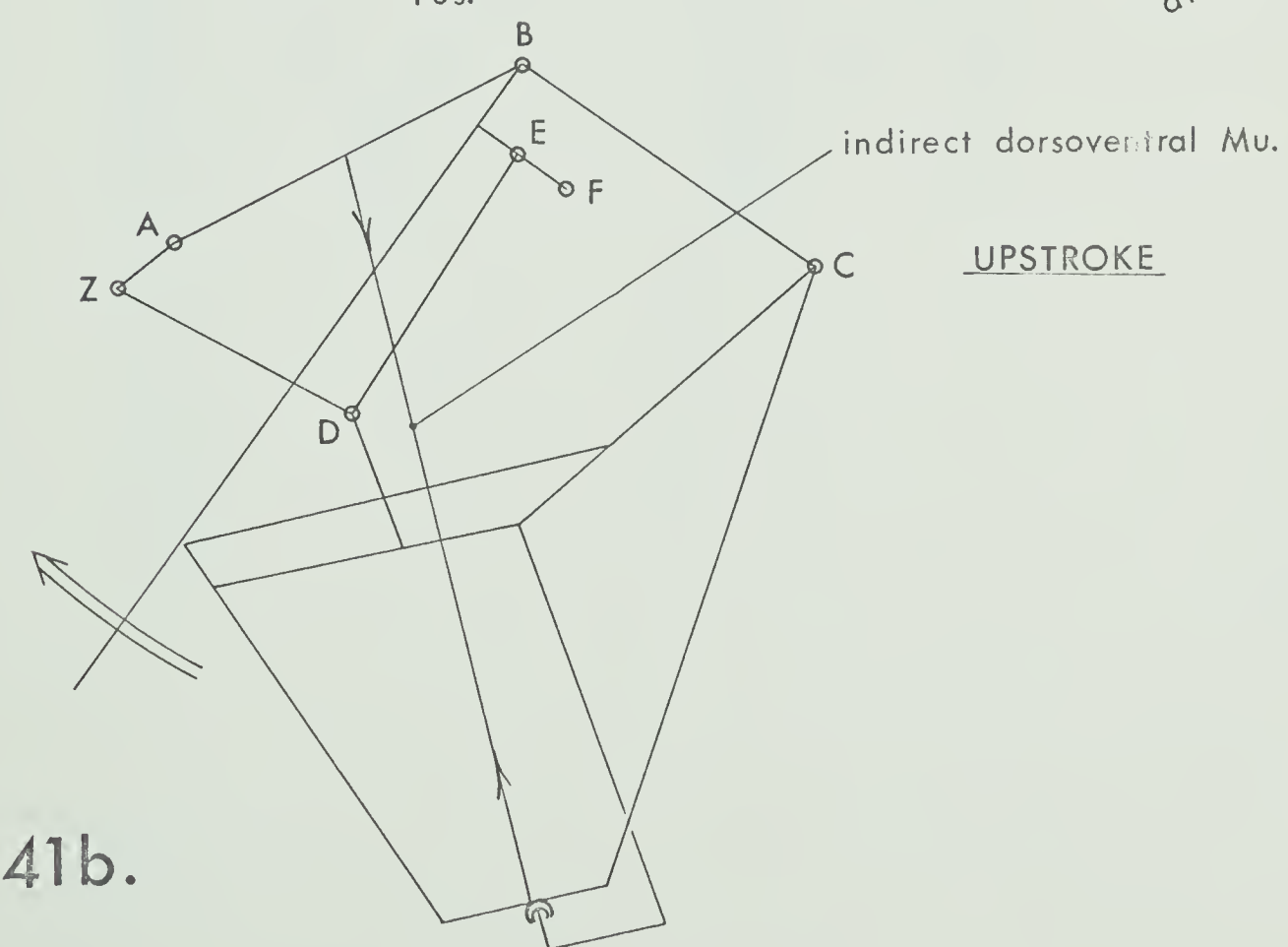
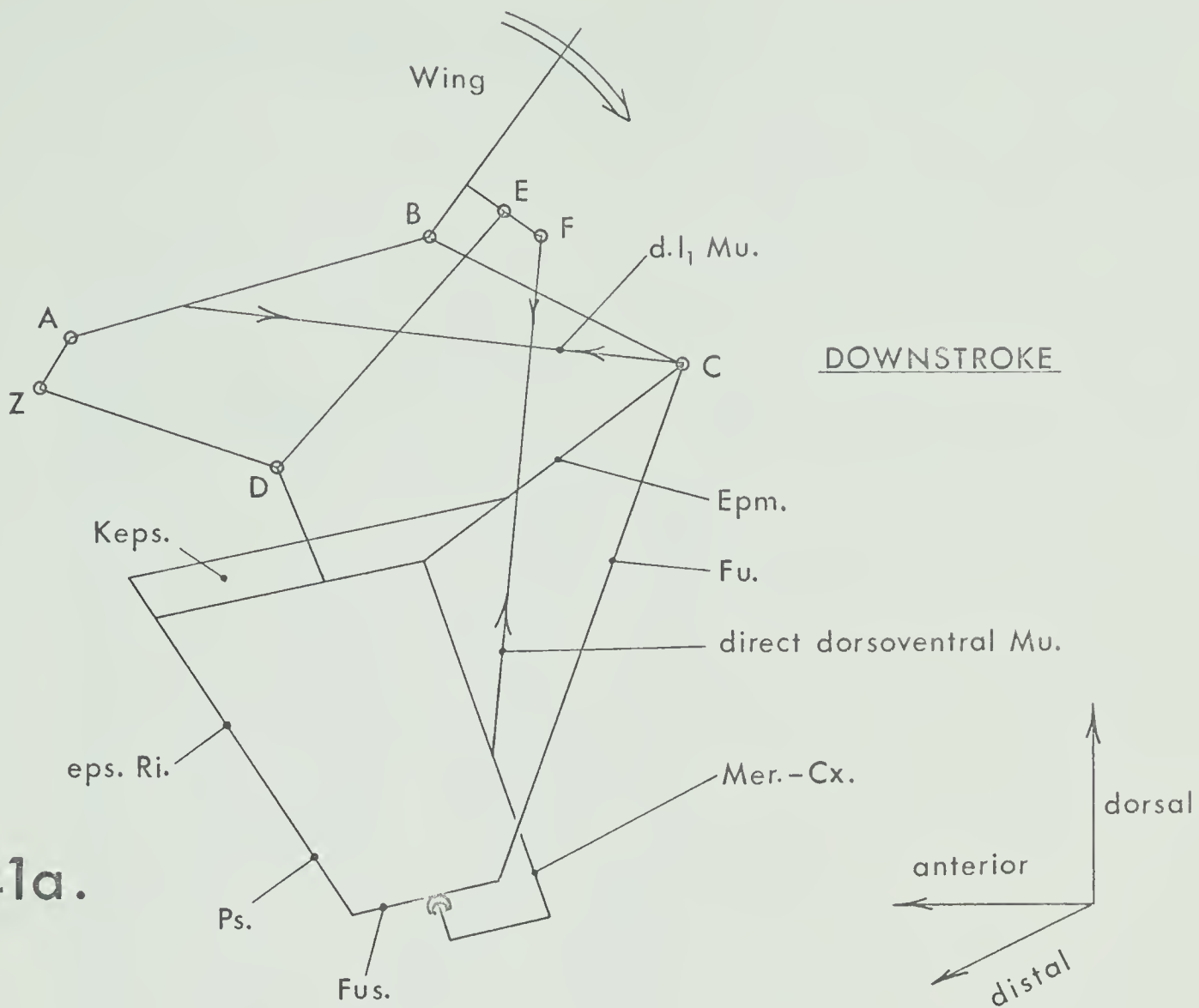
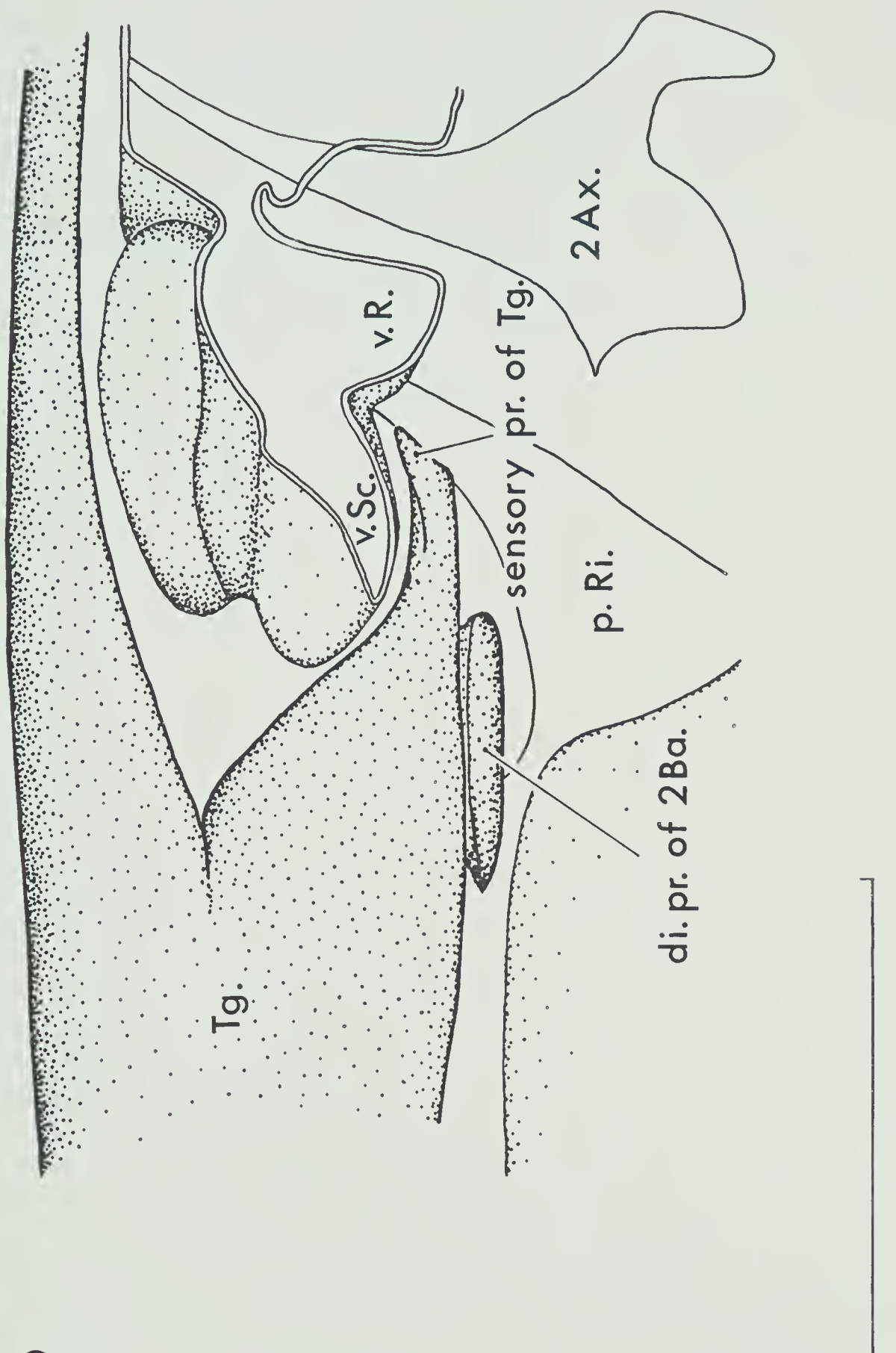
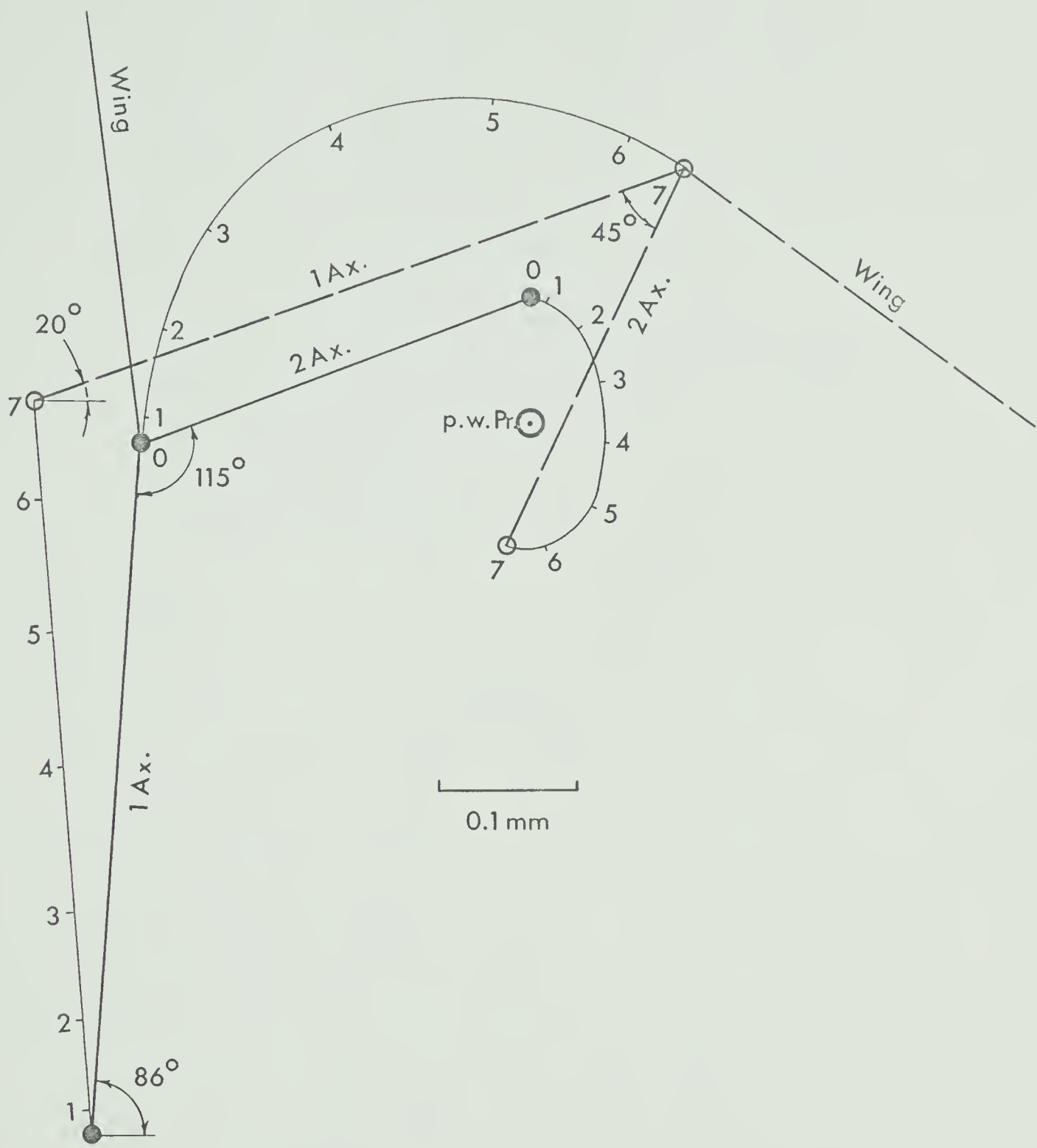


Fig. 42. Side view of the left tegula in position over  
the left fore wing base.



42.

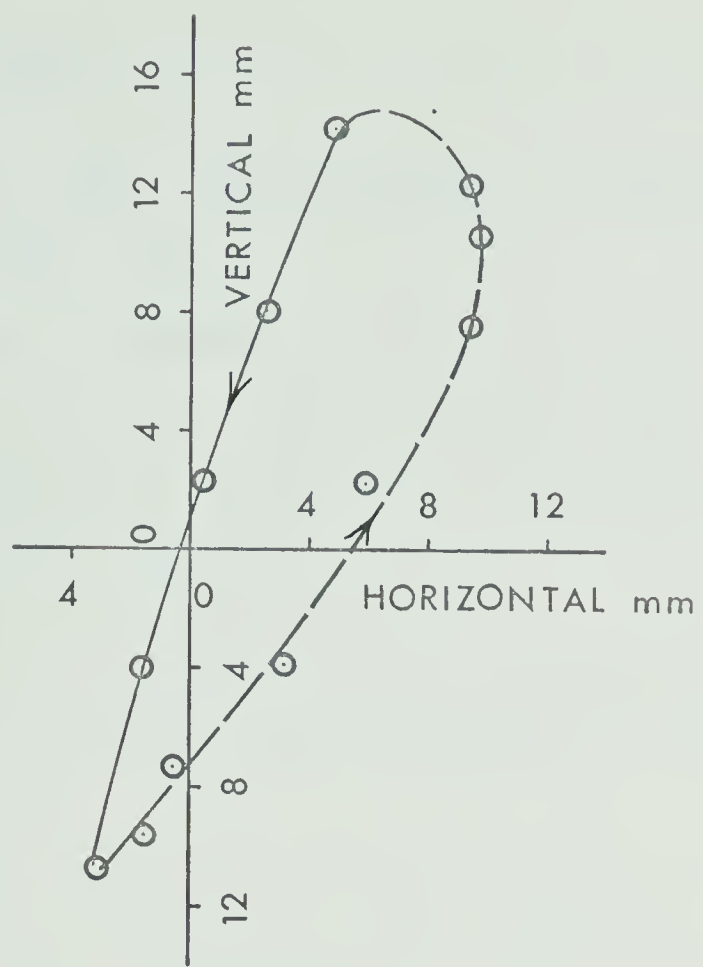
Fig. 43. Diagrammatic representation of the front view of the left mesothoracic first and second axillary limiting positions in flight. The solid lines indicate the maximum upstroke positions; the broken lines, the maximum downstroke positions. All positions are relative to a stationary pleural wing process in the maximum upstroke position.



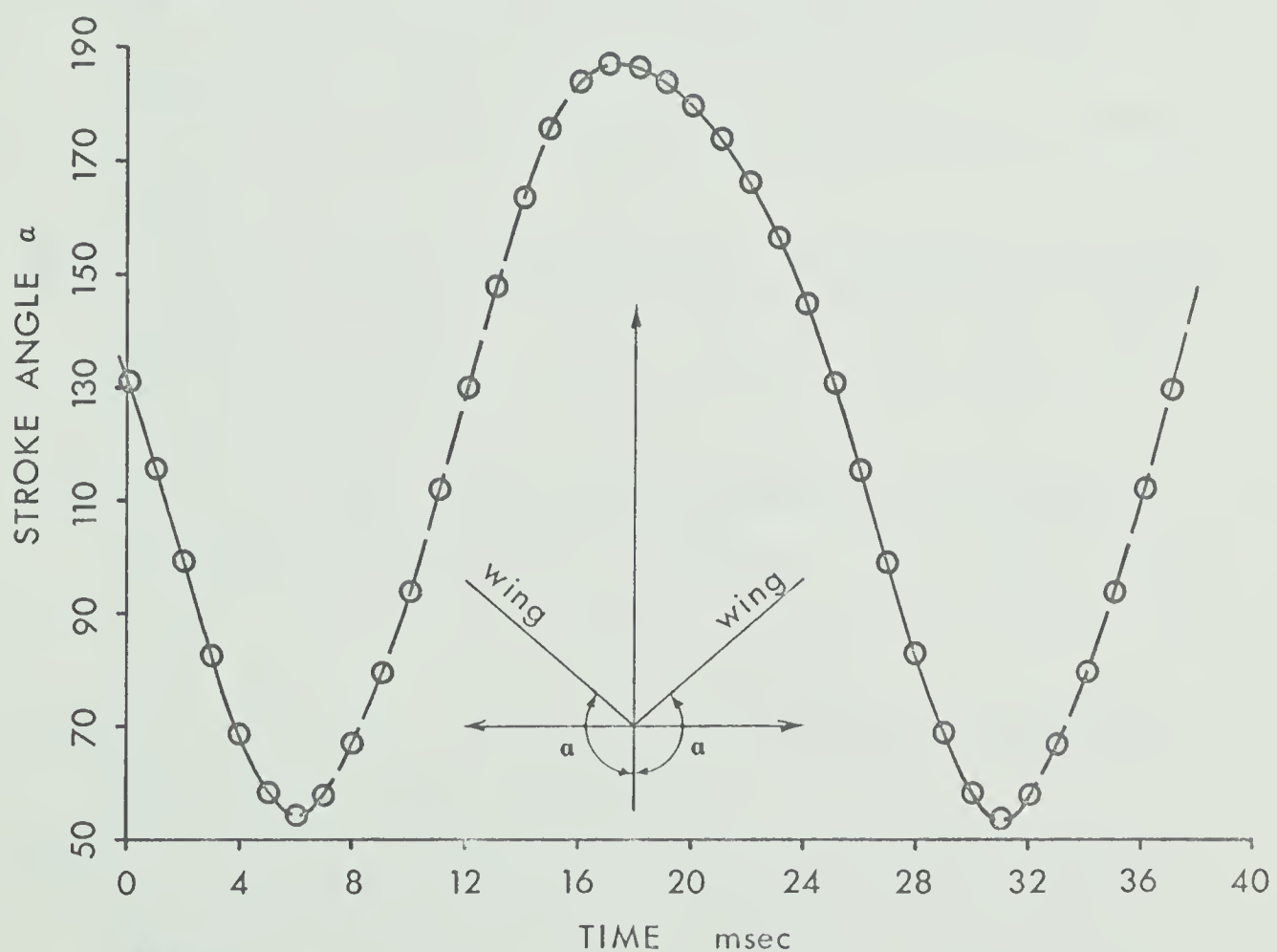
43.

Fig. 44. Side view of the mean left fore wing path for three individuals. The wing is taken to be a stiff extension of the radius 15mm from the first axillary-subcostal ligament. Broken lines indicate wing pronation during the stroke; solid lines, wing supination during the stroke.

Fig. 45. Mean variation of the frontal angle made by the wing to the ventral axis of a single insect with time. Broken lines indicate wing pronation during the stroke; solid lines, wing supination during the stroke.



44.



45.



## 8. Literature Cited

Alexander, R. McN. 1968. Animal mechanics. Sidgwick and Jackson, London. 346 pp.

Baird, J. L. 1964. Comparative physiology of insect flight: a study of the dynamic aspects of insect flight. Ph.D. thesis, University of Connecticut. University Microfilms, Inc., Ann Arbor, Michigan. 155 pp.

Barber, S.B. and J.W.S. Pringle. 1966. Functional aspects of flight in belostomatid bugs (Heteroptera). Proc. R. Soc. (B) 164:21-39.

Berlese, A. 1909. Gli Insetti. Milan. 1004 pp.

Boettiger, E.G. 1957. The machinery of insect flight, pp. 117-142. In Recent advances in invertebrate physiology. B.T. Scheer (ed.). University of Oregon Publications, Eugene, Oregon.

Boettiger, E.G. and E. Furshpan. 1952. The mechanics of flight movements in Diptera. Biol. Bull. mar. biol. Lab. Wood's Hole 102:200-211.

Carboneil, C.S. 1948. The thoracic muscles of the cockroach *Periplaneta americana* (L.). Smithson. misc. Coll. 107(2): 1-23.

Chadwick, L.E. 1959. The furcopleural muscles of Lepidoptera. Ann. ent. Soc. Amer. 52:665-668.

Ehrlich, P.R. and D.E. Davidson. 1961. The internal anatomy of the monarch butterfly, *Danaus plexippus* L. (Lepidoptera: Nymphalidae). Microentomology 24(3):85-133.



Ewer, D.W. and L.S. Naylor. 1967. The pterothoracic musculature of *Deropeltis erythrocephala*, a cockroach with a wingless female, and the origin of wing movements in insects. J. ent. Soc. sth. Afr. 30:18-33.

FitzPatrick, J.L.G. 1952. Natural flight and related aeronautics, Vol naturel et aeronautique allié, Nautr Flug und verwandte Luftschiffahrt. Institute of the Aeronautical Sciences. FF-7, 118 pp.

Greenewalt, C.H. 1960. Dimensional relationships for flying animals. Proc. Amer. phil. Soc. 104:1-605.

Hocking, B. 1953. The intrinsic range and speed of flight of insects. Trans. R. ent. Soc. Lond. 104:223-345.

Imms, A.D. 1957. A general textbook of entomology. Methuen, London. 9th edition. 886 pp.

Jensen, M. 1956. Biology and physics of locust flight. III. The aerodynamics of locust flight. Phil. Trans. R. Soc. B. 239: 511-552.

Jensen, M. and T. Weis-Fogh. 1962. Biology and biophysics of locust flight. V. Strength and elasticity of insect cuticle. Phil. Trans. R. Soc. 245:137-168.

Kammer, A.E. 1967. Muscle activity during flight in some large Lepidoptera. J. exp. Biol. 47:277-295.

Michener, C.D. 1952. The Saturniidae (Lepidoptera) of the western hemisphere. Morphology, phylogeny, and classification. Bull. Amer. Mus. nat. Hist. 98:335-501.



Nachtigall, W. and D.M. Wilson. 1967. Neuro-muscular control of dipteran flight. *J. exp. Biol.* 47:77-97.

Nüesch, H. 1953. The morphology of the thorax of *Telea polyphemus* (Lepidoptera). *J. Morph.* 93:589-609.

Pantin, C.F.A. 1948. Notes on microscopical technique for zoologists. Cambridge. 77 pp.

Parsons, M.C. 1960. Skeleton and musculature of the thorax of *Gelastocoris oculatus* (Fabricius) (Hemiptera-Heteroptera). *Bull. Mus. comp. Zool. Harv.* 122:299-357.

Pringle, J.W.S. 1957. Insect flight. Cambridge University Press, Cambridge 199 pp.

---

\_\_\_\_\_. 1965. Locomotion: flight, pp. 283-329. In M. Rockstein (ed.). *Physiology of Insecta*. vol. 11. Academic Press, London. 905 pp.

---

\_\_\_\_\_. 1968. Comparative physiology of the flight motor, pp. 163-223. In J.W.L. Beament, J.E. Treherne, and V.B. Wigglesworth (eds.) *Advances in insect physiology*. vol. 5. Academic Press, London. 361 pp.

Ritter, W. 1911. The flying apparatus of the blow-fly. *Smithson. misc. Coll.* 56(12):1-79.

Roeder, K.D. 1951. Movements of the thorax and potential changes in the thoracic muscles of insects during flight. *Biol. Bull.* 100:95-106.

Russenberger, von H. and M. Russenberger. 1959. Bau und Wirkungsweise des Flugapparates von Libellen. *Mitt. Naturforsch. Ges. Schaffhausen.* 27:1-88.



Sharplin, J. 1963a. A flexible cuticle in the wing bases of Lepidoptera. Can. Ent. 95:96-100.

\_\_\_\_\_ 1963b. Wing base structure in Lepidoptera.

I. Fore wing base. Can. Ent. 95:1042-1050.

\_\_\_\_\_ 1963c. Wing base structure in Lepidoptera.

II. Hind wing base. Can. Ent. 95:1121-1145.

\_\_\_\_\_ 1964. Wing folding in Lepidoptera. Can. Ent. 96:148-149.

Smart, J. 1959. Notes on the mesothoracic musculature of Diptera. Smithson. misc. Coll. 137:331-364.

Snodgrass, R.E. 1927. Morphology and mechanism of the insect thorax. Smithson. misc. Coll. 80(1):1-108.

\_\_\_\_\_ 1929. The thoracic mechanism of a grasshopper, and its antecedents. Smithson. misc. Coll. 82(2):1-111.

\_\_\_\_\_ 1935. Principles of insect morphology.

McGraw-Hill, New York. 667 pp.

Sotovalta, O. 1954. The effect of wing inertia on the wing stroke frequency of moths, dragonflies, and cockroach.

Ann. Ent. Fenn. 20:93-101.

Tiegs, O.W. 1955. The flight muscle of insects - their anatomy and histology with some observations on the structure of striated muscle in general. Phil. Trans. R. Soc. B. 238:221-347.

Weis-Fogh, T. 1960. A rubber-like protein in insect cuticle. J. exp. Biol. 37:889-907.



Weis-Fogh, T. and M. Jensen. 1956. Biology and physics of locust flight. I. Basic principles in insect flight. A critical review. Phil. Trans. R. Soc. B. 239:415-585.

Wilson, D.M. 1962. Bifunctional muscles in the thorax of grasshoppers. J. exp. Biol. 39:669-677.

---

1968. The nervous control of insect flight and related behaviour, pp. 289-334. In J.W.L. Beament, J.E. Treherne and V.B. Wigglesworth (eds.). Advances in insect physiology. vol. 5. Academic Press, London. 361 pp.

---

and T. Weis-Fogh. 1962. Patterned activity of co-ordinated motor units, studied in flying locusts. J. exp. Biol. 39(4):669-677.









**B29937**